An-Najah National University

Faculty of Graduate Studies

CdSe Thin Film Photoelectrochemical Electrodes:

Combined Electrochemical and Chemical Bath Depositions

By

Nour Nayef Abdul-Rahman

Supervisors

Prof. Hikmat S.Hilal

Dr. Ahed Zyoud

This Thesis is Submitted in Partial Fulfillment of the Requirements for the Degree of Master of Chemistry, Faculty of Graduate Studies, An- Najah National University, Nablus, Palestine.

2014

CdSe Thin Film Photoelectrochemical Electrodes: Combined Electrochemical and Chemical Bath Depositions

By

Nour Nayef Abdul-Rahman

This Thesis was defended successfully on17/9/2014 and approved by:

Defense Committee Members	**Signature**
1. Prof. Hikmat Hilal / Supervisor	.....
2. Dr. Ahed Zyoud / Co-Supervisor	.....
3. Dr. Abdel-Rahman Abo-Libdeh / External examiner	.....
4. Dr. Samar AL Shakhshir / Internal examiner	.....

Dedication

To My Great Parents
My Loving Sisters and Brothers,
All my Dear Friends,
My Doctors at both the University of Jordan and An-Najah National University
To everyone who supports me, encourages me, and loves me
To my lovely country "Palestine".

ACKNOWLEDGEMENTS

First and foremost, I would like to thank Allah who is my source of strength and to whom I owe all what I have been able to do and accomplish. Then my deepest appreciation and gratitude go to my supervisors Prof. Hikmat S. Hilal and Dr. Ahed Zyoud for their invaluable support and guidance during the course of this work.

I would also like to thank the members of the examination committee for their help and valuable comments on this thesis. Many thanks are due to DaeHoon Park, Dansuk Industrial Co., LTD. #1239-5, Jeongwang-Dong, Shiheung-Si, Kyonggi-Do, 429-913, South Korea, for XRD measurements.

Sincere thanks go to my parents for their endless support in everything I've ventured in my life, and to my friends for their assistance, for listening to my complaints and particularly for all the fun we have had during this period. Thanks are also due to the technical staff in the laboratories and all employees at the chemistry department in An-najah National University, for the help and the encouragement they provided at all times.

الإقرار

أنا الموقع أدناه مقدم الرسالة التي تحمل العنوان:

CdSe Thin Film Photoelectrochemical Electrodes:

Combined Electrochemical and Chemical Bath Depositions

أقر بأن ما اشتملت عليه هذه الرسالة هو نتاج جهدي الخاص، باستثناء ما تمت الاشارة اليه حيثما ورد، وأن هذه الرسالة ككل أو أي جزء منها لم يقدم من قبل لنيل أي درجة أو لقب علمي أو بحثي لدى أي مؤسسة تعليمية أو بحثية أخرى.

Declaration

The work provided in this thesis, unless otherwise referenced, is the researcher's own work, and has not been submitted elsewhere for any other degrees or qualifications.

Student's name: اسم الطالب: نور نايف جميل عبد الرحمن

Signature: التوقيع: نور عبد

Date: التاريخ ١٧/ ٩/ ٢٠١٤

List of Contents

List of Tables

List of Figures

List of Abbreviations

Symbol	Abbreviation
E_{bg}	Energy band gap
λ_{bg}	Wavelength band gap
CB	Conduction band
VB	Valance band
eV	Electron- volt
SCs	Semiconductors
PEC	Photoelectrochemical cell
PV	Photovoltaic
E_f	Fermi energy level
E_c	Conduction band energy
E_V	Valance band energy
E_{redox}	Redox energy level
SCL	Space charge layer
Red	Reductant
Ox	Oxidant
ECD	Electrochemical deposition
CBD	Chemical band energy
ECD/CBD	Combined between electrochemical and chemical bath methods
FTO	Fluorine doped tin oxide

V_{oc}	Open-circuit potential
J_{SC}	Short circuit current density
J-V	Current density potential
η	Conversion efficiency
FF	Fill factor
DC	Direct current
MP-Sil matrix	Matrix of tetra (-4-pyridyl) porpbyrinatomanganese (III/II) sulfate embedded inside polysiloxane
XRD	X-ray diffraction
PL	Photoluminescence

CdSe Thin Film Photoelectrochemical Electrodes: Combined Electrochemical and Chemical Bath Depositions

By
Nour Nayef Abdul-Rahman
Supervisors
Prof.Hikmat S.Hilal
Dr. Ahed Zyoud

Abstract

CdSe thin films have been deposited onto FTO/glass substrates by three different techniques, electrochemical deposition (ECD), chemical bath deposition (CBD) and combined method based on electrochemical deposition (ECD) followed by chemical bath deposition (CBD). The films were comparatively characterized by a number of techniques (photoluminescence spectra, electronic absorption spectra and XRD measurements). Photoelectrochemical (PEC) characteristics of the electrodes including current density-voltage (J-V) plots, conversion efficiency (η) and fill factor (FF) were then studies. The PEC measurements indicate that the CdSe films are n-type in electrical conduction, and optical absorption measurements show that the band gap

range for the prepared films is estimated to be 2.06-2.30 eV. XRD results show that the three systems involved nano-sized CdSe particles with cubic type crystals. The new ECD/CBD-CdSe electrode exhibited higher photo-electrochemical conversion efficiency (η% ~ 4.40) than either ECD- or CBD-CdSe film electrodes. This supports the basic hypothesis of this work where the ECD/CBD film is assumed to combine the advantages of both

ECD-CdSe film (good adherence to FTO/glass substrate) and CBD-CdSe film (suitable film thickness) together.

Various parameters were studied here, in order to enhance both ECD- and ECD/CBD thin film electrodes, including: Deposition times, annealing temperatures, cooling rate control and covering the prepared films with electro-active matrix of tetra (-4-pyridyl) porpyrinatomanganese (III/II) sulfate embedded inside polysiloxane films (MnPyP/Polysil) matrices, followed by additional heating of the coated films at 120ºC. CBD-CdSe films enhancement was investigated in an earlier study [18]. Annealing is undesirable in this study, since heating may increase the kinetic energy of the particles and may thus increase their disorder and arrange them in a random manner. On the other hand, lower annealing temperature (150 ºC) gave higher PL intensity, clearer electronic absorption, better PEC characteristics and higher crystallinity than 350 ºC annealing temperature.

Higher annealing temperatures increased the possibility of the film distortion and Se evaporation from the film. Cooling rate (slow or fast cooling) also affected films characteristics (XRD, PL and electronic absorption spectra, photo J-V plots).

Covering the films with MP-Sil matrix followed by additional heating of the coated films at 120ºC enhanced PL and electronic absorption spectra, photo J-V plots, conversion efficiency and fill factor. MP-Sil matrix coating seems to behave as a charge transfer catalyst at the solid/liquid interface and to protect the film from oxidation.

Chapter One

Introduction

1.1 What is so special about solar energy?

No one can deny the attention that solar energy has gained especially in recent years, and this is increasing with the increasing demand for energy. Solar energy is regarded as the best source of energy since the world's main energy sources used today (such as fossil fuels and coal) are non – renewable. Fossil fuels also hurt the environment by emitting carbon oxides, sulfur oxides and other gases which cause green house effect. In one day, solar radiation provides the world more energy than our current population would consume in 27 years. In fact, "The amount of solar energy striking the earth over a three-day period is equal to the energy stored in all fossil energy sources [1].

The ability to convert sun radiant power into electrical energy has many advantages including [2]:

a) Pollution free, which will solve the global energy problems.
b) Renewable energy source has long life time.
c) Freely available source.
d) Does not need expensive distribution net works.
e) There is no noise pollution in solar cells.

Despite the many advantages of solar energy technology, there are disadvantages which include [3]:

a) Solar energy is unreliable source of energy. Cloudy skies and storms reduce its effectiveness, at night the solar equipment will be useless. So we still need other sources of energy.

b) Solar energy equipments are relatively costly to manufacture, at least nowadays.

c) Large areas of land are needed for the solar energy installations.

d) Battery chargers are needed so that solar powered devices can be used at night. These batteries are large and heavy and need storage area. They also need replacement from time to time which means more money is needed.

In spite of these disadvantages of solar energy technology, the advantages are still considered since it is a promising renewable and long lasting source of energy. Scientists are working nowadays to overcome the disadvantages.

Solar energy technology uses special materials in converting the solar light into electrical power. Such materials are mostly semiconductors (SCs).

1.2 Energy band gap (E_{bg}) and semiconductors

To differentiate between insulators, semiconductors and conductors, the concept of energy band gap should be known. Energy band gap (E_{bg}) is defined as the energy difference between the upper edge of the valance

band (VB) and the lower edge of the conduction band (CB). Substances with large band gaps above ~ 4 eV are generally insulators, those with smaller band gaps are semiconductors, while conductors have zero band gap energy [4], as illustrated in Figure (1.1).

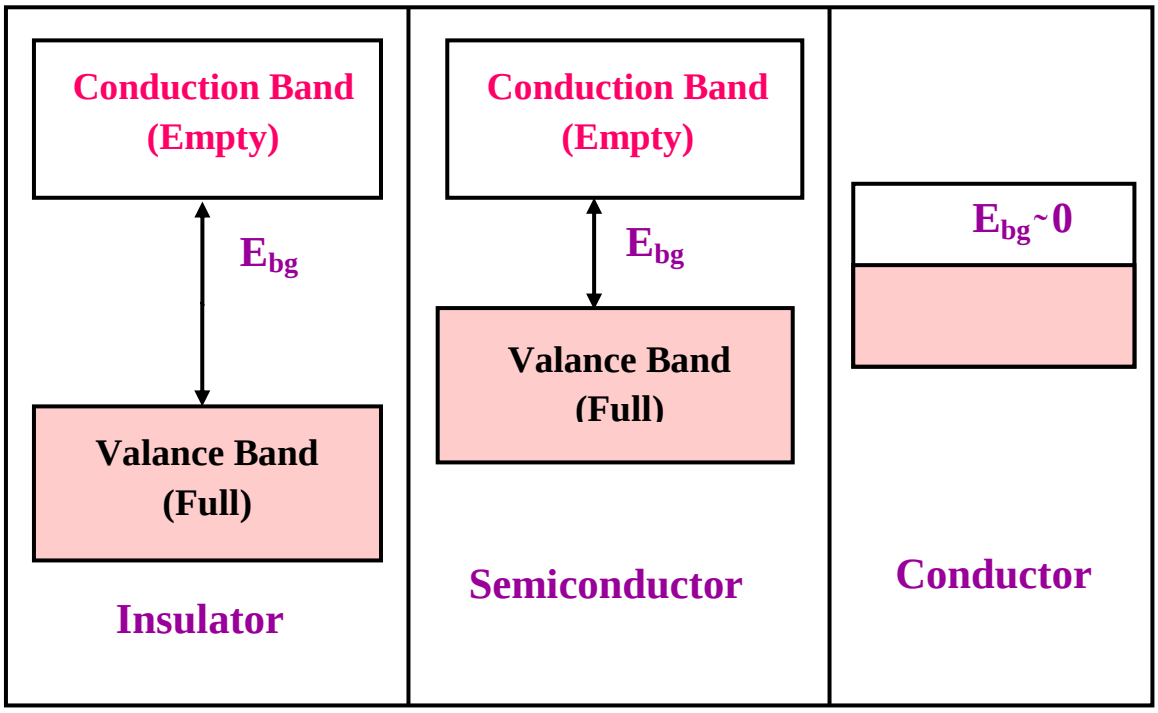

Figure (1.1): Band gap energies in solids. *Reproduced from* [5].

Semiconductor materials at absolute zero don't conduct electricity, since the electrons in the filled valance band cannot reach the empty conduction band due to the energy band gap.

Charge carriers could be created by rising temperature (thermal generation mechanism). The thermally excited electrons jump from the valance band to the conduction band and undertake conduction [4].

1.2.1 Types of semiconductor materials

There are two types of semiconductors, intrinsic SCs and extrinsic SCs.

a) Intrinsic semiconductors

In an intrinsic semiconductor (undoped semiconductor), when an electron transfers to the conduction band, a vacancy is left in the valance band (called hole). The number of excited electrons is equal to the number of holes in this type of semiconductor, Figure (1.2) [4-6].

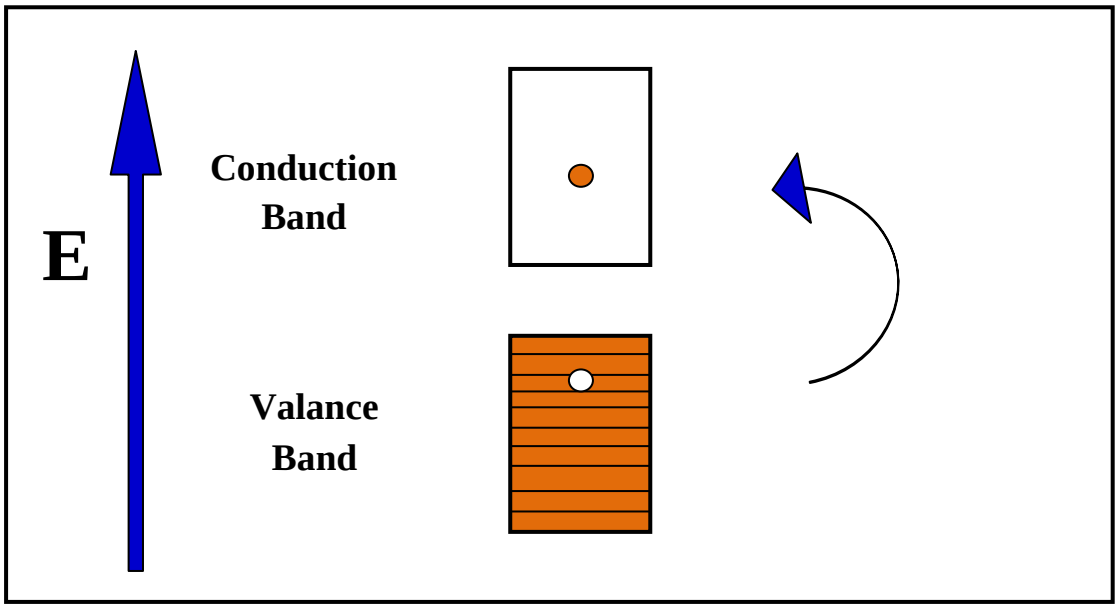

Figure (1.2): Thermal generation of charge carriers in intrinsic semiconductor. *Reproduced from* [6].

b) Extrinsic semiconductors

Doping is defined as "Introducing impurities (dopants) into an intrinsic semiconductor (SC) for the purpose of enhancing its electrical properties ". The new SC resulting from this process is called extrinsic SC.

Doping process involves chemically changing the crystal lattice by adding impurities into the forbidden band gap region. This means adding energy levels into it. These energy levels could be close to either conduction band or valance band.

So two cases may result here. If the dopants are electron donor, with energy levels near the conduction band, then large population of electrons is thermally excited to the conduction band. The semiconductor is called n-type in this case, Figure (1.3a). In the p-type semiconductor, the dopants are electron acceptors with energy levels near the valance band. Electrons are captured from the valance band creating large population of positive charge carriers (holes), Figure (1.3b), [4-6].

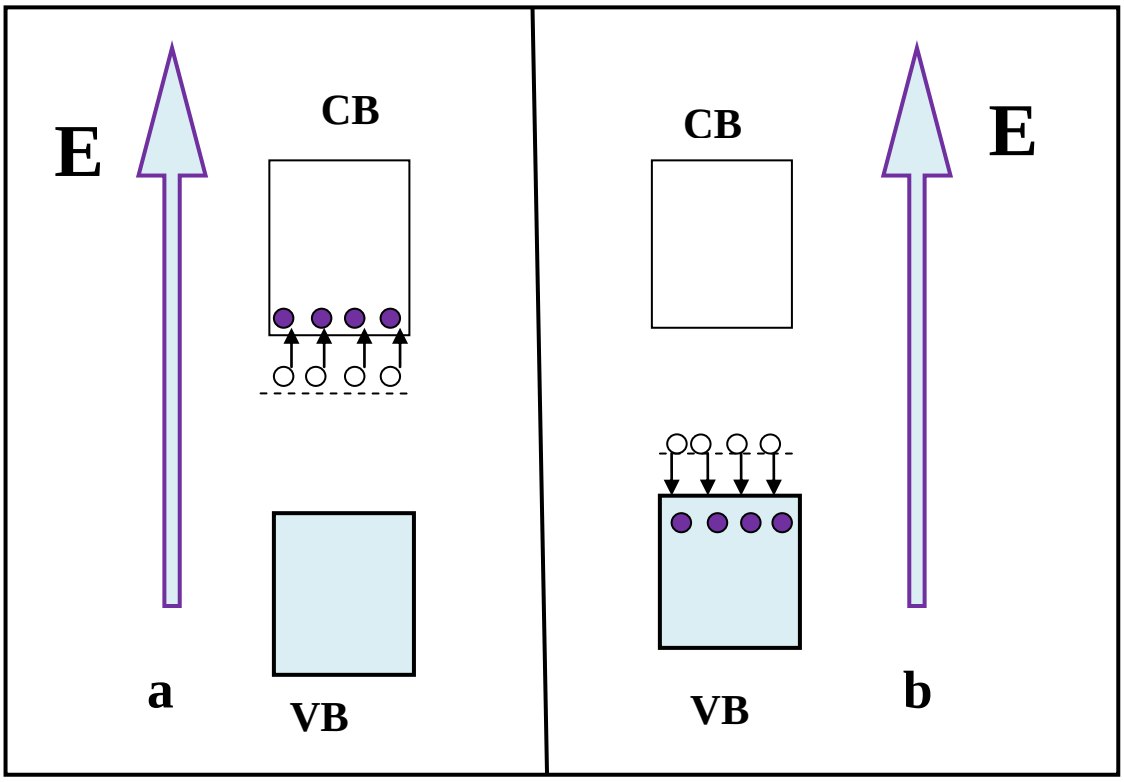

Figure(1.3) : Extrinsic types of semicondctors a) n-type SC, b) p-type SC. *Reproduced from* [4].

1.2.2 How photo excitation occurs in SCs ?

The photo sensitivity in SCs depends on energy band gap E_{bg}. The photo excitation occurs by photons with energy greater than, or equal to, the E_{bg}. In terms of wavelength λ_{bg}, the photons with wavelength shorter than a threshold wavelength will excite electrons from valenece band (VB), while photons with wavelength longer than λ_{bg} will have no excitation effect. A relationship between E_{bg} and λ_{bg} is shown below where λ_{bg} has units of nanometers (nm) while E_{bg} has units of electron- volts (eV):

$$\lambda_{bg}\,(\text{nm}) = 1240/\, E_{bg}\,(\text{eV}) \quad \ldots\ldots\ldots\ldots\ldots\ldots\ldots\ldots\ldots\ldots\ldots\ldots\ldots\ldots \quad (1)$$

For solar energy application, the suitable band gap energy for maximum efficiency conversion of sunlight to electricity is in the range 1.5-2.5eV, (800-400 nm in terms of wavelength λ_{bg} range) which is the visible region in the solar spectrum. This is a suitable range for giving a stable semiconductor as well [7].

Light absorbing properties of semiconductors differ between the direct band gap and the indirect band gap types. In the direct band gap SCs, the photon with energy equal to the direct band gap energy is absorbed creating a hole and an electron. In the in-direct band gap SCs, a hole, an electron and a phonon (vibrated motion in the lattice with certain energy) will result by the absorption process. The indirect transition occurs at a lower energy than the direct transition in many semiconductors. As a result of that the

absorption coefficient rises less steeply with increasing photon energy for the indirect band gap transition than for a direct band gap transition [6-8].

1.3 Types of solar systems

In addition to thermal solar systems, there are two major types of solar systems used to convert the solar light into electricity: Photovoltaic (PV) cells and photo electrochemical (PEC) cells.

1.3.1 Photovoltaic (PV) cell

A PV cell involves two layers of semiconductors (n and p types) to build p-n junction as shown in Figure (1.4). When a beam of light strikes the solar cell, electrons excite from valance band to conduction band leaving holes in the valance band.

Electrons move downhill to n-type through the solid junction and holes move upward towards p-type side. Barrier potential in the cell produces a voltage so called photovoltage, which drives a current through a circuit [9].

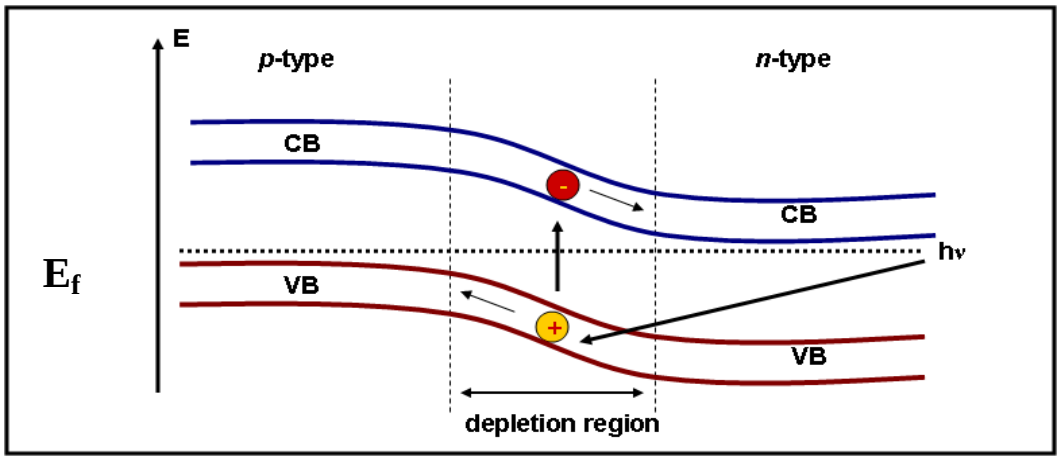

Figure (1.4): Creation of an electron-hole pair upon absorption of a photon with wavelength equal or shorter than threshold wavelength [9].

1.3.2 Photoelectrochemical cells (PECs)

PECs are popular devices used to convert light into electricity. When a certain SC is immersed in a suitable electrolyte solution, a PEC system will be created, the Fermi level (E_f) is an important parameter for semiconductor electrochemistry, it is defined as the energy level at which the probability of being occupied by an electron is equal to half. Considering n-type SC, the Fermi level (E_f) in SC is above the Fermi level in the electrolyte (E_{redox}) as shown in Figure (1.5).

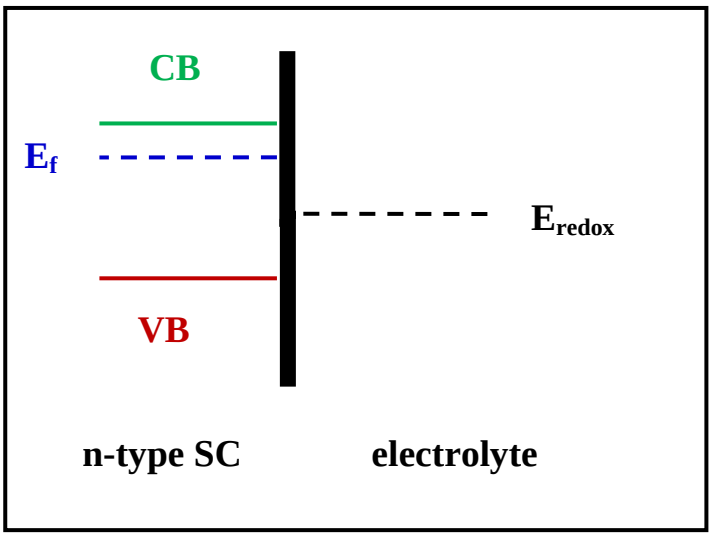

Figure (1.5): n-type semiconductor in PEC cell before equilibrium. *Reproduced from* [7].

Electrons will move from the CB of the SC to the E_{redox} until thermal equilibrium occurs. The Fermi levels of the SC and the electrolyte become the same. This equilibrium will produce a positive space charge layer (SCL). The conduction and the valence band edges will bend upward as shown in Figure (1.6) [21].

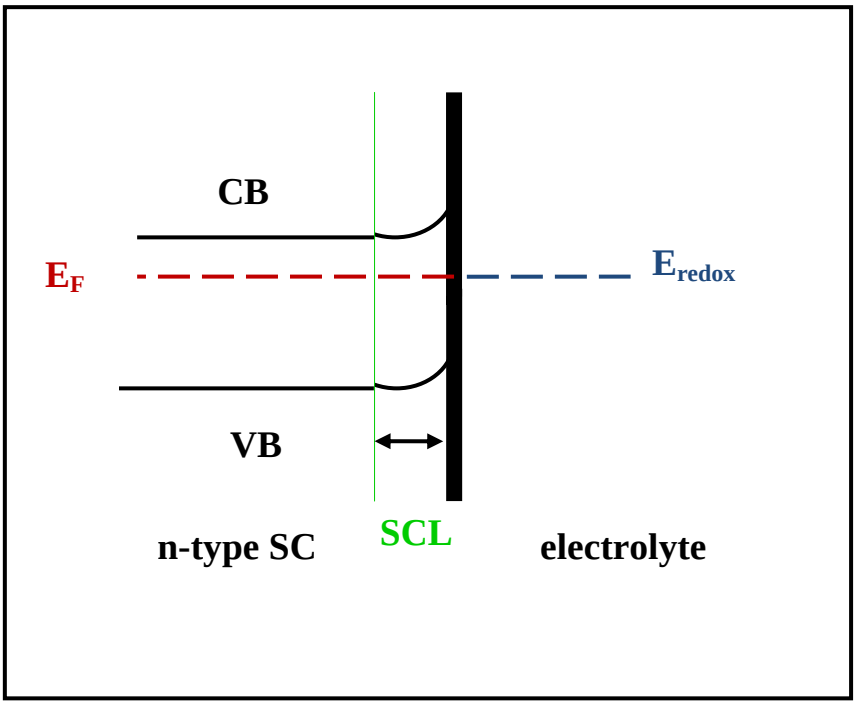

Figure (1.6): n-type semiconductor in PEC cell at equilibrium. *Reproduced from* [4].

For p-type SC, the same thing occurs, but the Fermi level of the p-type SC is below the Fermi level of the electrolyte [21].

PEC cells are expected to be more economic in solar light conversion into electricity than PV cells. This is because PV systems are costly and need special conductions to manufacture. Therefore, currently the cost of electricity created from PV cells is about 3-5 times the cost of coal or natural gas powered electrical plants. In PEC

cells, solar energy can be stored in the form of conventional fuel and converted to electrical energy as well. Moreover PEC cells can be fabricated and modified easily [19].

1.4 Photo current generation in PEC cells

Assuming n-type SC, electrolyte junction and a beam of light passes through, photons with energies larger than the E_{bg} are absorbed. Thus, electrons excited from the valance band into the conduction band leaving holes in the valance band [4-7].

When light absorption creates a population of excited holes and electrons, the electron concentration (called majority carriers) slightly changes, while the hole concentration (called minority carriers) increases rapidly. Thus photo-effects are greatest when minority carriers dominate the electrode response. This occurs when the electrode is biased to form a depletion layer (with positive potential) and the photo-generated minority carriers migrate towards the electrode-electrolyte interface [4- 7].

Photo- effects happen in SC when the wavelength of incident light is shorter than the threshold wavelength. With longer wave length the SC is insensitive to light. Information can be provided from this phenomenon about type of band gap energy (direct or indirect E_{bg}), [4-7].

Recombination is another important phenomenon related to photo-effects in the PEC. The excited hole and electron annihilate one another with heat or a photon evolution. Recombination can occur directly with the electron descending from the conduction band edge to the hole at the valance band edge, or indirectly via intermediate energy levels (bulk or surface states).

Recombination lowers the magnitude of photo-effect, and lowers the efficiency of PEC cell [4-7].

When n-type semiconductor electrode is biased sufficiently positive of potential of flat band (V_{fb}), the dark currents are very low, due to the blocking effect of the depletion layer. Irradiation of the semiconductor through the electrolyte with light ($\lambda < \lambda_{bg}$) yields anodic photocurrents, Figure (1.7) [4-7].

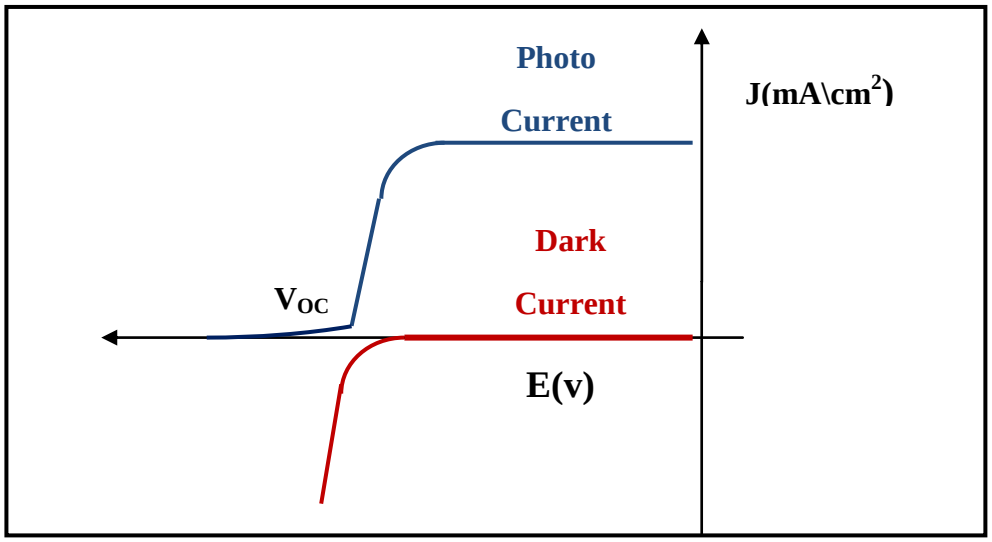

Figure (1.7): Typical dark current and photocurrent voltammograms for n-type SC. *Reproduced from* [4].

The anodic photocurrents appear from the flux of holes that arrive at the surface. After the absorbed light creates an electron-hole pair in the depletion layer, the two charge carriers are separated by the electric field in the depletion layer. The electron moves toward the bulk, while the hole migrates toward the surface, oxidizing the reduced species, Figure (1.8) [4-7].

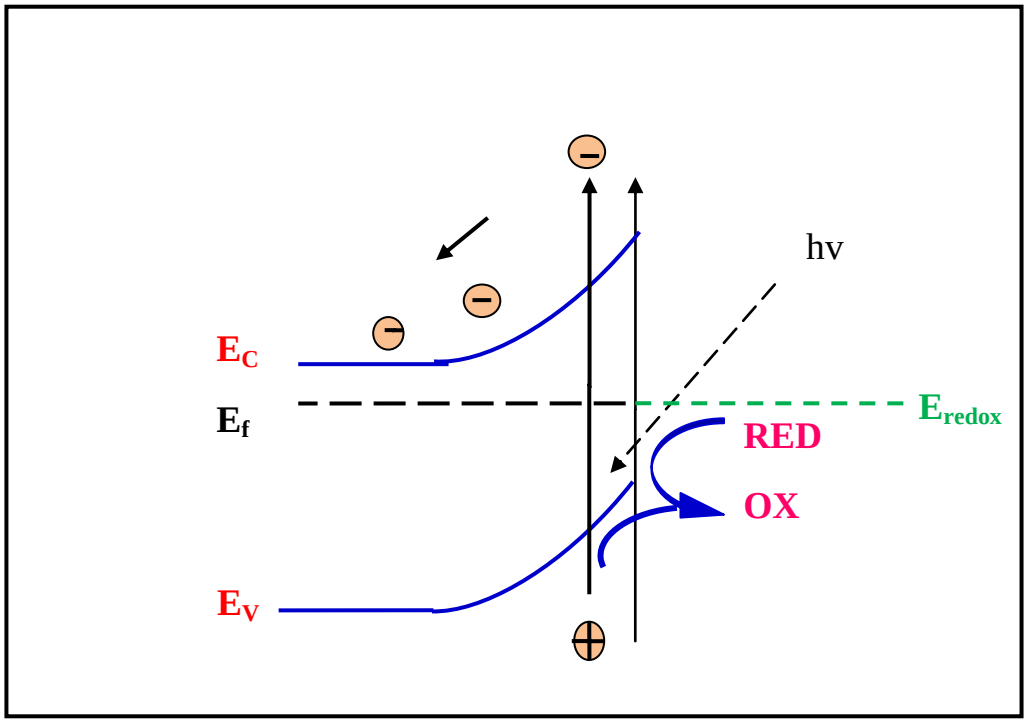

Figure (1.8): Photocurrent generation at n-type SC. Photo generated holes move to the surface and oxidize solution reduced species. *Reproduced from* [7].

The shape of the photocurrent voltammogrm depends on the energy distribution of the incident photons. The recombination rate, the absorption coefficient of the semiconductor and the diffusion distance of the excited hole and electron, all affect the resulting photo current. It should be noted that photocurrent occurs only in the case of band bending [4].

1.5 Dark current generation

Dark current occurs if the electrons transfer from the n-type semiconductor conduction band to the electrolyte solution. At equilibrium, an energy barrier is created by bending in both conduction and valence bands. The electrons must exceed this barrier before transfer occurs. This could be done by applying a negative potential ($\triangle E_1$) to provide electrons with enough energy to overcome this barrier. As a result space charge layer

(SCL) disappears and flat band potential occurs, Figure (1.9), [4-7]. Therefore, dark current should occur in case of flat bands.

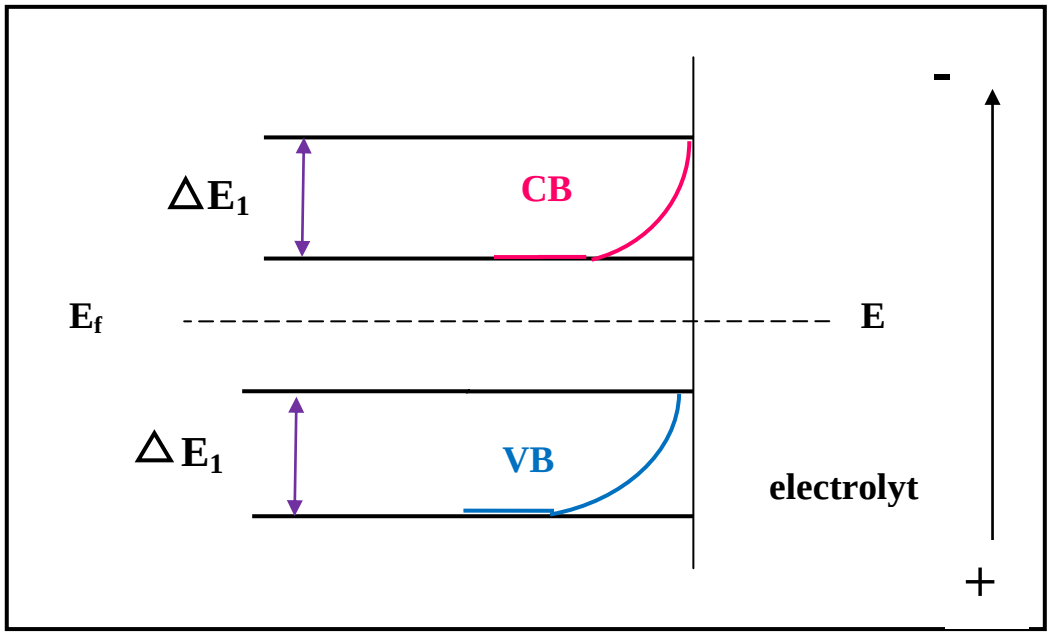

Figure (1.9): Dark current in n-type semiconductor, *Reproduced from* [4].

1.6 Thin film electrode technology

Thin film Semiconductor electrodes are emerging as alternative to conventional monolithic semiconductor electrodes, and thus thin film electrodes are becoming popular for PEC processes. Due to many features such as the low cost since much less material is used, more enhanced efficiency is expected in thin film technology [16].

Many different methods were used to deposit CdSe thin films, such as chemical vapor deposition (CVD), physical vapor deposition (PVD), chemical bath deposition (CBD), electrochemical deposition (ECD), successive ionic layer adsorption and reaction (SILAR) and atomic layer deposition (ALD) [17-18]. Each method has its own advantages and

shortages. ECD and CBD are known to be convenient and low cost demanding. ECD gives good contact while CBD gives soundly thick films. Combining the two techniques together may thus give combined advantages. Such technique has been first used in CdS thin film electrode preparation [17] but not in CdSe thin films.

1.7 Cadmium Selenide

Cadmium selenide has gained great attention in material science, due to its wide range of applications in optoelectronics such as laser diodes, electro conductive electrodes, solar control coatings and photo electrochemical solar cells [10]. Moreover, CdSe-based materials have potential uses in biomedical imaging. Human tissue is permeable to far infra-red light. By injecting appropriately prepared CdSe nanoparticles into injured tissue, it may be possible to image the tissue in the injured areas. CdSe material is transparent to infra-red (IR) light and has seen limited use in windows for instruments utilizing IR light. The material is also highly luminescent [11].

CdSe has three known crystalline forms: Wurtzite (hexagonal), zinc blende (cubic) and rock-salt (cubic) [12]. The CdSe form can be converted to the wurtzite structure by heating. The transition starts at 130 °C, and completes at 700 °C within a day. The rock-salt form only appears under high pressure, Figure (1.10) [13].

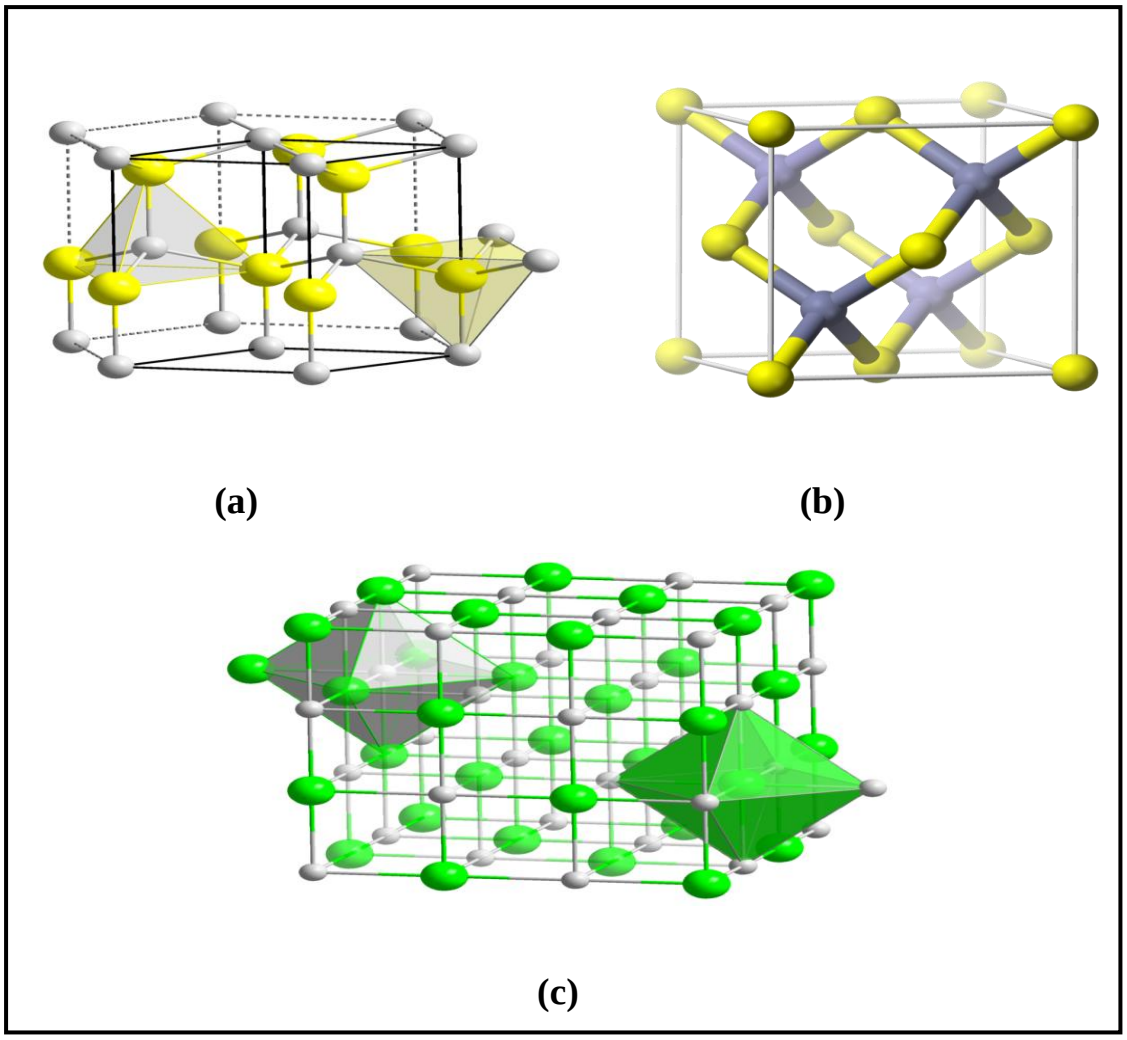

Figure (1.10): Crystal structure of CdSe with a) wurtzite (hexagonal) form, b) zinc blende (cubic) form, c) rock –salt (cubic) form, [14].

Cadmium selenide is n-type semiconductor. The band gap energy for CdSe nanoparticle thin films is in the range of 1.70 – 2.1 eV [22, 35]. The band gap is thus suitable for solar spectrum and efficient photo-conversion processes [15].

1.8 Objectives

The main objective of this work is to obtain stable and efficient CdSe thin film onto fluorine doped tin oxide/glass (FTO/glass) substrates. The electrodes will be used in photoelectrochemical (PEC) processes.

The preparation method will involve combination of CBD and ECD techniques together. Such a technique has been used in CdS thin film electrode preparation [16]. We wish to use the same technique here and apply it again in preparing CdSe films deposited onto FTO/glass, for the first time.

Technical objectives are:

1) Prepare CdSe nano thin film electrodes by using ECD followed by CBD onto FTO/glass electrodes. The ECD is expected to yield good contact between CdSe film and the FTO surface. CBD gives soundly thick films, and is known for its ease of preparation.

2) Examine film efficiency in light-to-electricity conversion by measuring PEC characteristics (short circuit current density J_{sc} , dark current density-potential (J-V) plots , open–circuit photo potential V_{oc}, conversion efficiency η and fill factor FF) of the new prepared CdSe film electrodes .

In this study, several methods will be used to enhance efficiency and stability of CdSe films and achieve our objectives, including:

1) Pre-annealing the CdSe thin film electrode at different temperatures.

2) Controlling the film cooling rate.

3) Covering the prepared CdSe thin films with metalloporphyrine MnP ions embedded inside polysiloxane polymer matrix.

In this study, CdSe thin films will be prepared by ECD, CBD and by combined ECD/CBD techniques. Comparison between these preparation methods will be made.

1.9 Hypothesis

Our new technique will enhance PEC characteristics of the thin film electrode. This is based on the following assumptions:

1) ECD makes a better contact between CdSe film particles and FTO/Glass surface than CBD.

2) If the ECD method is followed by CBD, two layers will result. Annealing the two CdSe layers will homogenize them together with high crystalline quality.

3) As a result of annealing process for the electodes, higher PEC efficiency and stability should be obtained

4) Coating the CdSe thin films with polymeric electro-active matrix, worked well on CBD- CdSe thin film electrodes [18]. Similar results are expected for combined ECD/CBD- CdSe thin film electrodes in this work.

5) Further modification, such as cooling rate control may also affect CdSe film quality.

1.10 Novelty of this work

This work involves many novel concepts and ideas, including:

- As far as we know, a preparation technique for CdSe thin films is proposed by combination between ECD and CBD for the first time.
- As far as we know, the ECD/CBD-CdSe thin film coverage with polymer/metaloporphyrin matrix will be examined as PEC working electrode for the first time.
- As far as we know, effect of annealing temperature on the ECD/CBD-CdSe thin films will be investigated here for the first time.
- As far as we know, effect of cooling rate in the pre-annealed ECD/CBD-CdSe thin films will be investigated here for the first time.
- As far as we know, effect of deposition time on the ECD/CBD-CdSe thin films will be investigated here for the first time.
- As far as we know, CdSe thin film prepared by ECD technique with a modified procedure will be investigated here for the first time.
- As far as we know, ECD-CdSe thin film coverage with polymer/metalophyrine will be investigated here for the first time.
- As far as we know, effect of annealing temperature on the ECD-CdSe thin films will be investigated here for the first time.
- As far as we know, effect of cooling rate on the pre-annealed new ECD-CdSe thin films will be investigated here for the first time.

- As far as we know, comparing between ECD-CdSe thin films, CBD-CdSe thin films, and ECD/CBD- CdSe thin films will be investigated here for the first time.

Chapter Two

Materials and Methods

2.1 Materials

Different chemicals were used in this work. $CdCl_2.2H_2O$, $Na_2S.XH_2O$, elemental sulfur and acetone were purchased in pure form from Sigma-Aldrich. NH_4Cl, $Na_2S_2O_3$, HCl were purchased in pure form from (SDFCL). FTO/glass substrates were purchased from Sigma-Aldrich, and triethanolamine (TEA) from Sun pharm LTD. Tetrapyridyl porphyrin (H_2TPyP) complex was kindly donated by Mrs. Najat Al-Daqqa, An – Najah National University.

2.2 Pretreatment of FTO/glass substrate

In order to obtain good adherence and CdSe film uniformity, FTO/Glass substrates were cleaned before CdSe film deposition process by washing with soap, then with distilled water followed by immersion in dilute solution of HCl (10% v/v) for 1 hour using ultrasonic cleaning bath, the substrates were then rinsed with distilled water, and immersed in acetone for 1 hour using ultrasonic cleaning bath. Finally, the substrates were rinsed with distilled water and then dried with nitrogen stream.

2.3 Preparation of selenium ions

Ordinarily, selenium is not soluble in water. To prepare selenium ions in the form of (Na_2SeSO_3), selenium powder was mixed with sodium sulfite

and refluxed at 90ºC for about 15 hours. To prepare 200 mL of (0.25 M) Na_2SeSO_3 solution, sodium sulfite (40.0 g) was added to 200 mL of distilled water. Then, Se powder (4.0 g) was added. Fresh Na_2SeSO_3 solution was filtered and stored for the deposition processes.

2.4 CdSe thin film preparations

Preparation techniques of CdSe thin films involved electrochemical deposition ECD, chemical bath deposition CBD, and the two techniques combined together ECD/CBD.

2.4.1 Electrochemical deposition (ECD) technique

The electrochemical cell used in CdSe thin film deposition consisted of a FTO/ glass substrate as working electrode, platinum as a counter connected to internal reference electrode, aqueous electrolyte containing (0.008M) $CdCl_2.H_2O$ and (0.005M) Na_2SeO_3.

The procedure that followed in this technique is taken based on literature [22-23], with making our own modification.

At first cadmium chloride solution (1.60 mL, 0.50 M) was mixed with selenium ions solution (2.00 mL, 0.25 M) in a volumetric flask (100 mL)

and filled with distilled water to the mark, continues stirring until the entire solid dissolved in distilled water. The solution was transferred to the deposition bath cell, then 2-3 drops of ammonium solution was added to control the pH value of the solution which was around 11. The substrates

were then immersed vertically into the deposition bath against the wall of the cell containing the reaction mixture.

The deposition was done at room temperature after nitrogen gas bubbling inside the solution prior to deposition for 5 minutes to remove any dissolved O_2. The nitrogen flow on the surface of solution was continued during deposition to avoid O_2 leakage. The electrolyte was continuously stirred at a moderate speed with the help of a magnetic stirrer during the electrodeposition. The deposition potential was fixed at a constant voltage (- 1.0 volt vs Ag/AgCl) using DC stripping. Thin films were deposited in different periods of time.

After deposition, the samples were taken out of the bath, washed with distilled water and dried by blowing air and preserved for characterization. Figure (2.1) shows the experimental arrangement for ECD technique.

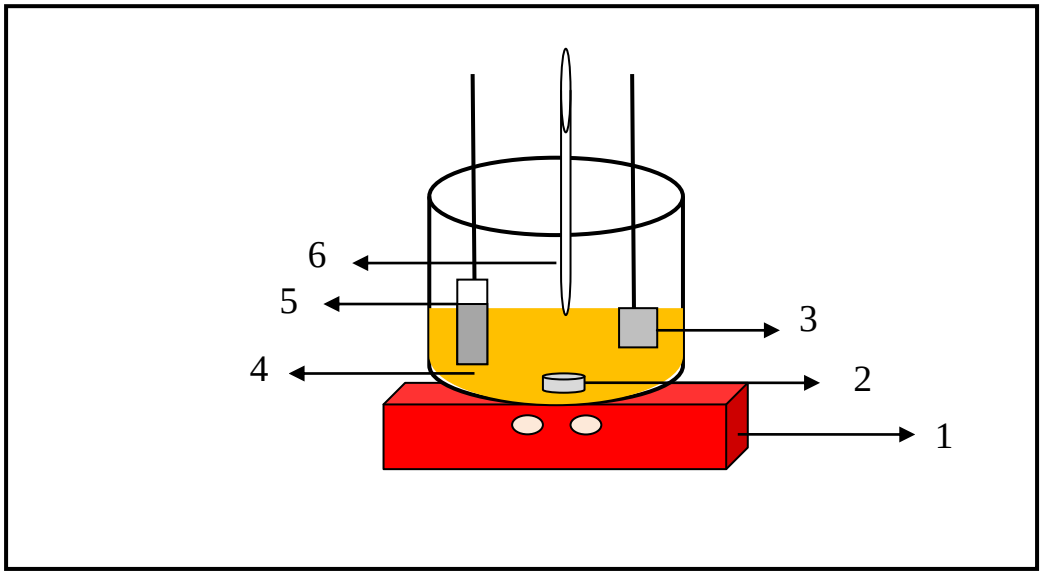

Figure (2.1): The experimental arrangment for the ECD-preparation of CdSe film. 1) magnetic stitter plate, 2) magnetic stirrer , 3) platinum electrode, 4) solution containing the required ions, 5) CdSe thin film, 6) nitrogen flow.

2.4.2 Chemical bath deposition (CBD) technique

The procedure followed in this technique is taken based on literature [10-24], with making our own modification. The chemical bath involved (5.00 mL, 0.50M) $CdCl_2$, (5.00 mL, 7.4M) Triethanolamine (TEA), (2.50mL, 13.4M) NH_3, (8.00 mL, 0.25 M) Na_2SeSO_3 and distilled water (20 mL). All materials were added according to this order in the reaction container. The final pH value of the solution became ~11. Pre-cleaned FTO/glass substrate was then inserted vertically into the mixture. The deposition was allowed to proceed at 70ºC for 4 hours with continuous stirring during the deposition process. The coated substrate was then removed, washed well with distilled water and allowed to dry. The system was tightly closed with rubber sealing. The solution color changed from colorless to pale yellow to bright orange and finally to red wine color during the deposition process.

2.4.3 ECD/CBD combined technique

The CBD technique, described above was applied to the prepared ECD – CdSe films forming two non-homogeneous layers of CdSe films.

2.5 Preparation of electro-active (MP-Si) matrix

Commercial R.T.V made polysiloxane paste (Sil) and tetra (-4-pyridyl) porphyrinatomanganese (III) sulfate (MP) complex, Figure (2.2), were used in preparing of MP-Sil matrix for CdSe thin film surface modification.

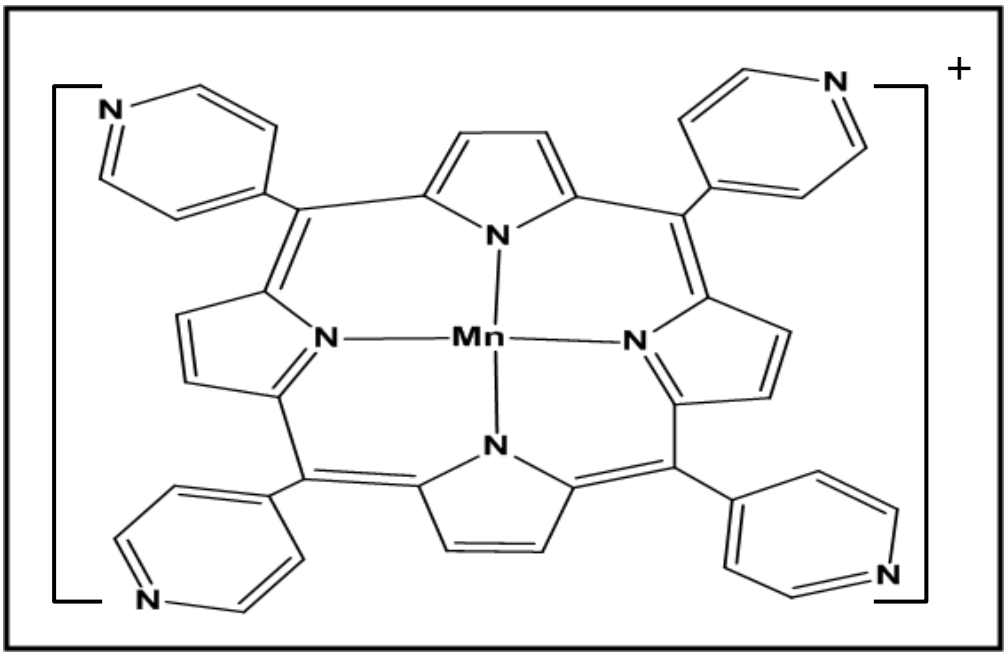

Figure (2.2): Tetra (-4-pyridyl)porphyrinatomanganese (III) sulfate (MP) complex [25].

MP complex was prepared by vigorously refluxing H_2TPyP (81.70 mg, 0.132 mmol) with excess manganese (II) sulfate (1.53 mg, 0.91 mmol) of N, N-dimethylformamide (DMF) (60.0 mL) for 10 hours. DMF was then evaporated under reduced pressure in order to reach concentrated solution.

Air was passed through the mixture to oxidize Mn^{+2} to Mn^{+3}. The resulting mixture was chromatographed over activated neutral alumina using DMF as eluant. Elute fractions with the characteristics absorption at 462, 569 and 620 nm were stored in the dark [25-27].

MP was prepared by dissolving (0.01 mg, 1.37 x 10^{-5} mole), each one in 1.0 mL methanol. A dilute solution of the polysiloxane paste (Sil) in acetic acid was prepared by dissolving 0.01 mg of the polysiloxane paste in 20.0 mL dichloromethane (CH_2Cl_2). MP-Sil matrix was prepared by adding the MP solution to the Sil solution in 1:4 (v/v) ratio respectively. Figure (2.3)

shows the electronic absorption spectra of MP complex embedded in Sil polymer, [25-27].

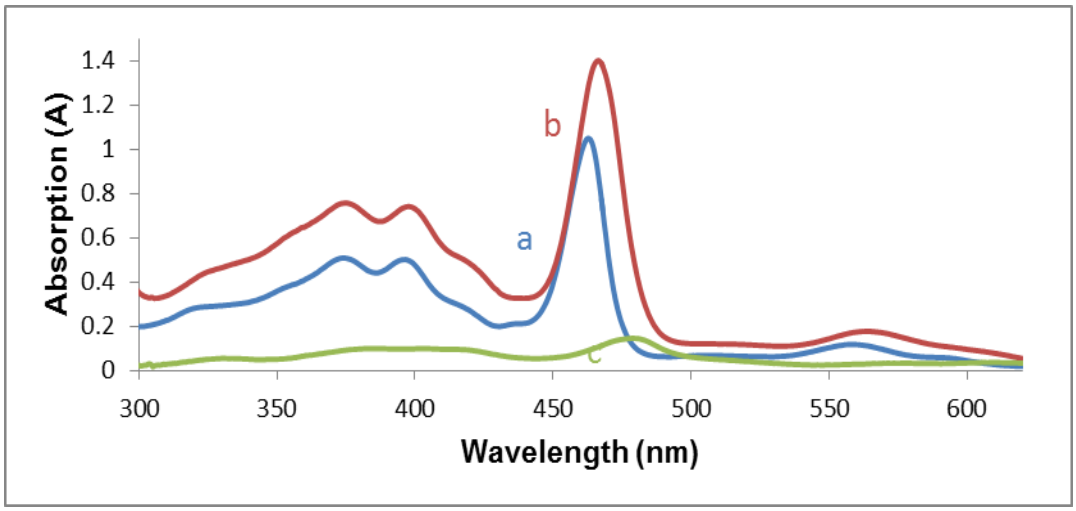

Figure (2.3): The electronic absorption spectra for: a) MnP solution in methanol, b) MnP-Sil solution, c) MnP-Sil on naked FTO [28].

2.6 Modification of CdSe thin films

To modify the prepared CdSe thin films, different methods were applied including: annealing process, cooling rate control and coating the prepared thin films with MP-Sil matrix, [18].

2.6.1 Annealing process

A thermostated horizontal tube furnace (Lindberg Hevi-Duty Control Tube Furnance) was used in this process. The temperature of the furnance was raised to the desired temperature (150°C, 250°C and 350°C) under nitrogen atmosphere, the prepared CdSe thin films were then inserted in a 30 cm long Pyrex cylinder which was then placed inside the tube furnace. The annealing process was continued for one hour at the constant desired temperature, Figure (2.4).

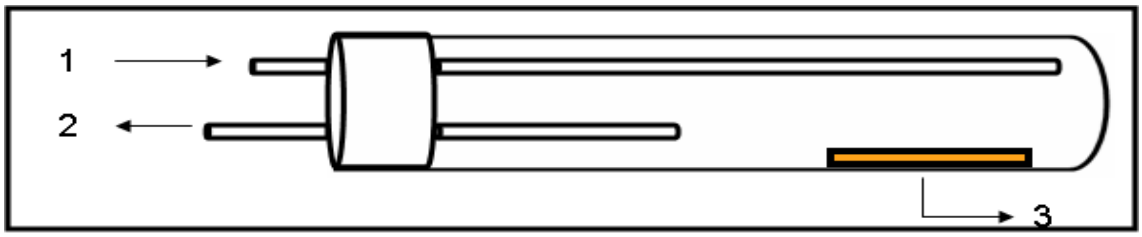

Figure (2.4): The annealing system, 1) nitrogen input, 2) nitrogen output, 3) CdSe thin film, [9].

2.6.2 Cooling rate control

(a) Fast cooling (quenching)

After annealing process, the Pyrex cylinder containing the CdSe thin film was taken out from the furnace and left to cool under N_2 atmosphere to room temperature within 15 minutes.

(b) Slow cooling

After annealing process, the furnace was shut down and left to cool slowly under N_2 atmosphere to room temperature. The slow cooling needed two hours or less with average cooling rate equal to 2°C/min.

2.6.3 Coating with MP-Sil matrix

CdSe thin film was covered by immersing it in the MP-Sil matrix for 5 seconds. The organic solvent mixture (dichloromethane/methanol) was then allowed to evaporate off, leaving a transparent thin layer of MP-Sil matrix on the surface of CdSe thin film. The coated CdSe thin film was annealed 120 ºC under N_2 atmosphere for 15 minutes, and then allowed to rapidly cool to room temperature under N_2 atmosphere.

2.7 Film characterization

2.7.1 Electronic absorption spectra

The electronic absorption spectra for the prepared CdSe thin films were investigated on a Shimadzu UV-1601 spectrometer at room temperature. The wavelength range was 400-800 nm.

2.7.2 Fluorescence spectrometry

To determine the band gap value, the emission fluorescence spectra (for the prepared CdSe thin films) were measured on a Perkin-Elmer LS 50 luminescence spectrometer. The excitation wavelength was 385 nm. To remove the undesired reflected shorter wavelengths; a cut- off filter (500 nm and shorter wavelength) were used.

2.7.3 X-ray diffraction (XRD)

Crystal structure and crystallinity of CdSe thin film were investigated by PANalytical X'Pert PRO X-ray diffractometer (XRD), where CuKα rays were used. XRD measurements were kindly conducted in Industrial Co., LTD. #1239-5, Jeongwang-Dong, Shiheung-Si, Kyonggi-Do, 429-913, South Korea.

2.8 PEC cell

The PEC cell consisted of CdSe thin film electrode (as working electrode), a platinum counter electrode connected to internal reference electrode, all in redox couple solution. Poly sulfide NaOH/S^{-2} /S_x^{-2} system Na_2S (0.10

M), NaOH (0.10 M), S (0.10 M) was used as a redox couple for all PEC measurements. High purity nitrogen (99.9999%) was bubbled through the solution for at least 5 minutes to remove the dissolved oxygen before each experiment, and was then kept bubbling over the solution during each experiment to avoid electrolyte oxidation, Figure (2.5).

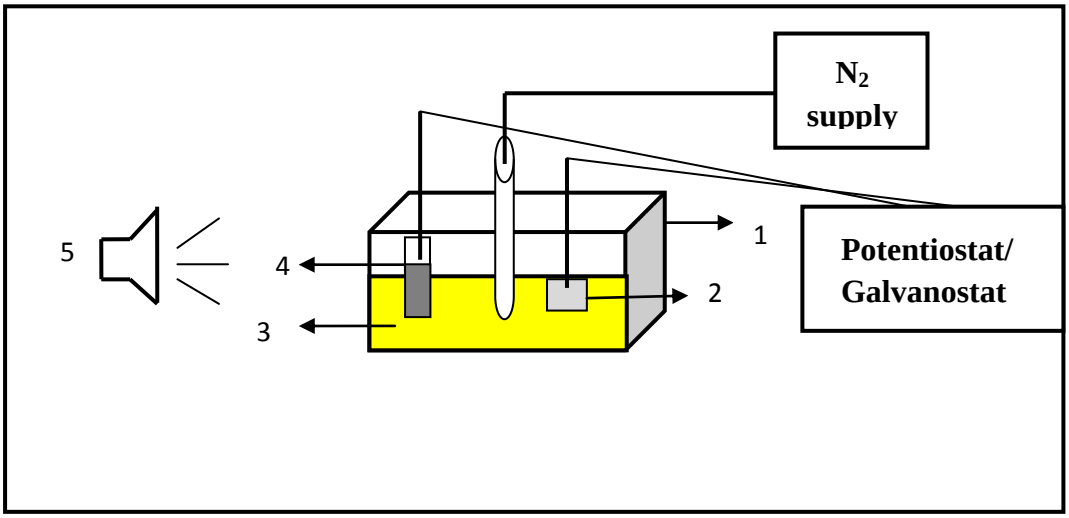

Figure (2.5): Schematic diagram for PEC measurement.1) rectangular cell, 2) platinum counter electrode, 3) poly sulfide NaOH/S^{-2} /S_x^{-2} redox couple solution 4) CdSe working electrode, 5) light source.

The internal reference was calibrated vs. AgCl/Ag reference, as shown in Figure (2.6).

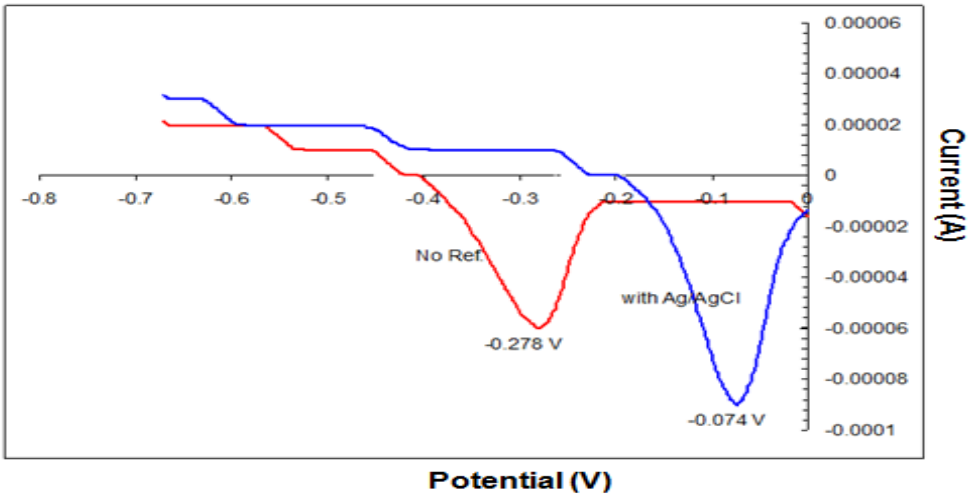

Figure (2.6): Reduction of copper ion in HCl electrolyte solution, on glassy carbon electrode [28].

From the Figure, the internal reference electrode showed 0.204 V more negative than AgCl/Ag reference. This means that the internal reference of potntiostat is equivalent to that of NHE [28].

A 50 Watt halogen spot solar simulator lamp was used for illumination. The lamp was placed at a defined distance from the working electrode. It has an intense converge of wide spectral range between 450-800 nm with high stability. The illumination intensity on the electrode was measured by a LX-102 light meter to be 34900 lux (equivalent to 0.00511 $W.cm^{-2}$).

2.9 Plots of current density versus potential

To measure the current density versus voltage (*J-V*) plots. A computer controlled Princeton Applied Research (PAR) Model 263A Potential/ Galvanostat was used in PEC measurements. For photocurrent experiments, the 50 Watt halogen spot lamp was used. In dark current experiments a thick blanket cover was used to achieve a complete darkness.

All experiments were done at room temperature, under N_2 atmosphere, using Poly sulfide $NaOH/S^{-2}/S_x^{-2}$ system Na_2S(0.10 M), NaOH (0.10 M), S (0.10 M) as redox solution.

Chapter Three

Results

CdSe thin films were prepared using ECD, CBD and ECD/CBD techniques. Various parameters were studied here for both ECD- and ECD/CBD- CdSe thin films including: deposition times, annealing temperatures, cooling rate and covering the films with MnP-Sil matrix. Enhancement of CBD-CdSe thin films was investigated in an earlier study [18]. Comparison between ECD-CdSe thin films, CBD-CdSe thin films and ECD/CBD-CdSe thin films was made.

Part I

Electrochemically deposited (ECD) thin film electrodes

CdSe thin films prepared by electrochemical deposition method were studied under different conditions by using different techniques including PL emission spectra, electronic absorption spectra and XRD. PEC studies including dark J-V plots, photo J-V plots, conversion efficiency, value of short-circuit current and fill-factor (FF) were performed.

3.1 ECD thin film characteristics

Characteristics of CdSe films were investigated by using different techniques as shown below.

3.1.1 XRD measurements for CdSe thin film electrodes

The crystallite size and structural phase of the ECD-CdSe nanocrystalline thin films have been determined using XRD measurements. CdSe may exist in either cubic (zinc-blende type) or hexagonal (wurtzite type) structure or sometimes a mixture of both phases [41]. XRD measurements were obtained for ECD-CdSe thin films with different parameters including annealing temperature, cooling rate and covering the films with MnP-Sil matrix.

3.1.1.1 Effect of annealing on CdSe thin film electrodes

XRD measurements were obtained for naked CdSe film electrodes before and after annealing at 350 ºC and slow cooling. XRD data showed that both annealed and non-annealed films exhibited crystallinity. The average particle size for non- annealed ECD-CdSe was ~ 3.69 nm, Figure (3.1). The annealed film particle size was ~ 4.38 nm. Both films are in the cubic phase with the zinc-blende type of structure. This was based on comparison with earlier reports [35, 38-40]. Table (3.1) shows the positions of observed peaks.

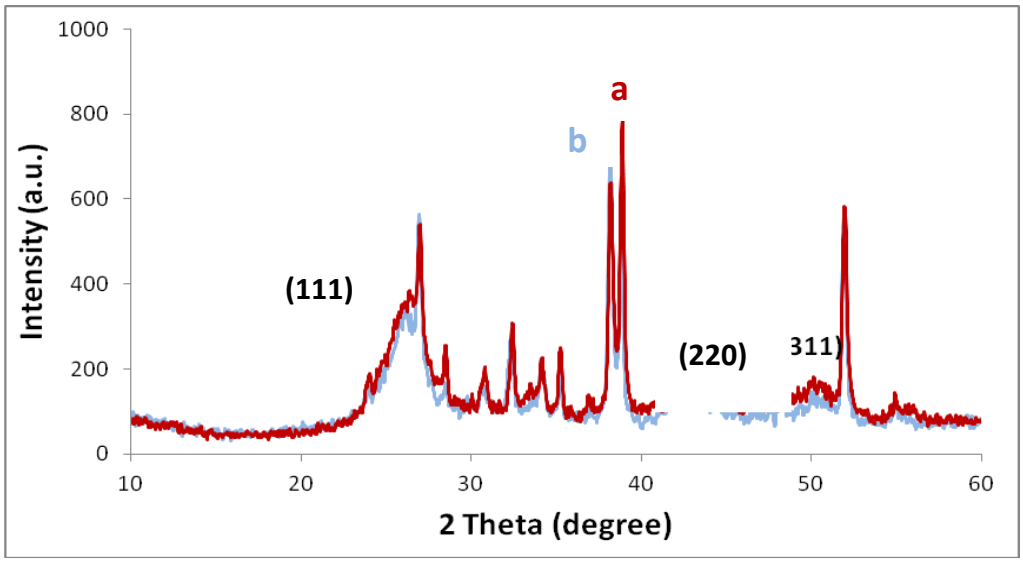

Figure (3.1): XRD patterns measured for naked ECD-CdSe thin film a) non-annealed, b) after annealing at 350 ºC and slowly cooled.

Table (3.1): XRD results for annealed and non-annealed ECD-CdSe film electrodes.

Position of observed peak (2 theta)		Plane	Reference	Particle size (nm)
Non-annealed	**26.34**	**C(111)**	**[38]**	**3.69**
	26.90	FTO subs	**[42]**	
	34.09	FTO subs	**[42]**	
	38.16	FTO subs	**[42]**	
	38.80	FTO subs	**[42]**	
	42.90	**C(220)**	**[38]**	
	50.32	**C(311)**	**[38]**	
	51.80	FTO subs	**[42]**	
Annealed	**26.40**	**C(111)**	**[38]**	**4.38**
	26.90	FTO subs	**[42]**	
	34.07	FTO subs	**[42]**	
	38.12	FTO subs	**[42]**	
	42.81	**C(220)**	**[38]**	
	50.14	**C(311)**	**[38]**	
	51.85	FTO subs	**[42]**	

3.1.1.2 Effect of annealing temperature on CdSe thin film electrodes

XRD measurements were obtained for ECD- CdSe thin film electrodes. The films were annealed at different temperatures (150 and 350 ºC) and slowly cooled. XRD data showed that both films exhibited crystallinity. The average particle size for ECD-CdSe film annealed at 150ºC was~4.47 nm, Figure (3.2). The particle size for the film annealed at 350 ºC was~3.51 nm. Both films are in the cubic phase with the zinc-blende type of structure. This was based on comparison with earlier reports [35, 38-40]. Table (3.2) shows the positions of observed peaks.

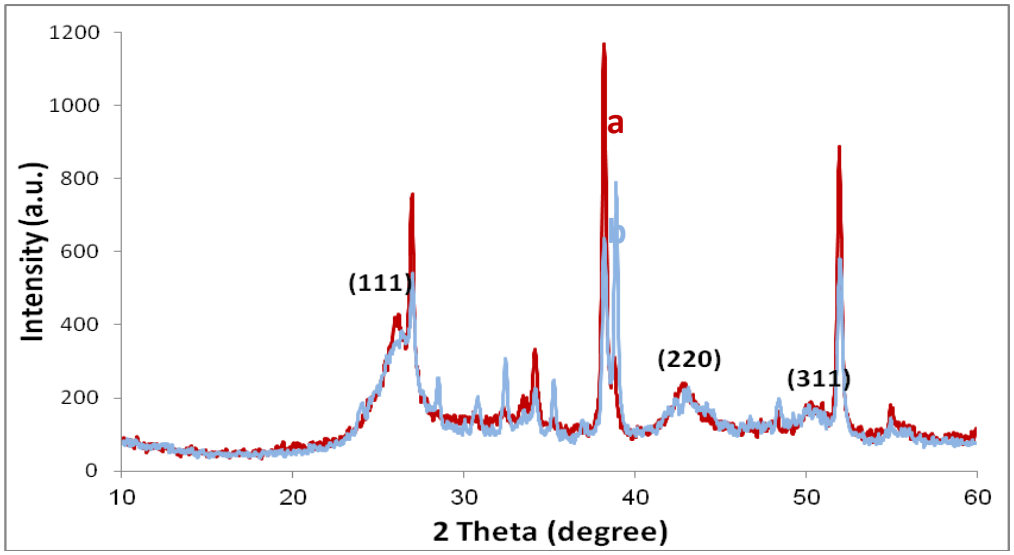

Figure (3.2): XRD patterns measured for naked ECD-CdSe thin film a) annealed at 150ºC and slowly cooled, b) annealed at 350 ºC and slowly cooled.

Table (3.2): XRD results for ECD-CdSe film electrodes annealed at different temperatures (150 and 350 ºC).

Position of observed peak (2 theta)		Plane	Reference	particle size(nm)
Annealed at 150 °C	**26.34**	**C(111)**	**[38]**	**4.47**
	26.90	FTO subs	[42]	
	34.08	FTO subs	[42]	
	38.12	FTO subs	[42]	
	38.23	FTO subs	[42]	
	42.88	**C(220)**	**[38]**	
	50.18	**C(311)**	**[38]**	
	51.85	FTO subs	[42]	
Annealed at 350 °C	**26.34**	**C(111)**	**[38]**	**3.15**
	26.90	FTO subs	[42]	
	34.07	FTO subs	[42]	
	38.12	FTO subs	[42]	
	42.81	**C(220)**	**[38]**	
	50.14	**C(311)**	**[38]**	
	51.85	FTO subs	[42]	

3.1.1.3 Effect of cooling rate on CdSe thin film electrodes

XRD measurements were obtained for slowly cooled and quenched ECD-CdSe thin film electrodes. XRD data showed that both films exhibited crystallinity. The average particle size for slowly cooled ECD-CdSe film was ~ 3.51 nm, Figure (3.3). The particle size for the quenched film was ~ 4.38 nm. Both films are in the cubic phase with the zinc-blende type of structure. This was based on comparison with earlier reports [35, 38-40]. Table (3.3) shows the positions of observed peaks.

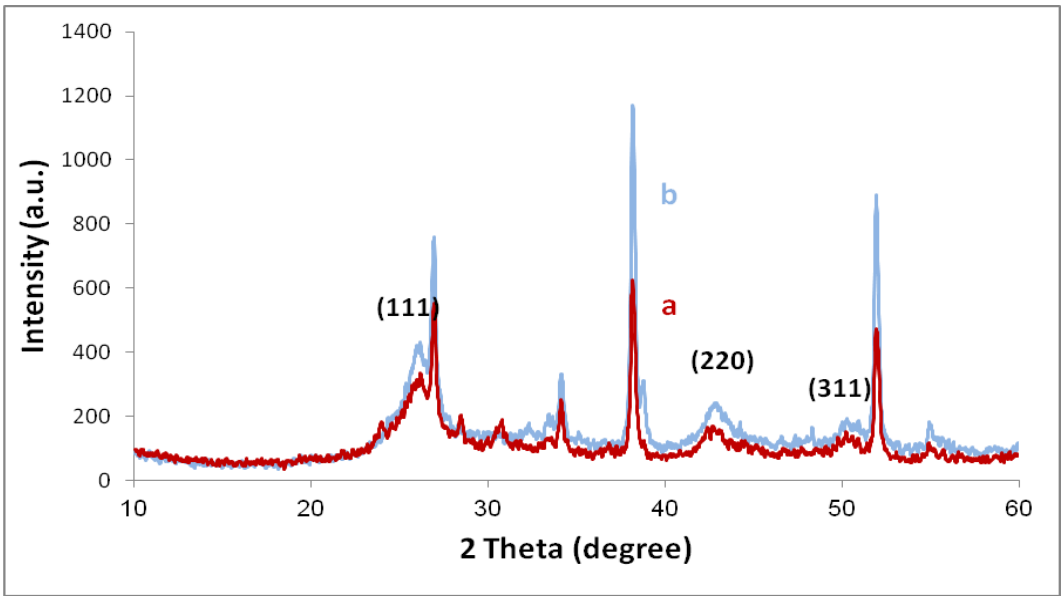

Figure (3.3): XRD patterns measured for naked ECD-CdSe thin film annealed at 350ºC, a) slowly cooled, b) quenched.

Table (3.3): XRD results for slowly cooled and quenched ECD-CdSe film electrodes (annealed at 350 ºC).

Position of observed peak (2 theta)		Plane	Reference	Particle size(nm)
Slowly cooled	**26.40**	**C(111)**	**[38]**	**3.51**
	26.96	FTO subs	[42]	
	34.07	FTO subs	[42]	
	38.12	FTO subs	[42]	
	42.81	**C(220)**	**[38]**	
	50.14	**C(311)**	**[38]**	
	51.85	**FTO subs**	**[30]**	
Quenched	**26.33**	**C(111)**	**[38]**	**4.38**
	26.91	FTO subs	[42]	
	34.07	FTO subs	[42]	
	38.11	FTO subs	[42]	
	42.66	**C(220)**	**[35]**	
	50.46	**C(311)**	**[35]**	
	51.88	FTO subs	[42]	

3.1.1.4 Effect of covering with MP-Sil matrix on CdSe thin film electrodes.

XRD measurements were obtained for naked and coated non-annealed ECD- CdSe thin film electrodes. XRD data showed that both films exhibited crystallinity. Both films are in the cubic phase with the zinc-blende type of structure. The average particle size for naked ECD-CdSe film was~3.69 nm, Figure (3.4). The particle size for the coated film was~ 3.31nm. This was based on comparison with earlier reports (35, 38-40). Table (3.4) shows the positions of observed peaks.

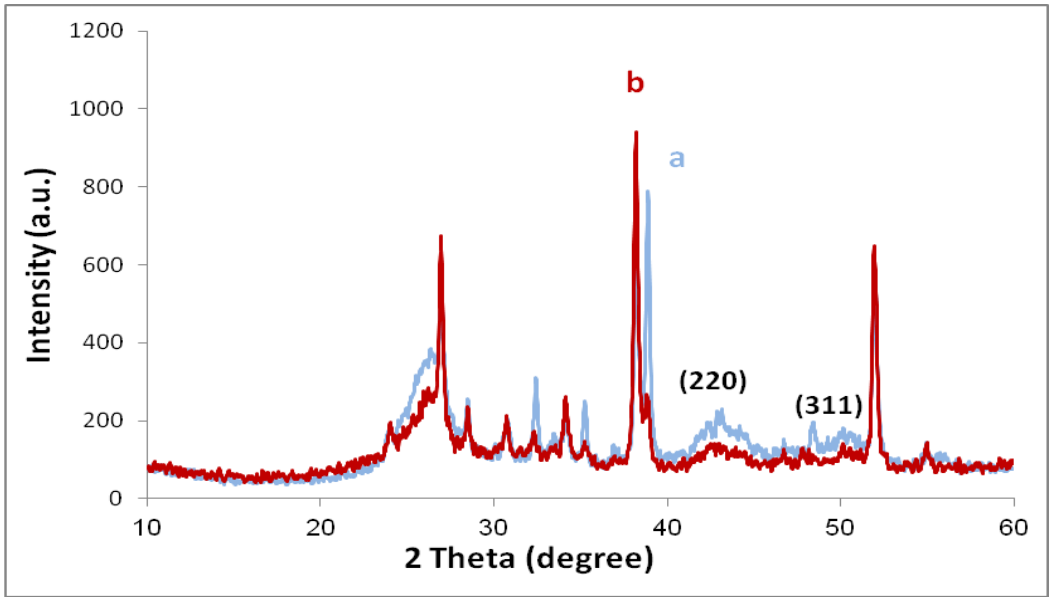

Figure (3.4): XRD patterns measured for non-annealed ECD-CdSe thin film non-annealed, a) naked, b) coated.

Table (3.4): XRD results for non-annealed naked and coated ECD-CdSe film electrodes.

Position of observed peak (2 theta)		Plane	Reference	Particle size(nm)
Naked	**26.34**	**C(111)**	[38]	**3.69**
	26.90	FTO subs	[42]	
	34.09	FTO subs	[42]	
	38.16	FTO subs	[42]	
	38.80	FTO subs	[42]	
	42.90	**C(220)**	[38]	
	50.32	**C(311)**	[38]	
	51.80	FTO subs	[30]	
Coated	**26.64**	**C(111)**	[38]	**3.31**
	34.18	FTO subs	[42]	
	38.16	FTO subs	[42]	
	42.86	**C(220)**	**[38]**	
	50.10	FTO subs	[42]	
	51.90	**C(311)**	[38]	

3.1.2 Photoluminescence spectra for CdSe thin film electrodes

Photoluminescence spectra were investigated for ECD-CdSe thin films under controlled parameters including deposition times, annealing temperatures, cooling rate and covering the films with MnP-Sil matrix.

3.1.2.1 Effect of deposition time on CdSe thin film electrodes

The effect of deposition time (15, 30, and 45 min) on the photoluminescence spectra of non- annealed CdSe thin films were studied, Figure (3.5). The systems were excited at wavelength 385nm. The Figure shows many weak peaks, the highest intensity peaks appeared at wavelength range of 630-530 nm with a band gap range (1.9-2.3) eV, in agreement with the band gap range of CdSe in literature [35]. The film

prepared in 15 min shows higher intensity than the other two films. Therefore it was used in all our study.

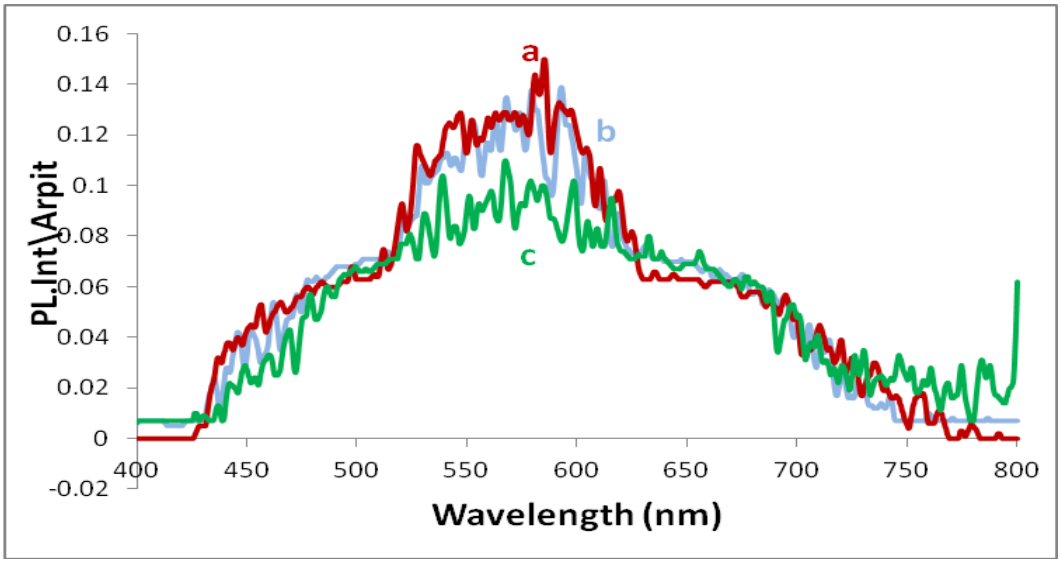

Figure (3.5): Photo-luminescence spectra for non-annealed ECD-CdSe thin film electrodes prepared in different deposition times: a) 15 min, b) 30 min, c) 45 min.

3.1.1.2 Effect of annealing temperature on CdSe thin film electrodes

The effect of annealing temperature (150, 250 and 350ºC) on the prepared on the photoluminescence spectra of the prepared CdSe thin films were studied, Figure (3.6). The systems were excited at wavelength 385nm. The Figure shows many weak peaks, the highest intensity peaks appeared at wavelength range of 630-530 nm with a band gap range (1.9-2.3) eV, which is consistent with the band gap range of CdSe in literature [22, 35]. The non –annealed film shows slightly higher intensity than the film annealed at 150 ºC, while the film annealed at 150 ºC shows higher intensity than the other counterparts annealed at 250 and 350 ºC.

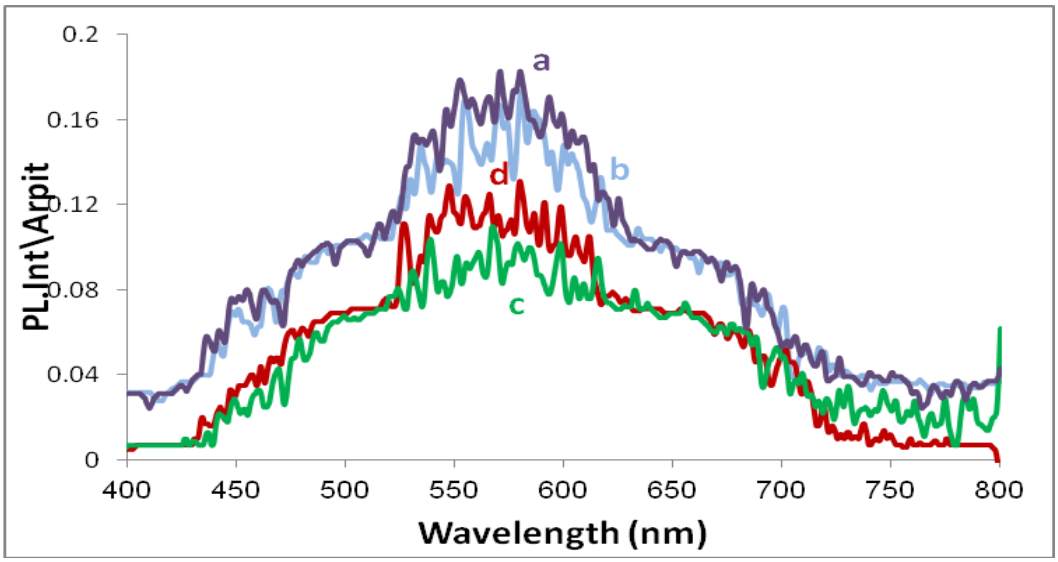

Figure (3.6): Photo-luminescence spectra for ECD-CdSe thin film electrodes prepared in 15 min, a) non-annealed, b) annealed at 150ºC, c) annealed at 250ºC , annealed at 350ºC.

3.1.2.3 Effect of cooling rate on CdSe thin film electrodes

The effect of cooling rate (fast and slow cooling) on the photoluminescence spectra of the pre annealed ECD -CdSe thin film electrodes, annealed at different temperatures (150, 250 and 350ºC), was investigated.

3.1.2.3.1 CdSe thin films annealed at 150 ºC

The effect of cooling rate (fast and slow cooling) on the photoluminescence spectra of the CdSe thin films annealed at 150 ºC under nitrogen for 1 hour was studied, Figure (3.7). The systems were excited at wavelength 385 nm. The Figure shows many weak peaks, the highest intensity peaks appeared at wavelength range of 620-540 nm with a band gap range (2.0-2.3) eV, which is consistent with the band gap range of CdSe in literature [22, 35].

The quenched film shows slightly higher intensity than the slowly cooled one.

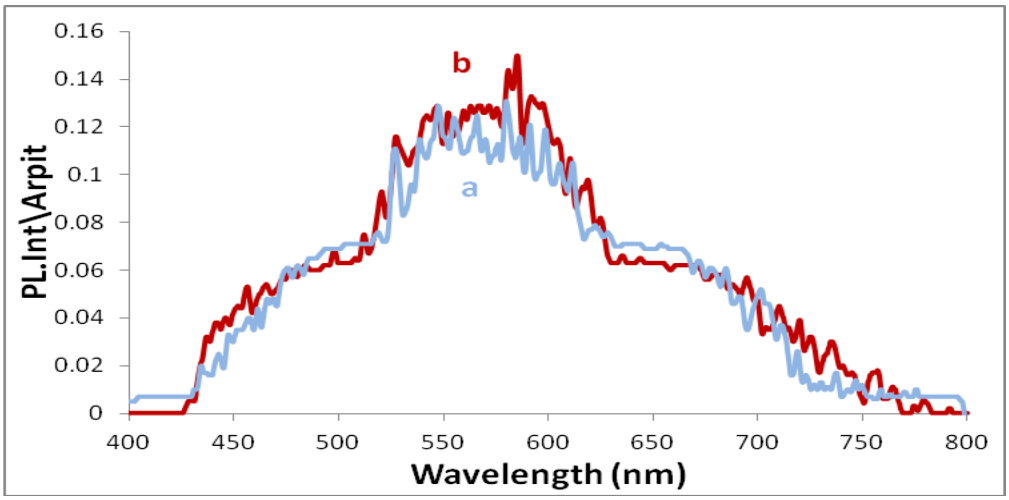

Figure (3.7): Photo-luminescence spectra for ECD-CdSe thin film electrodes prepared in 15 min and annealed at 150ºC, a) slowly cooled, b) quenched.

3.1.2.3.2 CdSe thin films annealed at 250 ºC

The effect of cooling rate (fast and slow cooling) on the photoluminescence spectra of the CdSe thin films annealed at 250 ºC under nitrogen for 1 hour was studied, Figure (3.8). The systems were excited at wavelength 385nm. The Figure shows many weak peaks, the highest intensity peaks appeared at wavelength range of 620-540 nm with a band gap range (2.0-2.2) eV, which is consistent with the band gap range of CdSe in literature [22, 35]. The peaks intensity is close to each other for both quenched and slowly cooled films.

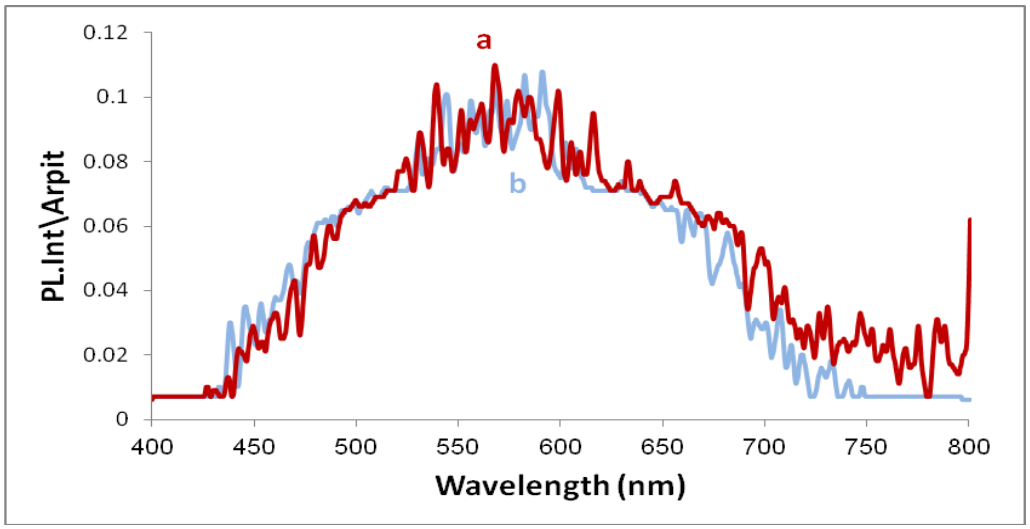

Figure (3.8): Photo-luminescence spectra for ECD-CdSe thin film electrodes prepared in 15 min and annealed at 250ºC, a) slowly cooled b) quenched.

3.1.2.3.3 CdSe thin films annealed at 350 ºC

The effect of cooling rate (fast and slow cooling) on the photoluminescence spectra of the CdSe thin films annealed at 350 ºC under nitrogen for 1 hour was studied, Figure (3.9). The systems were excited at wavelength 385nm. The Figure shows many weak peaks, the highest intensity peaks appeared at wavelength range of 600-550 nm with a band gap range (2.06-2.25) eV, which is consistent with the band gap range of CdSe in literature [22, 35]. The quenched film shows higher intensity than the slowly cooled one.

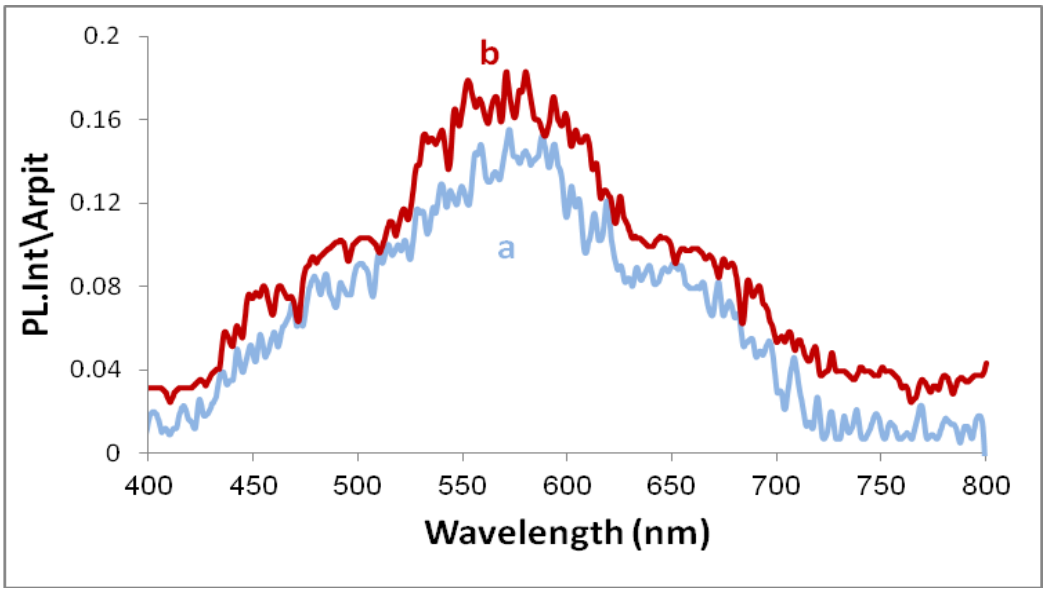

Figure (3.9): Photo-luminescence spectra for ECD-CdSe thin film electrodes prepared in 15 min and annealed at 350ºC, a) slowly cooled, b) quenched.

3.1.2.4 Effect of covering with MP-Sil matrix on CdSe thin film electrodes

The effect of covering with MP-Sil matrix on the photoluminescence spectra of the non- annealed CdSe thin films was studied, Figure (3.10). The systems were excited at wavelength 385 nm. The Figure shows many weak peaks, the highest intensity peaks appeared at wavelength range of 590-550 nm with a band gap range (2.10-2.25) eV, which is consistent with the band gap range of CdSe in literature [22, 35]. The coated film shows higher intensity than the naked one.

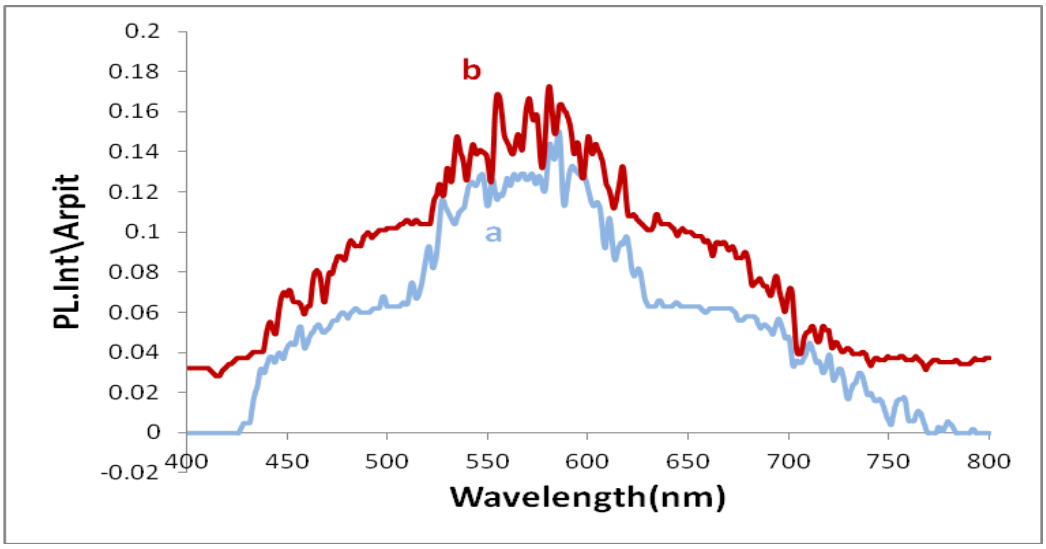

Figure (3.10): Photo-luminescence spectra for non-annealed ECD-CdSe thin film electrodes prepared in 15 min, a) naked, b) coated.

3.1.3 Electronic absorption spectra for CdSe thin film electrodes

Electronic absorption spectra were measured for CdSe thin films with changing different parameters including deposition times, annealing temperatures, cooling rate and covering the films with MnP-Sil matrix. It should be noted that the absorption spectra were inconclusive and difficult to analyze. This is due to ECD-CdSe films, being too thin.

3.1.3.1 Effect of deposition time on CdSe thin film electrodes

Electronic absorption spectra were measured for CdSe thin films deposited in different deposition times (15, 30, and 45 min), Figure (3.11). A relatively obvious absorption was observed for the film deposited in 15 min which is consistent with PL result. On the other hand, the absorption spectra for the films deposited for longer time were difficult to analyze and conclude. The film deposited in 15 min was used in all other preparations and further modifications in this study.

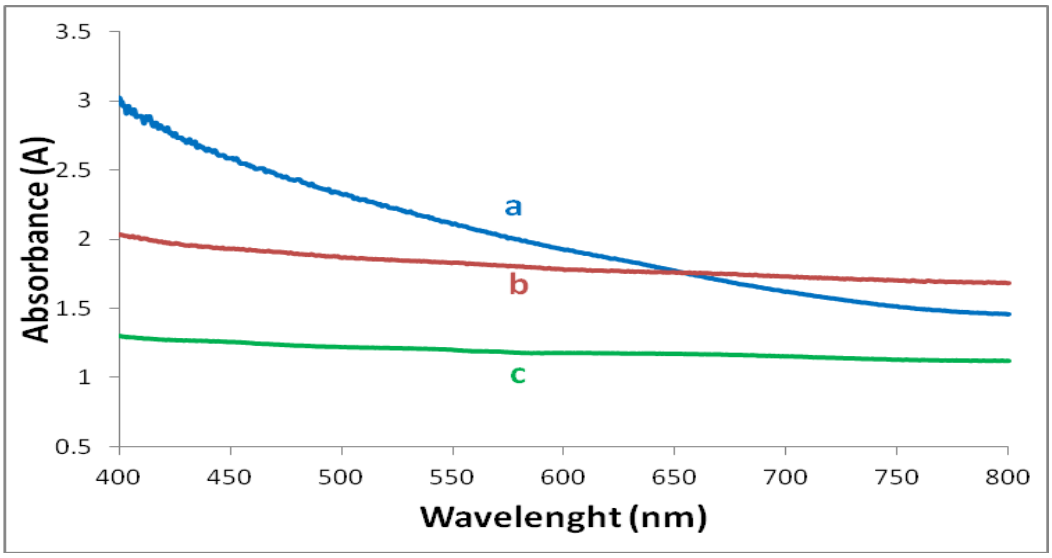

Figure (3.11): Electronic absorption spectra for ECD-CdSe thin films deposited in a) 15 min, b) 30 min, c) 45 min.

3.1.3.2 Effect of annealing temperature on CdSe thin film electrodes

Electronic absorption spectra were measured for CdSe thin films annealed at different temperatures (150, 250, and 350 ºC) under nitrogen for 1 hour,

Figure (3.12). A relatively obvious absorption spectra were observed for both the non-annealed film and the film annealed at 150 ºC. On the other hand, the absorption spectra for the films annealed at 250 and 350 ºC were inconclusive and difficult to analyze. This is consistent with PL result. The film annealed at 150 ºC showed some red shift from 570 nm (non-annealed) to 600 nm, with a decreasing in energy band gap value from 2.17 to 2.06 eV.

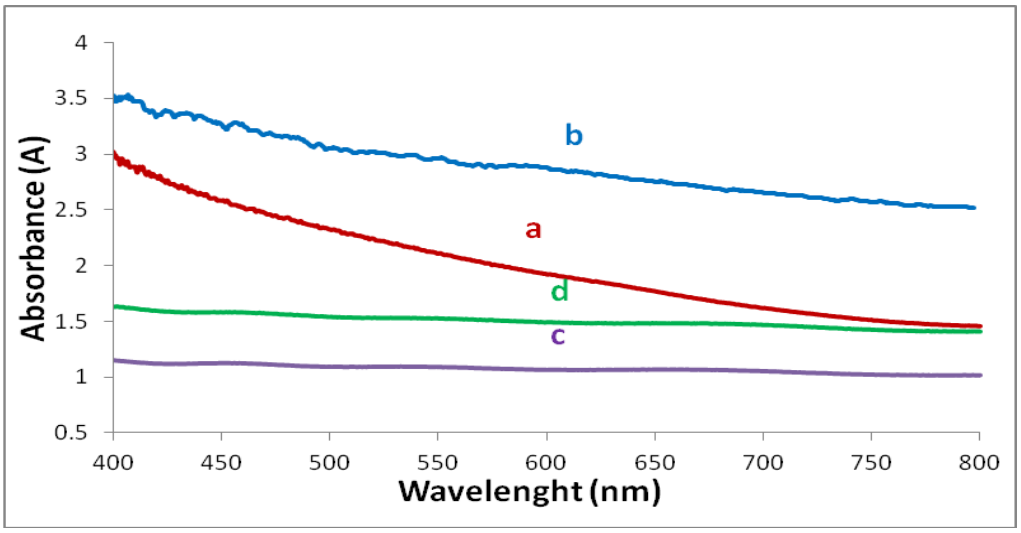

Figure (3.12): Electronic absorption spectra for ECD- CdSe thin films prepared in 15 min a) non-annealed, b) annealed at 150ºC, c) annealed at 250ºC, d) annealed at 350ºC.

3.1.3.3 Effect of cooling rate on CdSe thin film electrodes

The effect of cooling rate (fast and slow cooling) on the electronic absorption spectra of the pre annealed ECD -CdSe thin film electrodes at different annealing temperatures (150, 250 and 350ºC) under nitrogen for one hour was investigated. Only rough conclusion could be made based on these spectra.

3.1.3.3.1 CdSe thin films annealed at 150 ºC

Electronic absorption spectra were measured for slowly cooled and quenched CdSe thin films annealed at 150ºC**,** Figure (3.13). Despite the absorption spectra were difficult to analyze, the quenched film showed slightly clearer absorption than the slowly cooled one, which is consistent with the PL spectra result.

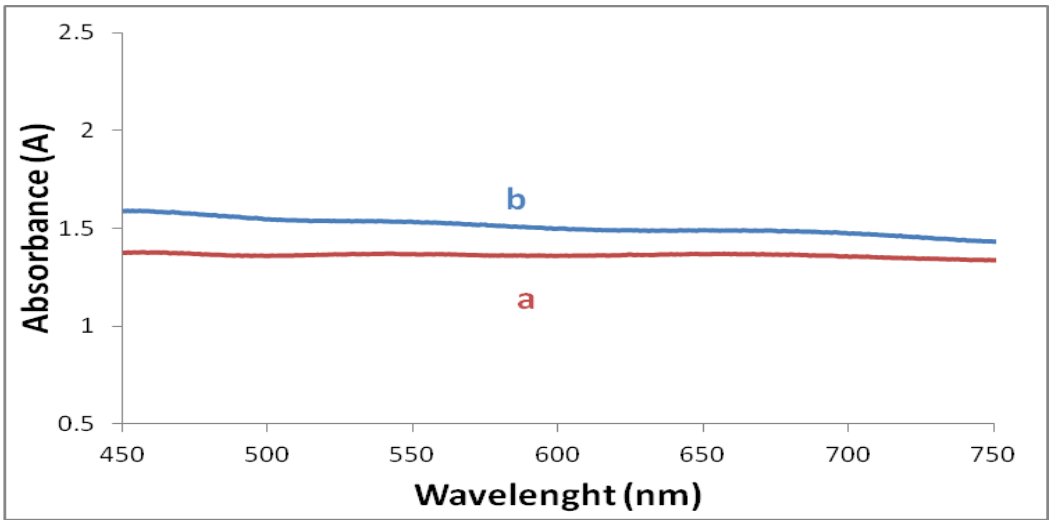

Figure (3.13): Electronic absorption spectra for ECD- CdSe thin films prepared in 15 min and annealed at 150 ºC, a) slowly cooled b) quenched.

3.1.3.3.2 CdSe thin films annealed at 250 ºC

Electronic absorption spectra were measured for slowly cooled and quenched CdSe thin films annealed at 250ºC**,** Figure (3. 14). Although the absorption spectra were difficult to analyze, the quenched film showed slightly clearer absorption than the slowly cooled one, which is consistent with the PL spectra result.

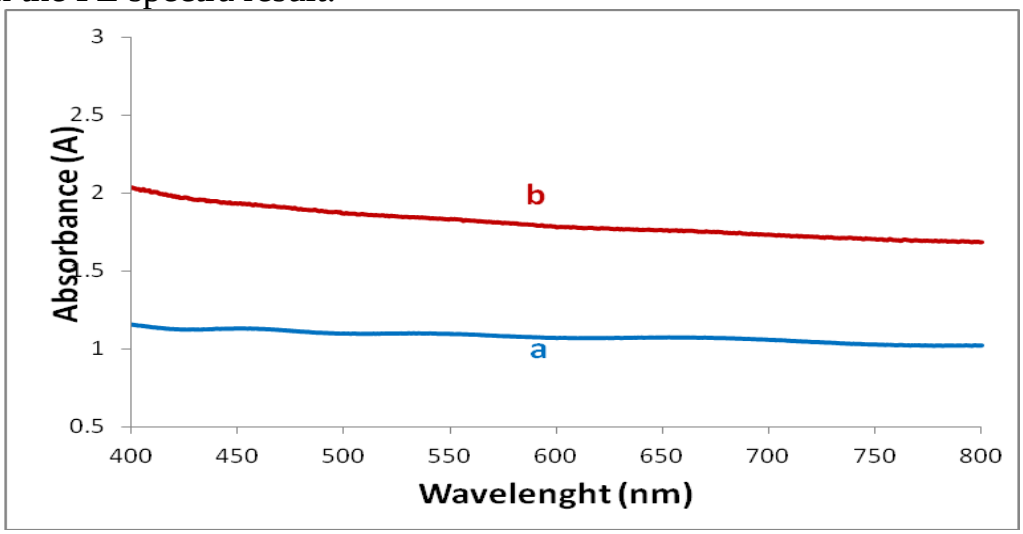

Figure (3.14): Electronic absorption spectra for the CdSe thin films prepared in 15 min and annealed at 250ºC a) slowly cooled, b) quenched.

3.1.3.3.3 CdSe thin films annealed at 350 ºC

Electronic absorption spectra were measured for slowly cooled and quenched CdSe thin films which annealed at 350ºC**,** Figure (3.15). A relatively obvious absorption was observed for the quenched film which is consistent with the PL spectra result. The slowly cooled film absorption spectra were difficult to analyze, this is due to ECD-CdSe films being too thin.

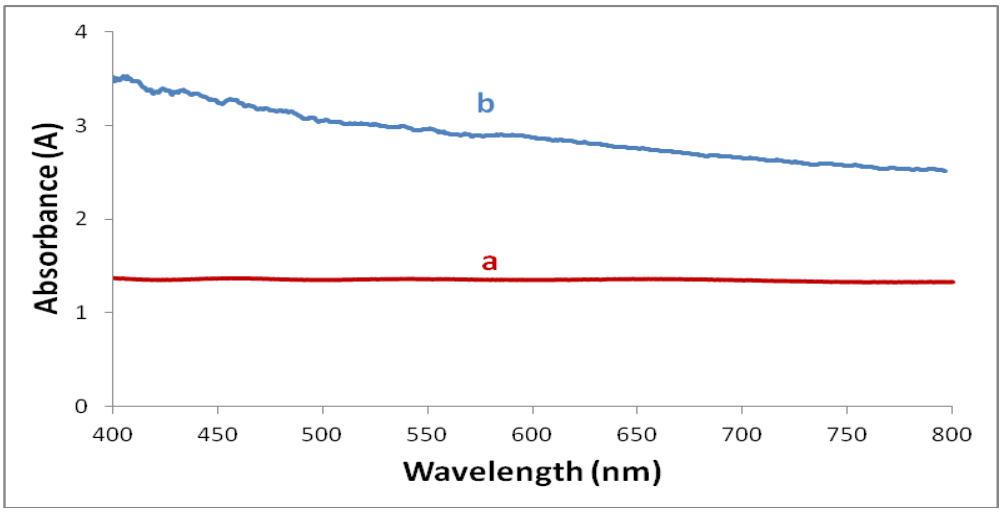

Figure (3.15): Electronic absorption spectra for the CdSe thin films prepared in 15 min and annealed at 350ºC a) slowly cooled, b) quenched.

3.1.3.4 Effect of covering with MP-Sil matrix on CdSe thin film electrode

The effect of covering with MP-Sil matrix on the electronic absorption spectra of the non- annealed CdSe thin films was studied**,** Figure (3. 16). Slightly clearer absorption was observed for the coated film which is consistent with the PL spectra result.

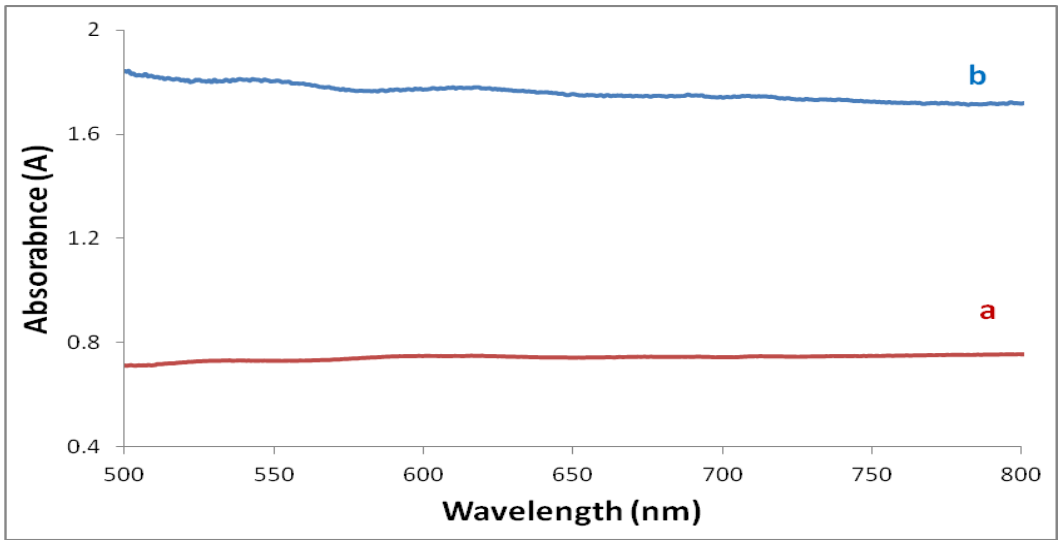

Figure (3.16): Electronic absorption spectra for non-annealed ECD- CdSe thin films prepared in 15 min a) naked, b) coated.

3.2 ECD thin film PEC studies

PEC characteristics, including dark J-V plots, photo J-V plots, value of short-circuit current and efficiency, were studied for ECD CdSe films in aqueous S^{2-}/S_x^{2-} redox couple at room temperature.

3.2.1 Dark *J-V* plots of CdSe thin film electrodes

Dark *J-V* plots were measured for ECD-CdSe thin film electrodes with different controlled parameters (deposition time, annealing temperature, cooling rate and covering with MP-Sil matrix). It should be noted that dark J-V plots were inconclusive in this study. This is due to current leakage in system during the experiment.

3.2.1.1 Effect of deposition time on CdSe thin film electrode

Dark *J-V* plots were measured for ECD-CdSe thin film electrodes deposited for different times, Figure (3.17). The positive dark current

occurred, due to current leakage in system during the experiment. Therefore, dark *J-V* plots don't give good indication here.

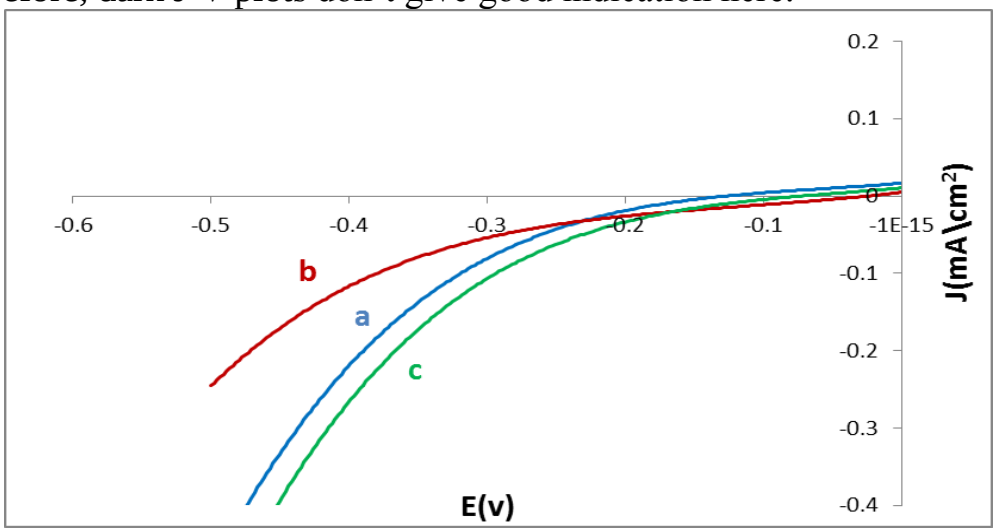

Figure (3.17): Dark *J-V* plots for ECD-CdSe thin film electrodes prepared in : *a)* 15 min, *b*) 30 min, c) 45 min. All measurements were conducted in aqueous S^{2-}/S_x^{2-} redox system at room temperature.

3.2.1.2 Effect of annealing temperature on CdSe thin film electrodes

Dark *J-V* plots were measured for ECD-CdSe thin film electrodes annealed at different temperatures, 150, 250, and 350 ºC, Figure (3.18). The positive dark current occurred, due to current leakage in system during the experiment. Therefore, dark *J-V* plots don't give good indication here.

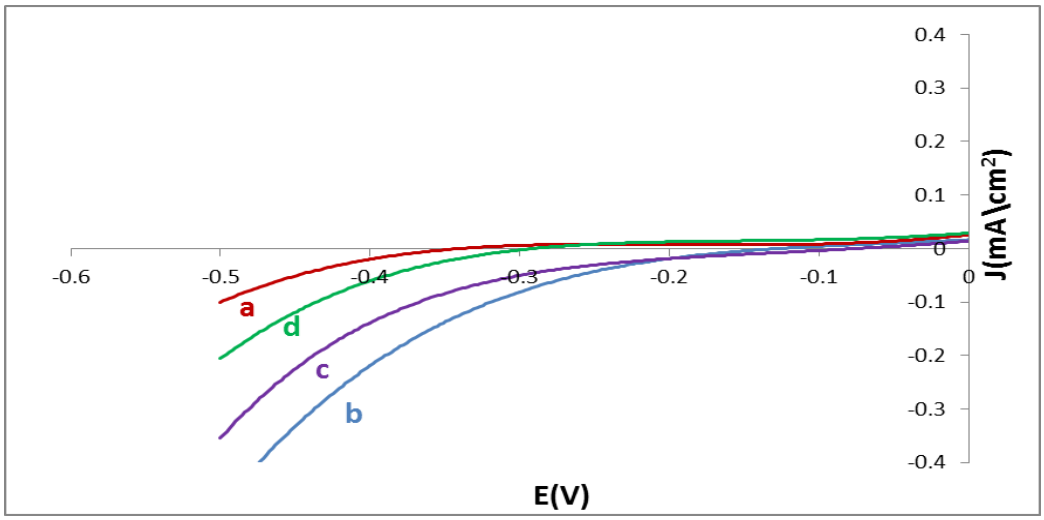

Figure (3.18): Dark *J-V* plots for ECD-CdSe thin film electrodes deposited in 15 min, *a)* non-annealed, *b*) annealed at 150ºC, c) annealed at 250ºC, d) annealed at 350ºC. All measurements were conducted in aqueous S^{2-}/S_x^{2-} redox system at room temperature.

3.2.1.3 Effect of cooling rate on CdSe thin film electrodes

Dark *J-V* plots were measured for slowly cooled and quenched ECD-CdSe thin film electrode**s** annealed at different temperatures (150ºC, 250ºC, and 350ºC) under nitrogen for 1 hour.

3.2.1.3.1 CdSe thin film annealed at 150ºC

Dark *J-V* plot was measured for slowly and quickly cooled ECD-CdSe thin film electrode**s**, Figure (3.19). The positive dark current occurred, due to current leakage in system during the experiment. Therefore, dark *J-V* plots don't give good indication here.

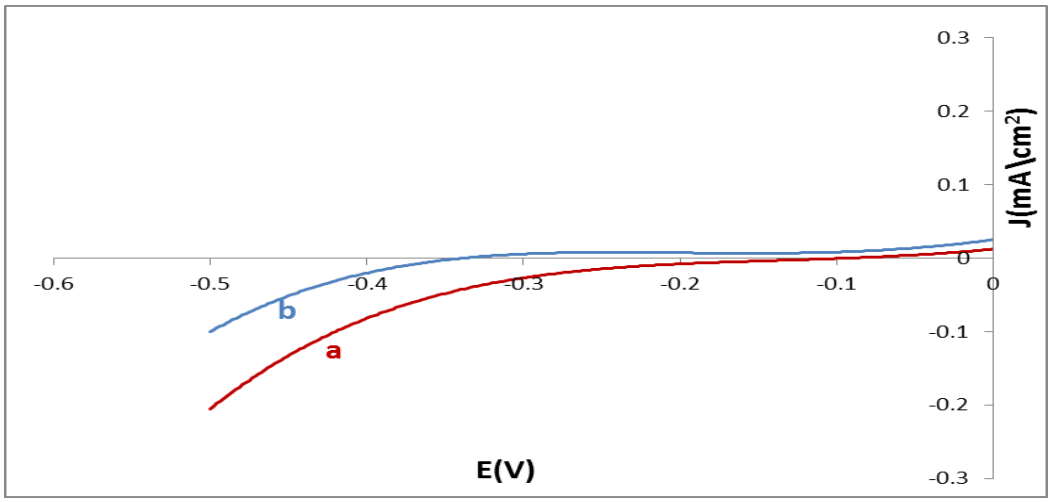

Figure (3.19): Dark *J-V* plots for ECD-CdSe thin film electrodes annealed at 150ºC, *a)* slowly cooled, *b*) quenched. All measurements were conducted in aqueous S^{2-}/S_x^{2-} redox system at room temperature.

3.2.1.3.2 CdSe thin films annealed at 250 ºC

Dark *J-V* plots were measured for slowly quickly cooled ECD-CdSe thin film electrode**s**, Figure (3.20). The positive dark current occurred, due to current leakage in system during the experiment. Therefore, dark *J-V* plots don't give a good indication in our study.

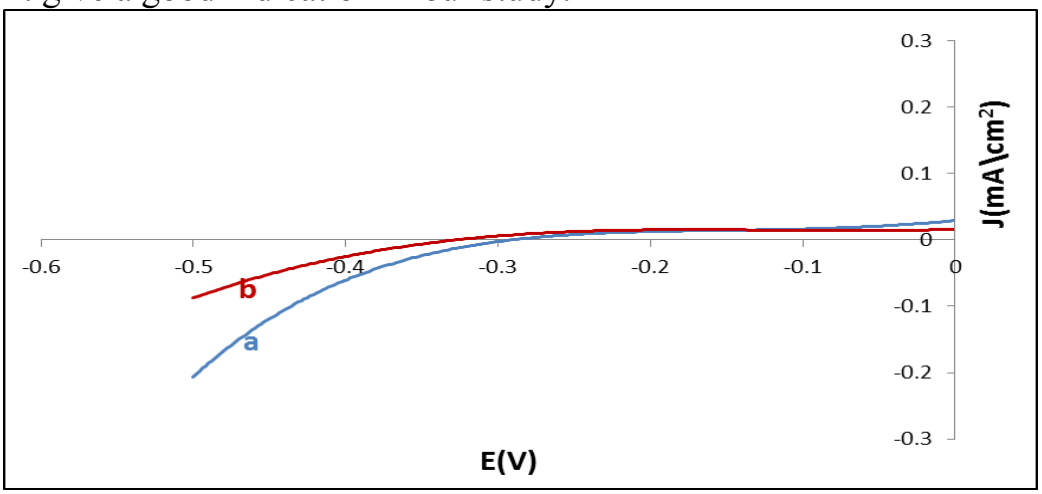

Figure (3.20): Dark *J-V* plots for ECD-CdSe thin film electrodes annealed at 250ºC prepared in 15 min, *a)* slowly cooled, *b*) quenched. All measurements were conducted in aqueous S^{2-}/S_x^{2-} redox system at room temperature**.**

3.2.1.3.3 CdSe thin films annealed at 350 ºC

Dark *J-V* plot was measured for slowly quickly cooled ECD-CdSe thin film electrodes, Figure (3.21). The positive dark current occurred, due to current leakage in system during the experiment. Therefore, dark *J-V* plots don't give good indication here.

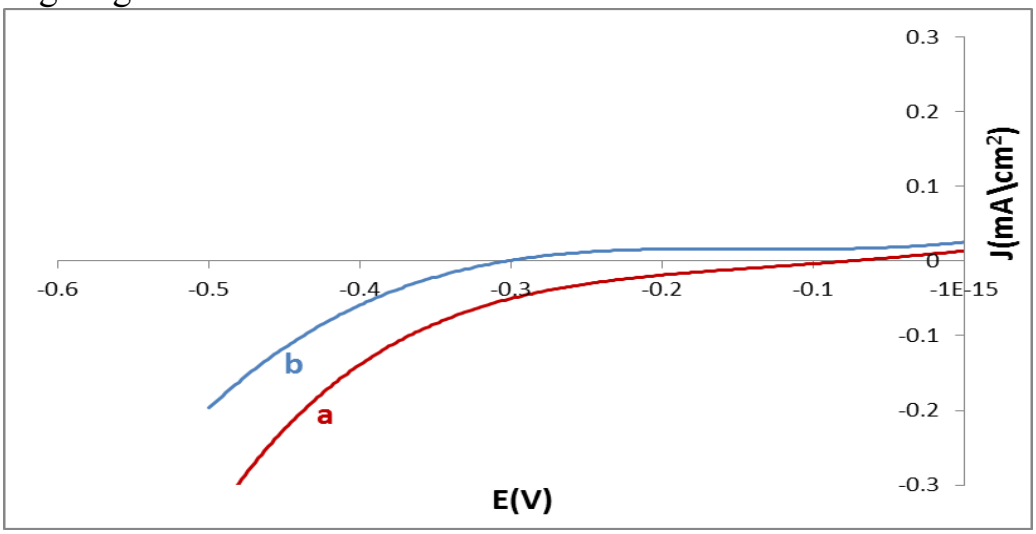

Figure (3.21): Dark *J-V* plots for ECD-CdSe thin film electrodes annealed at 350 ºC, *a)* slowly cooled, *b*) quenched. All measurements were conducted in aqueous S^{2-}/S_x^{2-} redox system at room temperature.

3.2.1.4 Effect of covering with MP-Sil matrix on CdSe thin film electrodes

Dark *J-V* plot was measured for naked and coated ECD-CdSe thin film electrodes, Figure (3.22). The positive dark current occurred, due to current leakage in the system during the experiment. Therefore, dark *J-V* plots don't give good indication here.

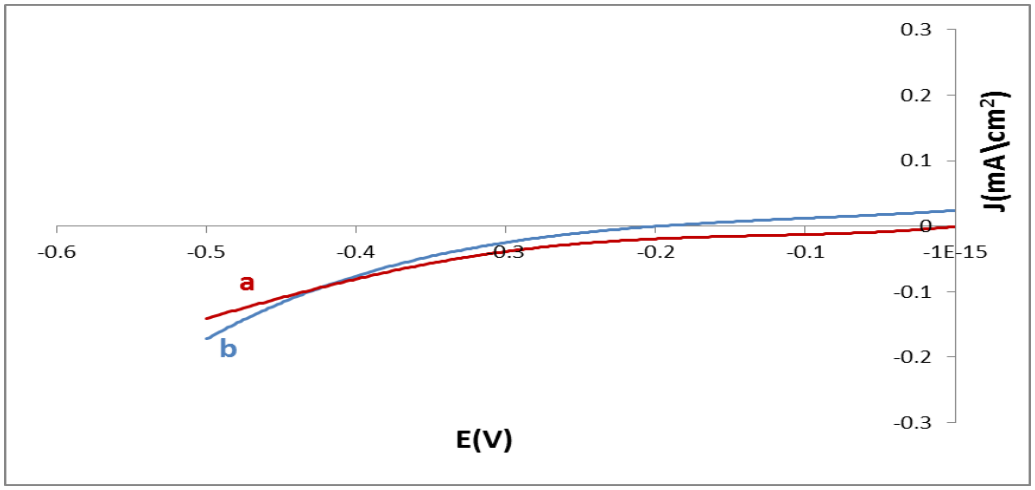

Figure (3.22): Dark *J-V* plots for non-annealed ECD-CdSe thin film electrodes prepared in 15 min, *a)* naked, *b*) coated. All measurements were conducted in aqueous S^{2-}/S_x^{2-} redox system at room temperature**.**

3.2.2 Photo *J-V* plots of CdSe thin film electrodes

Photo *J-V* plots were measured for ECD -CdSe thin film electrodes with different controlled parameters (deposition time, annealing temperature, cooling rate, and covering with MP-Sil matrix. The PEC measurements indicate that the CdSe films are n-type in electrical conduction.

3.2.2.1 Effect of deposition time on CdSe thin film electrodes

Photo *J-V* plots were measured for ECD -CdSe thin film electrodes prepared for different deposition times (15, 30 and 45 min), Figure (3. 23). The results of the Figure are summarized in Table (3.5).

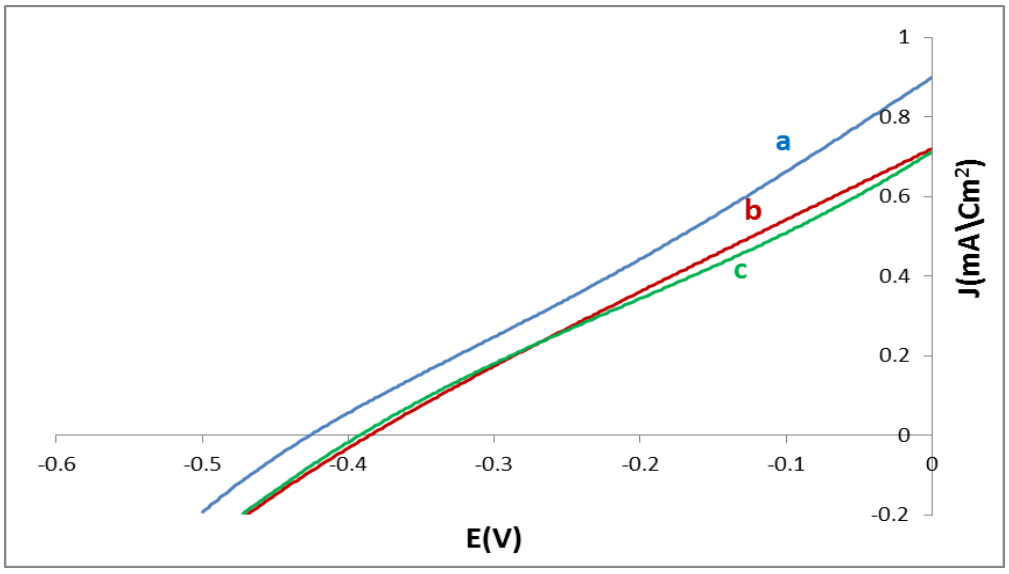

Figure (3.23): Photo J-V plots for ECD -CdSe thin film electrodes at different deposition time, a) 15 min, b) 30 min, c) 45 min. All measurements were conducted in aqueous S^{2-}/S_x^{2-} redox system at room temperature.

Table (3.5): Effect of deposition times on PEC characteristics of ECD-CdSe thin film electrodes.

sample	description	*Voc* (V)	*Jsc* (A/cm^2)	[a] η %	[b] *FF*%
a	15 min	-0.45	0.94×10^{-3}	1.72	20.08
b	30 min	-0.39	0.77×10^{-3}	0.95	25.60
c	45 min	-0.38	0.69×10^{-3}	0.74	25.93

[a] η (%) = [(maximum observed power density)/(reach-in power density)]×100%.

[b] FF = [(maximum observed power density)/ $J_{sc} \times V_{oc}$]×100%.

Voc values for the films deposited in 30, and 45 min were close to each other, on the other hand, the film deposited for 15 min showed the highest *Voc* and *Jsc* values, and gave the highest percent conversion efficiency (η % ~ 1.72) than the other two films, in agreement with the PL and the electronic absorption spectra results, Table (3.5).

3.2.2.2 Effect of annealing temperature on CdSe thin film electrodes

Photo *J-V* plots were measured for ECD -CdSe thin film electrodes annealed at different temperatures (150, 250, and 350ºC) and quenched, Figure (3.24). The results of the Figure are summarized in Table (3.6).

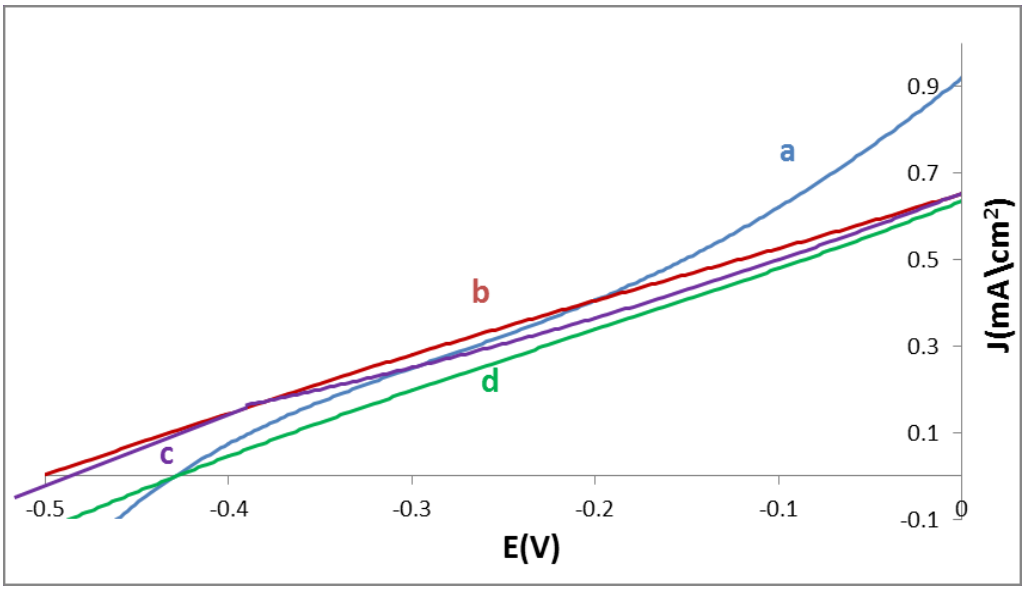

Figure (3.24): Photo J-V plots for naked ECD-CdSe thin film electrodes, a) non- annealed, b) annealed at 150 ºC, c) annealed at 250 ºC, d) annealed at 350 ºC. All measurements were conducted in aqueous S^{2-}/S_x^{2-} redox system at room temperature.

Table (3.6): Effect of annealing temperature on PEC characteristics of ECD-CdSe thin film electrode.

Sample	description	V_{oc} (V)	J_{sc} (A/cm^2)	[a] η %	[b] FF%
a	Non-annealed	-0.45	0.94×10^{-3}	1.72	20.08
b	150ºC	-0.49	0.69×10^{-3}	1.62	26.62
c	250ºC	-0.48	0.64×10^{-3}	1.24	23.24
d	350ºC	-0.44	0.62×10^{-3}	1.06	26.39

[a] η (%) = [(maximum observed power density)/(reach-in power density)]×100%.

[b] FF = [(maximum observed power density)/ J_{sc} ×V_{oc}]×100%.

V_{oc} values for the films annealed at different temperatures (150, 250, and 350ºC) were close to each other. The film annealed at 150 ºC showed the highest *Voc*, while the non- annealed one showed the highest J_{sc} value, and gave the highest percent conversion efficiency (η % ~ 1.72) than the annealed films, in agreement with the PL, the electronic absorption spectra and XRD results, Table (3.6).

3.2.2.3 Effect of cooling rate on CdSe thin film electrodes

Photo *J-V* plots were measured for ECD-CdSe thin film electrodes annealed at different temperatures (150, 250, and 350ºC) under N_2 atmosphere for 1 hour.

3.2.2.3.1 CdSe thin films annealed at 150ºC

Photo *J-V* plots were investigated for both slowly cooled and quenched ECD-CdSe thin film electrodes annealed at 150ºC under nitrogen, Figure (3. 25). The results of the Figure are summarized in Table (3.7).

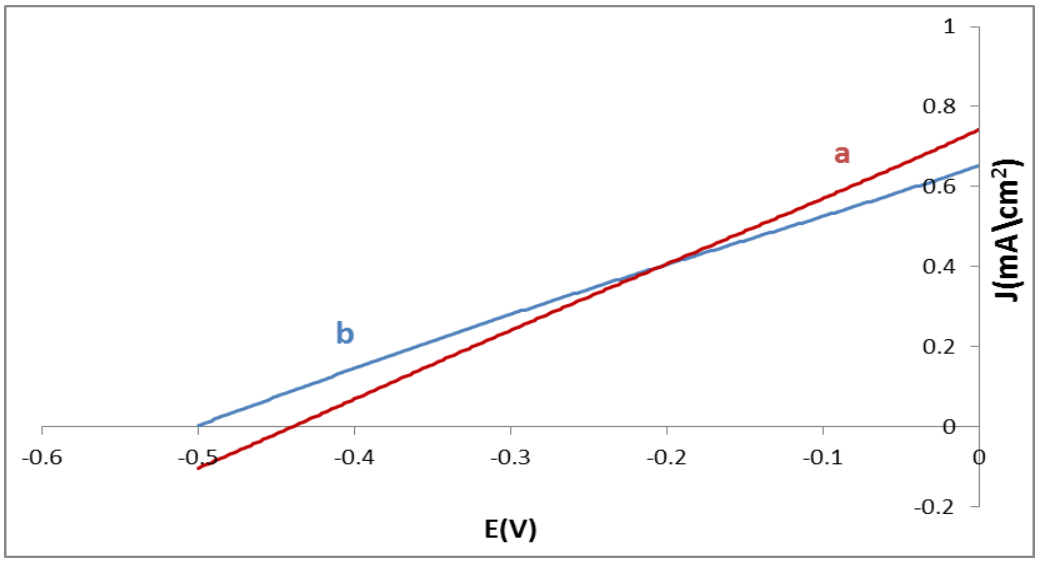

Figure (3.25): Photo J-V plots for ECD-CdSe thin film electrodes annealed at 150 ºC, a) quenched, b) slowly cooled. All measurements were conducted in aqueous S^{2-}/S_x^{2-} redox system at room temperature.

Table (3.7): Effect of cooling rate on PEC characteristics of ECD-CdSe thin film electrodes (annealed at 150 ºC).

sample	description	V_{oc} (V)	J_{sc} (A/cm^2)	[a] η %	[b] FF%
a	Quenched	-0.49	0.69×10^{-3}	1.62	26.62
b	Slowly cooled	-0.44	0.77	1.19	25.67

[a] η (%) = [(maximum observed power density)/(reach-in power density)]×100%.

[b] FF = [(maximum observed power density)/ J_{sc} ×V_{oc}]×100%.

The quenched film showed higher V_{oc} value, while the slowly cooled one showed higher J_{sc} value, the quenched film gave higher percent conversion efficiency (η % ~ 1.62) than the slowly cooled one, in agreement with the PL, the electronic absorption spectra and XRD results, Table (3.7).

3.2.2.3.2 CdSe thin films annealed at 250ºC

Photo *J-V* plots were investigated for both slowly cooled and quenched ECD- CdSe thin film electrodes which annealed at 250ºC under nitrogen. Figure (3. 26). The results of the Figure are summarized in Table (3.8).

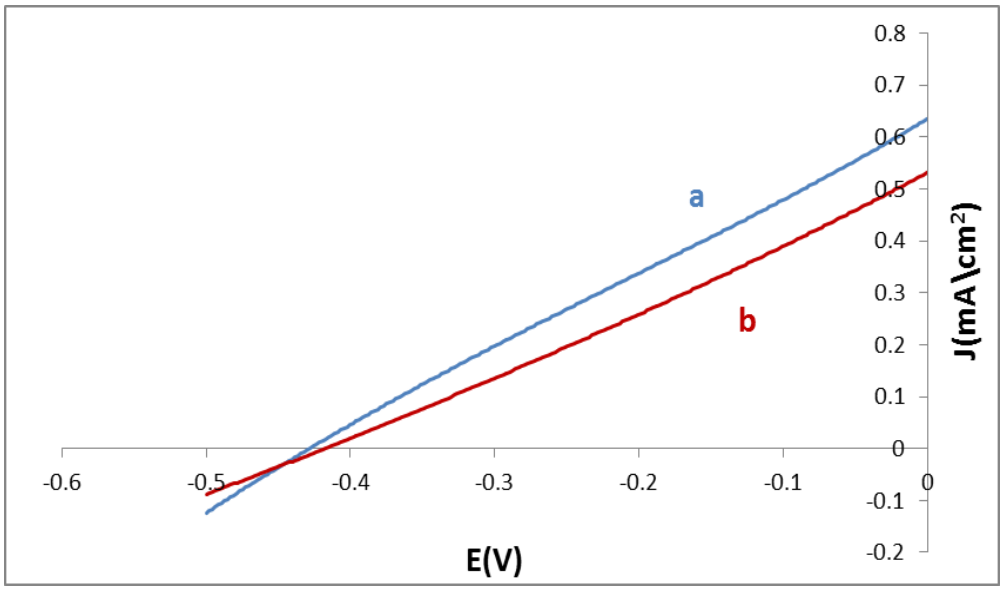

Figure (3. 26): Photo J-V plots for ECD -CdSe thin film electrodes annealed at 250 ºC, a) quenched, b) slowly cooled. All measurements were conducted in aqueous S^{2-}/S_x^{2-} redox system at room temperature.

Table (3.8): Effect of cooling rate on PEC characteristics of ECD-CdSe thin film electrodes (annealed at 250 ºC).

sample	description	V_{oc} (V)	Jsc (A/cm^2)	[a] η %	[b] FF%
a	Quenched	-0.48	0.64×10^{-3}	1.24	23.24
b	Slowly cooled	-0.43	0.52×10^{-3}	0.74	23.90

[a] η (%) = [(maximum observed power density)/(reach-in power density)]×100%.

[b] FF = [(maximum observed power density)/ J_{sc} ×V_{oc}]×100%.

The quenched film showed higher V_{oc} *and* Jsc values *and* it gave higher percent conversion efficiency (η % ~ 1.24) than the slowly cooled one. This is consistent with the PL spectra, the electronic absorption spectra and XRD results, Table (3.8).

3.2.2.3.3 CdSe thin films annealed at 350 ºC

Photo *J-V* plots were investigated for both slowly cooled and quenched ECD -CdSe thin film electrodes annealed at 350ºC under nitrogen. Figure (3. 27). The results of the Figure are summarized in Table (3.9).

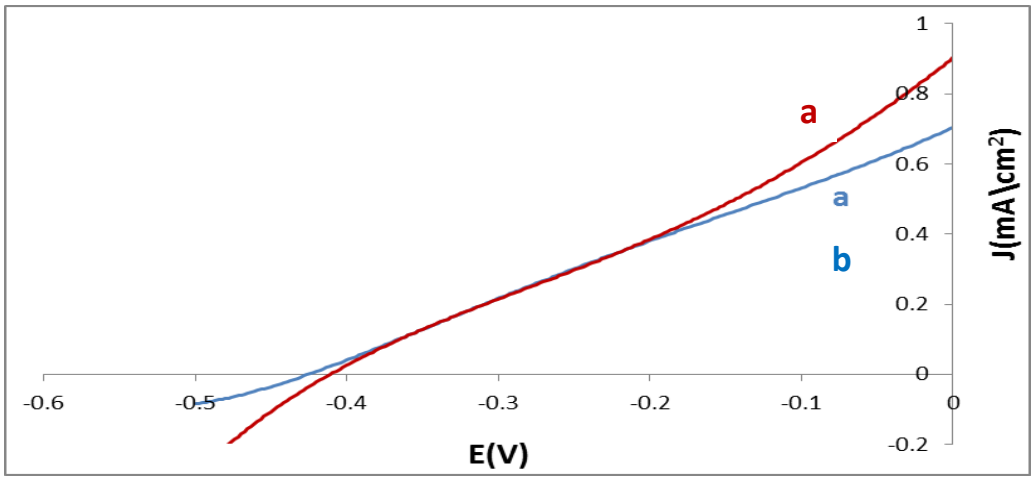

Figure (3.27): Photo J-V plots for ECD -CdSe thin film electrodes annealed at 350 ºC, a) quenched, b) slowly cooled. All measurements were conducted in aqueous S^{2-}/S_x^{2-} redox system at room temperature.

Table (3.9): Effect of cooling rate on PEC characteristics of ECD - CdSe thin film electrodes (annealed at 350 ºC).

sample	description	V_{oc} (V)	J_{sc} (A/cm^2)	[a] η %	[b] FF%
a	Quenched	-0.44	0.62×10^{-3}	1.06	26.39
b	Slowly cooled	-0.40	0.85×10^{-3}	0.79	25.29

[a] η (%) = [(maximum observed power density)/(reach-in power density)]×100%.

[b] FF = [(maximum observed power density)/ $J_{sc} \times V_{oc}$]×100%.

The quenched film showed higher V_{oc} value and higher percent conversion efficiency (η % ~ 1.06) than the slowly cooled one. This is consistent with the PL, the electronic absorption spectra and XRD results, Table (3.9).

3.2.2.4 Effect of covering with MP-Sil matrix on CdSe thin film electrodes

Photo *J-V* plots were investigated for both naked and coated types ECD - CdSe thin film electrodes, Figure (3. 28). The results of the Figure are summarized in Table (3.10).

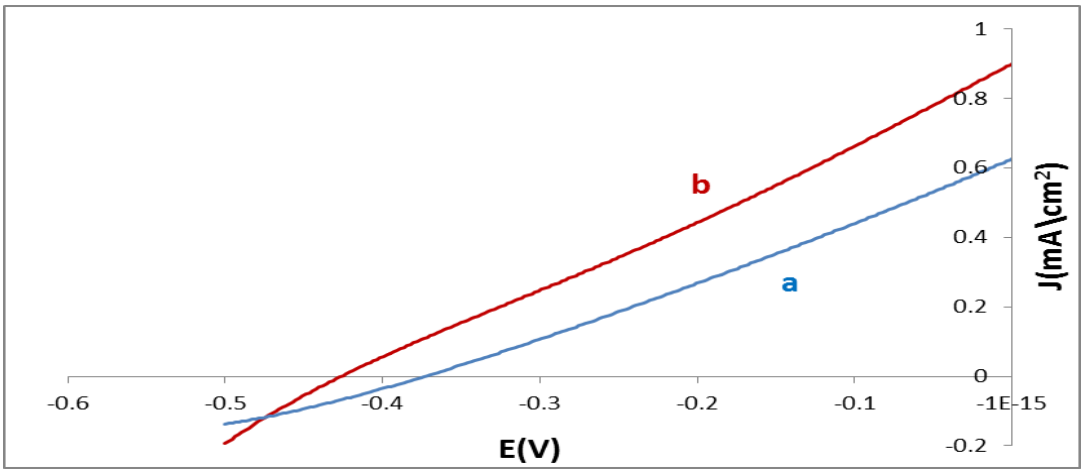

Figure (3.28): Photo J-V plots for non-annealed ECD -CdSe thin film electrodes, a) naked, b) coated. All measurements were conducted in aqueous S^{2-}/S_x^{2-} redox system at room temperature.

Table (3.10): Effect of covering with MP-Sil matrix on PEC characteristics of ECD-CdSe thin film electrode.

sample	description	*Voc* (V)	*Jsc* (A/cm^2)	[a] η %	[b] *FF*%
a	Naked	-0.37	0.62×10^{-3}	0.88	24.44
b	Coated	-0.44	0.85×10^{-3}	1.44	23.52

[a] η (%) = [(maximum observed power density)/(reach-in power density)]×100%.

[b] FF = [(maximum observed power density)/ $J_{sc} \times V_{oc}$]×100%.

The film coated with MP-Sil matrix showed higher V_{oc} and *Jsc values*, it also gave higher percent conversion efficiency ((η % ~ 1.44) than the naked one. In agreement with the PL and the electronic absorption spectra results, Table (3.10).

Part II

Combined electrochemical/chemical bath deposited (ECD/CBD) thin film electrodes

CdSe thin films prepared by the combined between electrochemical deposition and chemical bath deposition methods were studied under

different conditions by using different techniques including PL emission spectra, electronic absorption spectra and XRD. PEC studies including dark J-V plots, photo J-V plots, conversion efficiency, value of short-circuit current and fill-factor (FF) were also studied.

3.3 Combined ECD/CBD electrodes thin film characteristics

Characteristics of combined ECD /CBD CdSe films were investigated by using different techniques as shown below.

3.3.1 XRD measurements for CdSe thin film electrodes

The crystalline size and structural phase of the combined ECD/CBD -CdSe nanocrystalline thin films have been determined using XRD measurements. CdSe is known to exist in either cubic (zinc-blende type) or hexagonal (wurtzite type) structure or sometimes a mixture of both phases [41]. XRD measurements were obtained for combined ECD/CBD-CdSe thin films with different parameters including deposition times, annealing temperatures, cooling rate and covering the films with MnP-Sil matrix.

3.3.1.1 Effect of annealing on CdSe thin film electrodes

XRD measurements were obtained for naked ECD/CBD-CdSe thin film electrodes before and after annealing at 350 ºC and quenched. XRD data showed that both annealed and non-annealed ECD/CBD-CdSe thin films exhibited crystallinity. The average particle size for non-annealed ECD/CBD-CdSe was~ 4.13 nm, Figure (3.29). On the other hand, the

average particle size for ECD/CBD-CdSe was~ 4.32 nm after annealing at 350 ºC and quenched. Both Films are in cubic phase with the zinc-blende type phase. This was based on comparison with earlier reports [35, 38-41], Table (3.11) shows the positions of observed peaks.

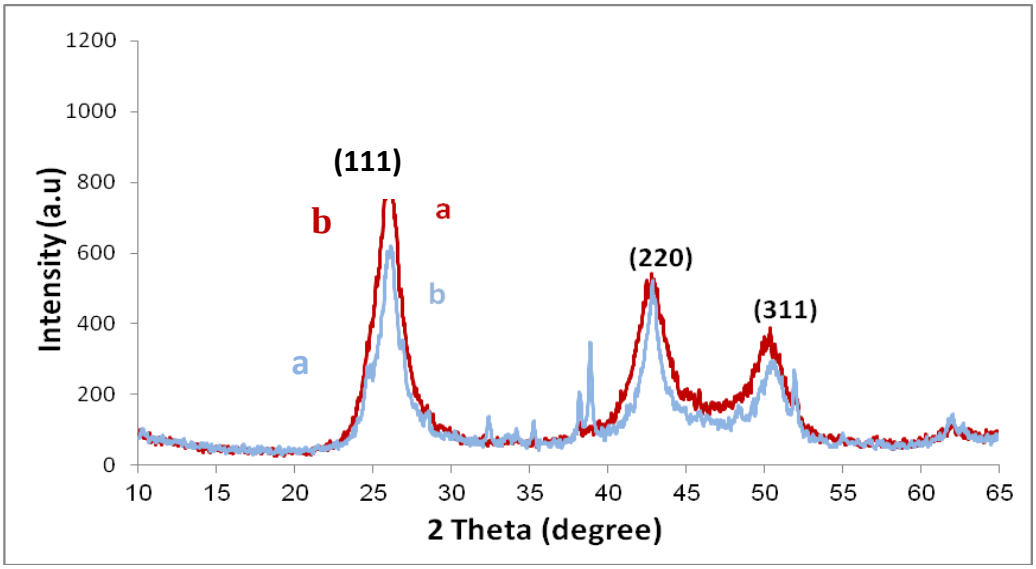

Figure (3.29): XRD patterns measured for naked ECD/CBD CdSe thin film a) non-annealed, b) after annealing at 350 ºC and quenched.

Table (3.11): XRD results for annealed and non-annealed ECD/CBD-CdSe film electrodes.

Position of observed peak (2 theta)		Plane	Reference	Particle size (nm)
Non-annealed	**25.97**	**C(111)**	[38]	**4.13**
	33.88	FTO subs	[42]	
	38.81	FTO subs	[42]	
	42.77	**C(220)**	[38]	
	50.41	**C(311)**	[38]	
	51.85	FTO subs	[42]	
Annealed	**25.86**	**C(111)**	[38]	**4.32**
	34.08	FTO subs	[42]	
	42.62	**C(220)**	[38]	
	50.10	**C(311)**	[38]	

3.3.1.2 Effect of annealing temperature on CdSe thin film electrodes

XRD measurements were obtained for naked ECD/CBD-CdSe thin film electrodes annealed at different temperatures (150 and 350 ºC) and quenched. XRD data showed that both annealed ECD/CBD-CdSe thin films exhibited crystallinity. The average particle size for ECD/CBD-CdSe annealed at 150 ºC ~ 3.32 nm, Figure (3.30). On the other hand, the average particle size for ECD/CBD-CdSe was ~ 3.19 nm after the film annealed at 350 ºC. Both Films are in cubic phase with the zinc-blende type phase. This was based on comparison with earlier reports (35, 38-40) only. Table (3.12) shows the positions of observed peaks. The peaks of FTO substrate don't appear here clearly due to the high thickness of the ECD/CBD CdSe thin film electrodes.

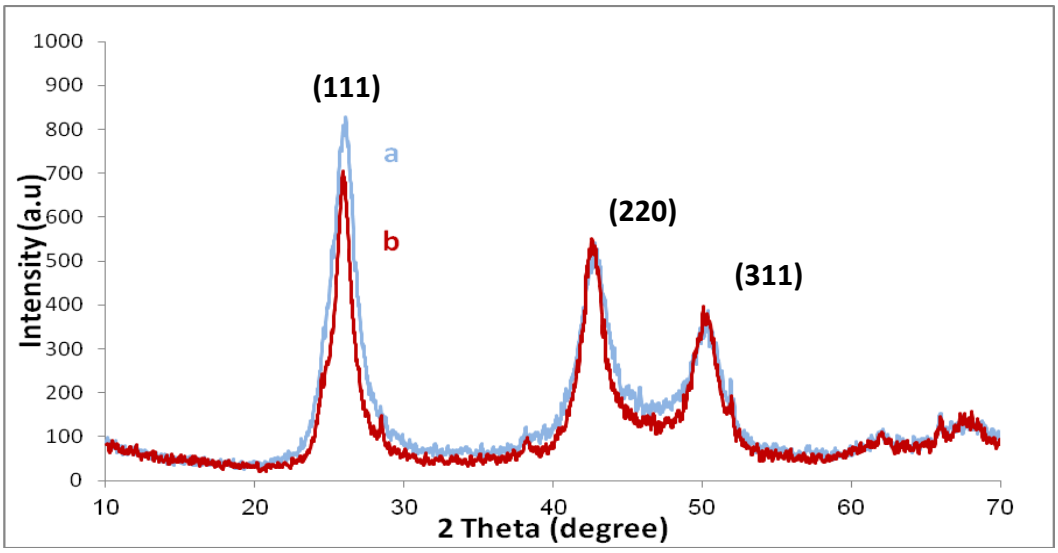

Figure (3.30): XRD patterns measured for naked ECD/CBD CdSe thin film a) annealed at 150 ºC and quenched, b) annealed at 350 ºC and quenched.

Table (3.12): XRD results for ECD/CBD-CdSe film electrodes annealed at different temperature (150 and 350ºC) and quenched.

Position of observed peak (2 theta)		Plane	Reference	Particle size (nm)
Annealed at 150ºC	**25.89**	**C(111)**	[38]	**3.32**
	42.68	**C(220)**	[38]	
	50.23	**C(311)**	[38]	
Annealed at 350ºC	**25.86**	**C(111)**	[38]	**3.19**
	42.62	**C(220)**	[38]	
	50.10	**C(311)**	[38]	

3.3.1.3 Effect of cooling rate on CdSe thin film electrodes

XRD measurements were obtained for naked ECD/CBD-CdSe thin film electrodes, annealed at 150 ºC with slow and fast cooling. XRD data showed that both annealed and non-annealed ECD/CBD-CdSe thin films exhibited crystallinity. The average particle size for the slowly cooled film particle size was ~3.19 nm, Figure (3.31).The quenched ECD/CBD-CdSe was ~3.56 nm. Both films are in cubic phase with the zinc-blende type phase. .This was based on comparison with earlier reports [35, 38-40] only. Table (3.13) shows the positions of observed peaks and their significances. The peaks of FTO substrate don’t appear clearly here due to the high thickness of the ECD/CBD CdSe thin film electrodes.

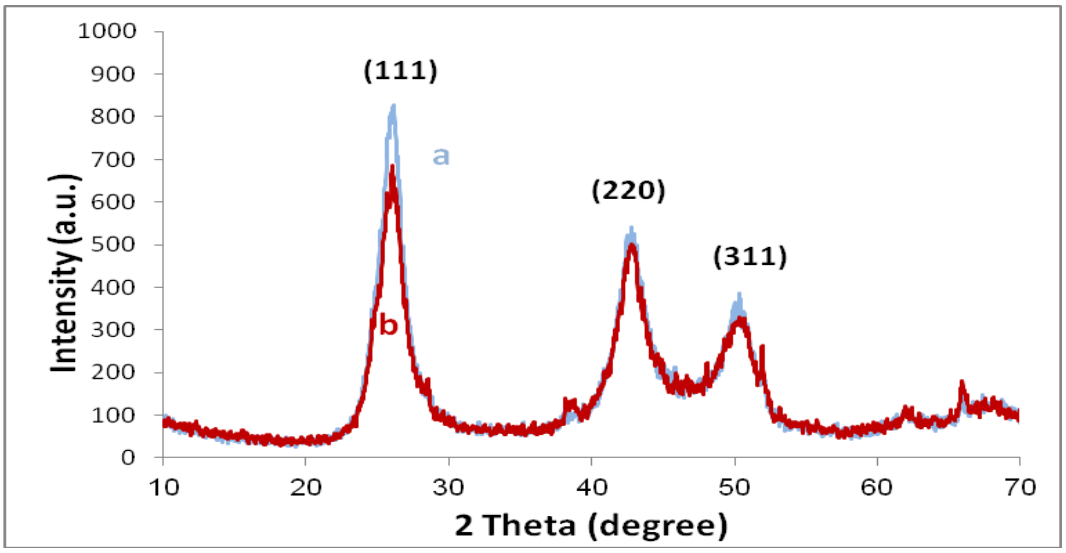

Figure (3.31) XRD patterns measured for naked ECD/CBD CdSe thin film annealed at 350 ºC a) slowly cooled, b) quenched.

Table (3.13): XRD results for quenched and slowly cooled ECD/CBD-CdSe film electrodes (annealed at 150 ºC).

Position of observed peak (2 theta)		Significance	References	Particle size (nm)
Quenched	**25.89**	**C(111)**	[38]	**3.56**
	42.68	**C(220)**	[38]	
	50.23	**C(311)**	[38]	
Slowly cooled	**25.91**	**C(111)**	[38]	**3.19**
	34.15	FTO subs	[42]	
	42.75	**C(220)**	[38]	
	50.09	**C(311)**	[38]	

3.3.1.4 Effect of covering with MP-Sil matrix on CdSe thin film electrodes

XRD measurements were obtained for naked and coated non-annealed ECD/CBD CdSe thin film. XRD data showed that both films exhibited crystallinity. Both Films are in cubic phase with the zinc-blende type phase. The average particle size for naked ECD/CBD-CdSe thin film was~ 3.41nm, Figure (3.32). The coated film particle size was~ 3.31 nm. This was based on comparison with earlier reports [35, 38-40] only. Table (3.14) shows the positions of observed peaks.

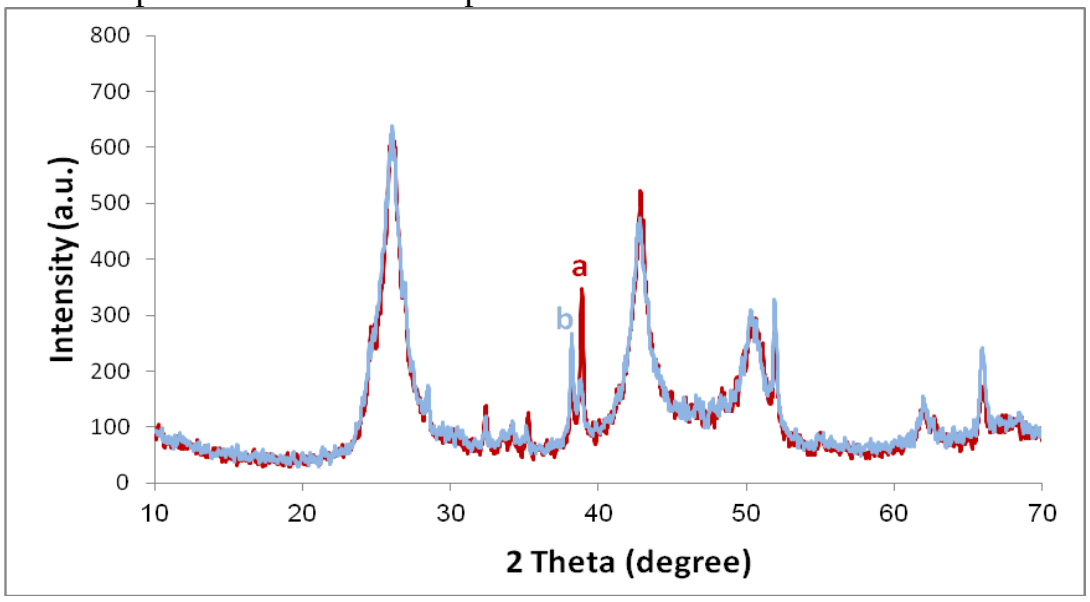

Figure (3.32): XRD patterns measured for non-annealed ECD/CBD CdSe thin film a) naked, b) coated.

Table (3.14): XRD results for naked and coated ECD/CBD-CdSe film electrodes

Position of observed peak (2 theta)		Plane	Reference	Particle size (nm)
Naked	**25.97**	**C(111)**	[38]	3.41
	33.88	FTO subs	[42]	
	38.81	FTO subs	[42]	
	42.77	**C(220)**	[38]	
	50.41	**C(311)**	[38]	
	51.85	FTO subs	[42]	
Coated	**25.93**	**C(111)**	[38]	3.31
	34.06	FTO subs	[42]	
	38.13	FTO subs	[42]	
	42.70	**C(220)**	[38]	
	50.35	**C(311)**	[38]	
	51.85	FTO subs	[42]	

3.3.2 Photoluminescence Spectra for CdSe thin film electrodes

Photoluminescence spectra were investigated for combined ECD/CBD - CdSe thin films with different parameters including deposition times, annealing temperatures, cooling rate and covering the films with MnP-Sil matrix.

3.3.2.1 Effect of deposition time on CdSe thin film electrodes

The effect of deposition time (15 min CBD and 120 min CBD), (15 min ECD and 240 min CBD) on the photoluminescence spectra of non-annealed CdSe thin films were studied, Figure (3.33). The systems were excited at wavelength 385 nm.

The Figure shows many weak peaks, the highest intensity peaks appeared at wavelength range of 600-570 nm with a band gap range (2.06- 2.21) eV. This is in agreement with band gap values range of CdSe thin films in literature [22, 35].The ECD/CBD-CdSe film deposited in longer time shows higher intensity than its counterpart, while in ECD-CdSe preparation method, the film deposited in shorter time shows higher intensity than the other deposited in longer time.

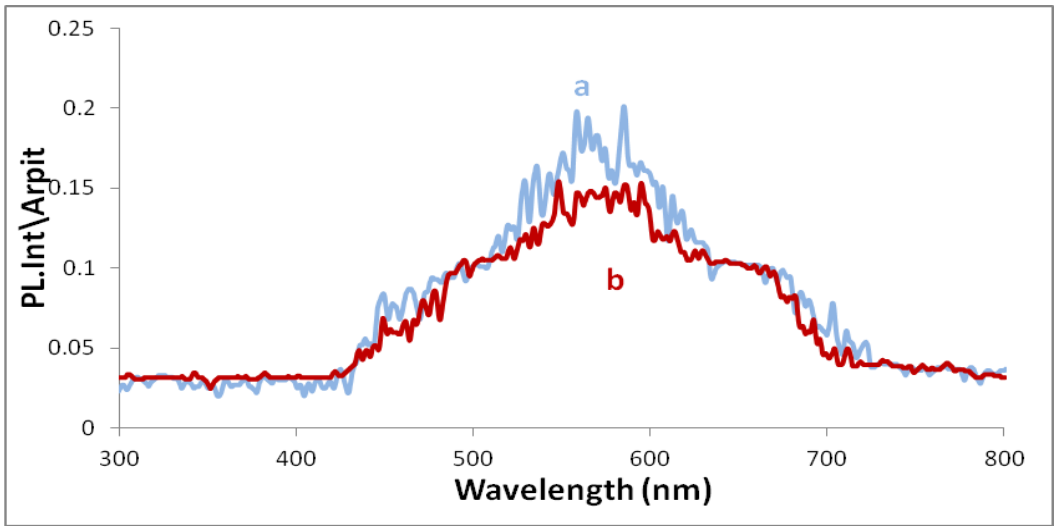

Figure (3.33): Photo-luminescence spectra for non-annealed ECD/CBD-CdSe thin film electrodes prepared in different deposition times, a) 15 min ECD and 240 min CBD, b) 15 min and 120 min CBD.

3.3.1.2 Effect of annealing temperatures on CdSe thin film electrodes

The effect of annealing temperatures (150, 250 and 350ºC) on the photoluminescence spectra of the prepared ECD/CBD-CdSe thin films was studied, Figure (3.34). The systems were excited at wavelength 385nm.

The Figure shows many weak peaks, the highest intensity peaks appeared at wavelength range of 600-550 nm with a band gap range (2.06-2.25) eV, which is consistent with the band gap range of CdSe thin films in literature

[22, 35]. The non-annealed film shows higher intensity than the annealed films. While the film annealed at 150 ºC shows higher intensity than the films annealed at higher temperature (250 and 350 ºC). Same results have been observed for the ECD-CdSe thin film electrodes.

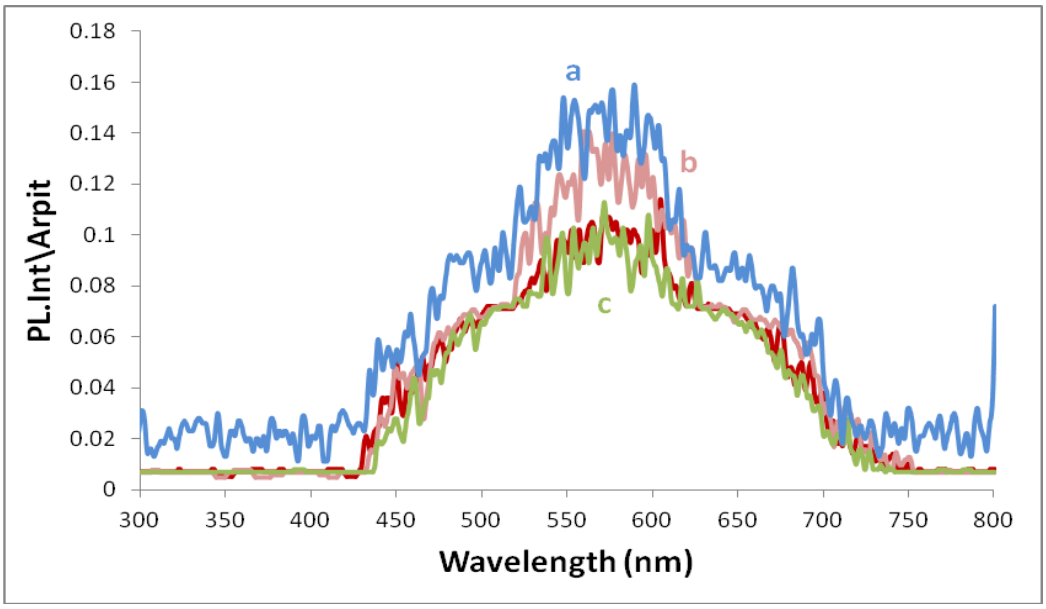

Figure (3.34): Photo-luminescence spectra for ECD-CdSe thin film electrodes, a) non-annealed, b) annealed at 150ºC, c) annealed at 250ºC , annealed at 350ºC **.**

3.3.1.3 Effect of cooling rate on CdSe thin film electrodes

The effect of cooling rate (fast and slow cooling) on the photoluminescence spectra of the pre annealed combined ECD\CBD -CdSe thin film

electrodes at different annealing temperatures (150, 250 and 350℃) under nitrogen for one hour on was investigated.

3.3.1.3.1 CdSe thin films annealed at 150 ºC

The effect of cooling rate (fast and slow cooling) on the photoluminescence spectra of the CdSe thin films annealed at 150 ºC under nitrogen for 1 hour was studied, Figure (3.35). The systems were excited at wavelength

385nm. The Figure shows many weak peaks, the highest intensity peaks appeared at wavelength range of 620-540 nm with a band gap range (2.0-2.2) eV, which is consistent with the band gap range of CdSe thin films in literature [22, 35]. The slowly cooled film shows higher intensity than the quenched one. While in ECD-CdSe thin films preparation method, the quenched film shows higher intensity than the slowly cooled one.

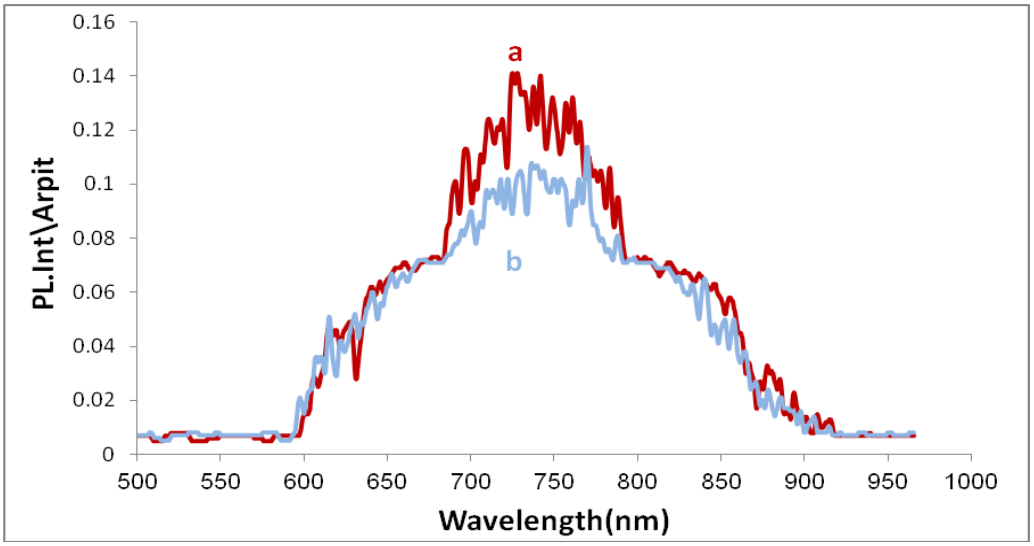

Figure (3.35): Photo-luminescence spectra for ECD\CBD-CdSe thin film electrodes annealed at 150℃, a) slowly cooled, b) quenched**.**

3.3.1.3.2 CdSe thin films annealed at 250 ºC

The effect of cooling rate (fast and slow cooling) on the photoluminescence spectra of the CdSe thin films annealed at 250 ºC under nitrogen for 1 hour was studied, Figure (3.36). The systems were excited at wavelength 385nm. The Figure shows many weak peaks, the intensities of the peaks were close to each other appeared at wavelength range of 600-540 nm with a band gap range (2.06-2.29) eV.

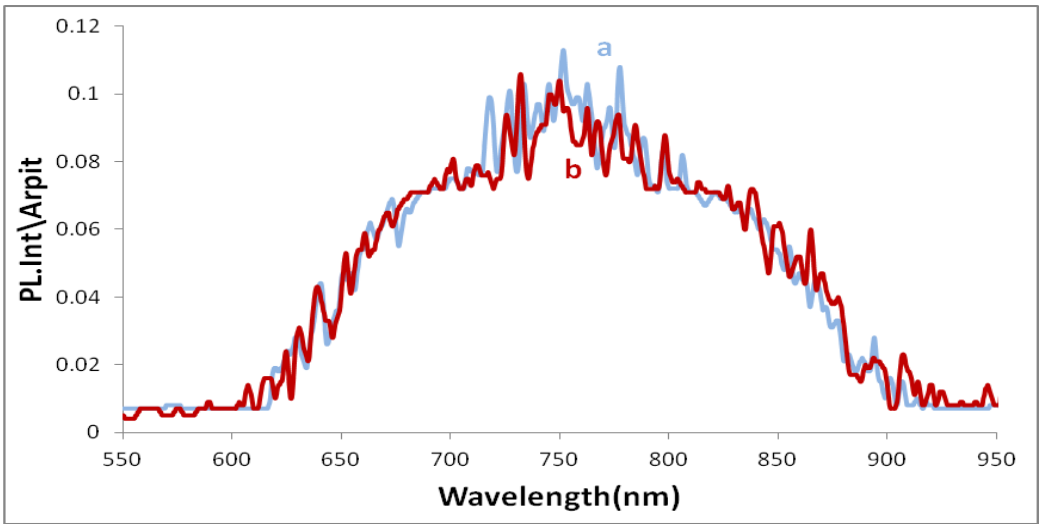

Figure (3.36): Photo-luminescence spectra for ECD\CBD-CdSe thin film electrodes annealed at 250℃, a) slowly cooled, b) quenched.

3.3.1.3.3 CdSe thin films annealed at 350 ºC

The effect of cooling rate (fast and slow cooling) on the photoluminescence spectra of the CdSe thin films annealed at 350 ºC under nitrogen for 1 hour

was studied, Figure (3.37). The systems were excited at wavelength 385nm. The Figure shows many weak peaks, the highest intensity peaks appeared at wavelength range of 600-550 nm with a band gap values range (2.06- 2.25) eV. The slowly cooled film shows slightly higher intensity than the quenched one.

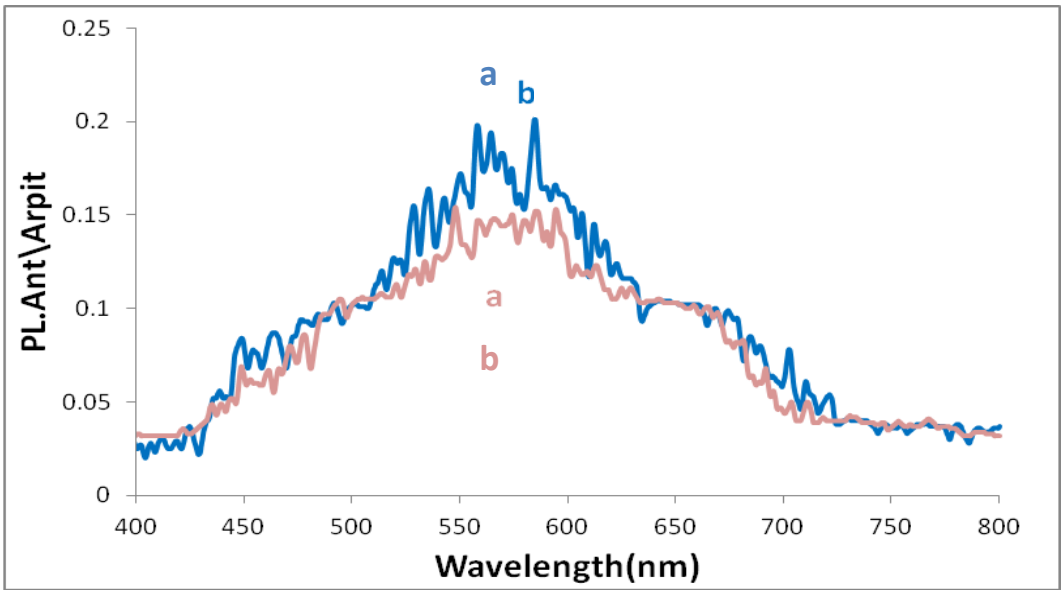

Figure (3.37): Photo-luminescence spectra for ECD-CdSe thin film electrodes annealed at 350 ºC, a) slowly cooled, b) quenched.

3.3.1.4 Effect of covering with MP-Sil matrix on CdSe thin film electrodes

The effect of covering with MP-Sil matrix on the photoluminescence spectra of ECD\CBD CdSe thin films, annealed at different temperatures (150, 250, and 350ºC) was studied.

3.3.1.4.1 CdSe thin film annealed at 150ºC

The effect of covering with MP-Sil matrix on the photoluminescence spectra of the ECD\CBD CdSe thin film annealed at 150ºC under nitrogen for 1 hour was studied, Figure (3.38). The systems were excited at wavelength 385 nm. The Figure shows many weak peaks, the highest intensity peaks appeared at wavelength range of 600-550 nm with a band gap range (2.06-2.25) eV, which is consistent with the band gap values range of CdSe in literature [22, 35]. The coated film shows slightly higher

intensity than the naked one, same result has been shown previously for the ECD-CdSe thin film.

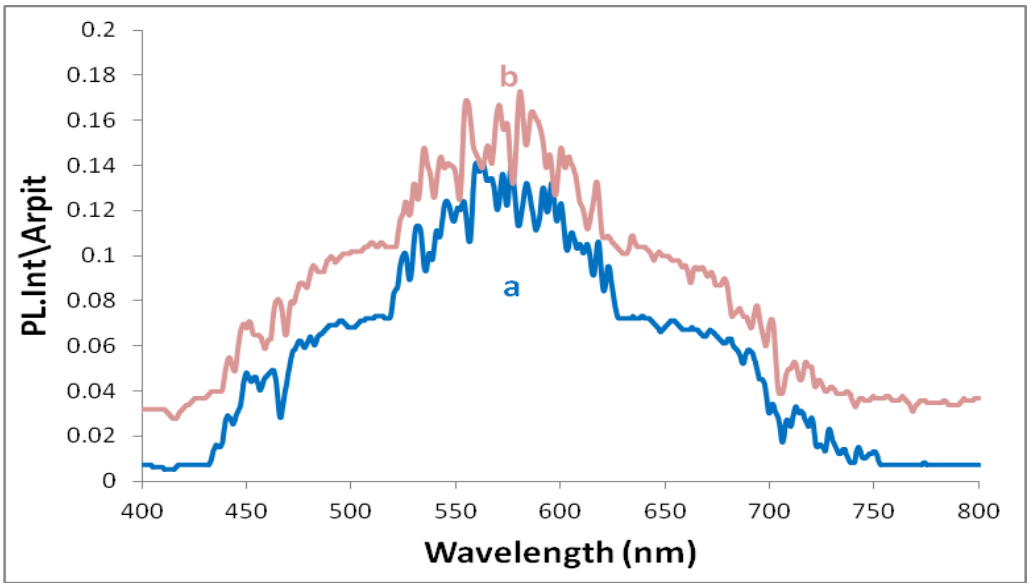

Figure (3.38): Photo-luminescence spectra for ECD\CBD-CdSe thin film electrodes annealed at 150℃, a) naked, b) coated.

3.3.1.4.2 CdSe thin film annealed at 250ºC

The effect of covering with MP-Sil matrix on the photoluminescence spectra of the ECD\CBD CdSe thin film annealed at 250ºC under nitrogen for 1 hour was studied, Figure (3.39). The systems were excited at wavelength 385nm. The Figure shows many weak peaks, the highest intensity peaks appeared at wavelength range of 620-540 nm with a band gap range (2.0-2.2) eV, which is consistent with the band gap range of CdSe in literature [22, 35]. The coated film shows higher intensity than the naked one.

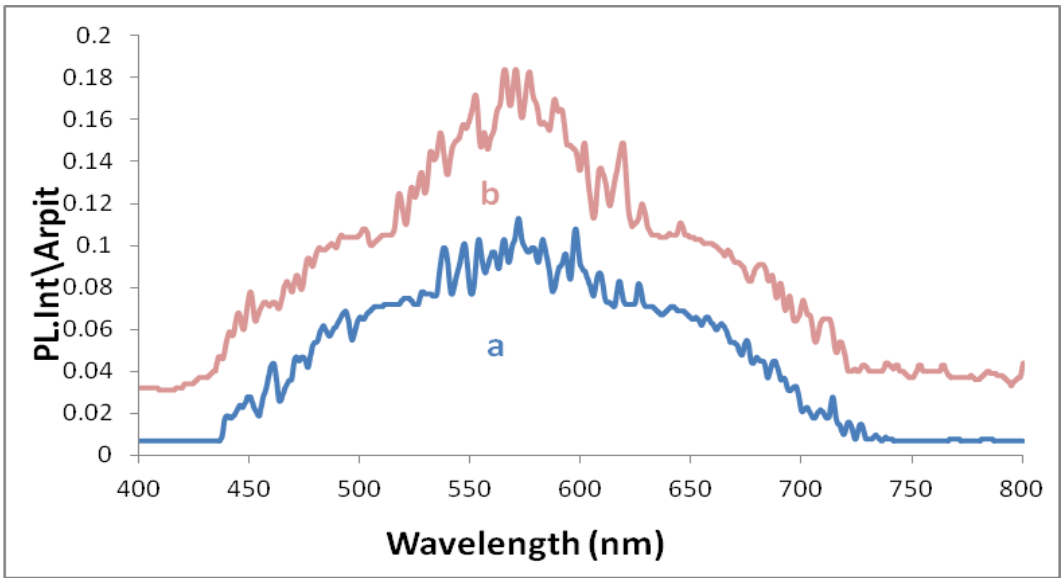

Figure (3.39): Photo-luminescence spectra for ECD\CBD-CdSe thin film electrodes annealed at 250℃, a) naked, b) coated.

3.3.1.4.3 CdSe thin film annealed at 350℃

The effect of covering with MP-Sil matrix on the photoluminescence spectra of the combined ECD\CBD CdSe thin film annealed at 350ºC under nitrogen for 1 hour was studied, Figure (3.40). The systems were excited at wavelength 385nm. The Figure shows many weak peaks, the highest intensity peaks appeared at wavelength range of 600-550 nm with a band gap range (2.06-2.25) eV, which is consistent with the band gap values range of CdSe thin films in literature [22, 35]. The coated film shows higher intensity than the naked one.

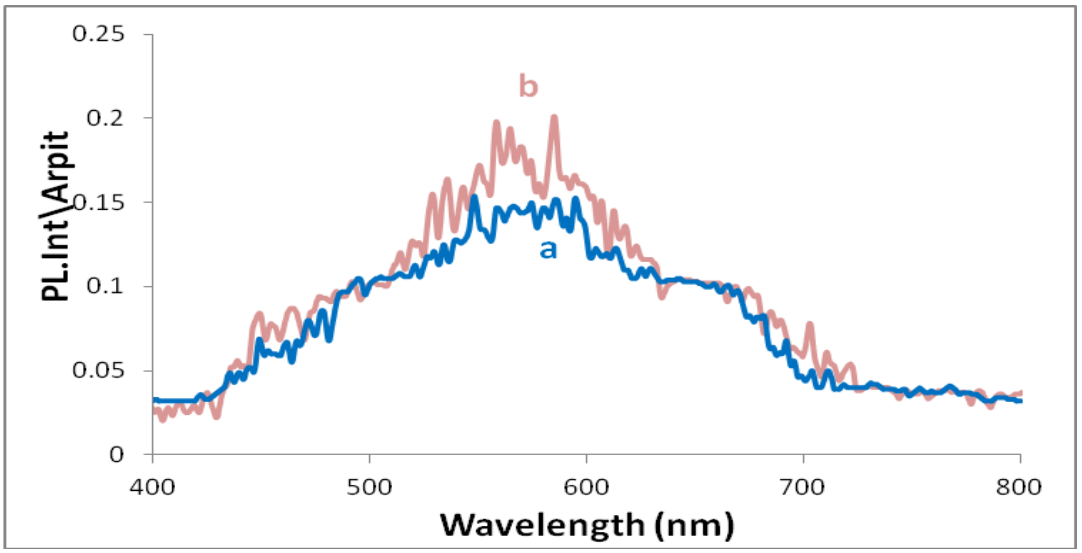

Figure (3.40): Photo-luminescence spectra for ECD\CBD-CdSe thin film electrodes annealed at 350ºC, a) naked, b) coated.

3.3.2 Electronic absorption spectra for CdSe thin film electrodes

Electronic absorption spectra were measured for ECD/CBD CdSe thin films with different controlled parameters, including deposition times,

annealing temperatures, cooling rate and covering the films with MnP-Sil matrix. It should be noted that that absorption spectra were inconclusive and difficult to analyze. This is due to the high thickness of ECD/CBD-CdSe films

3.3.2.1 Effect of deposition time on CdSe thin film electrodes

Electronic absorption spectra were measured for ECD/CBD -CdSe thin films prepared in different deposition times (15min ECD and120 min CBD), (15min ECD and 240 min CBD). Spectra could not be clearly observed here due to the thickness of the prepared film.

3.3.2.2 Effect of annealing temperatures on CdSe thin film electrodes

Electronic absorption spectra were measured for CdSe thin films annealed at different temperatures (150, 250 and 350 ºC) under nitrogen for 1 hour. Spectra could not be clearly observed here due to the thickness of the prepared film.

3.3.2.3 Effect of cooling rate on CdSe thin film electrodes

The effect of cooling rate (fast and slow cooling) on the electronic absorption spectra of the pre annealed ECD/CBD-CdSe thin film electrodes at different annealing temperatures (150, 250 and 350ºC) under nitrogen for 1 hour was investigated.

3.3.2.3.1 CdSe thin films annealed at 150 ºC

Clear electronic absorption spectra for slowly cooled and quenched CdSe thin films annealed at 150ºC can't be obtained here due to the thickness of the prepared films.

3.3.2.3.2 CdSe thin films annealed at 250 ºC

Clear electronic absorption spectra for slowly cooled and quenched CdSe thin films annealed at 250ºC can't be obtained here due to the thickness of the prepared films.

3.3.2.3.3 CdSe thin films annealed at 350 ºC

Clear electronic absorption spectra for slowly cooled and quenched CdSe thin films annealed at 350ºC can't be obtained here due to the thickness of the prepared films.

3.3.1.4 Effect of covering with MP-Sil matrix on CdSe thin film electrodes

The effect of covering with MP-Sil Matrix on the electronic absorption spectra of the CdSe thin films annealed at different times (150, 250, and 350ºC) under nitrogen atmosphere for 1 hour was studied**.**

3.3.1.4.1 CdSe thin films annealed at 150 ºC

The effect of covering with MP-Sil matrix on the electronic absorption spectra of the CdSe thin films annealed at 150 ºC under nitrogen atmosphere for 1 hour was studied. Spectra could not be clearly observed here due to the thickness of the prepared films.

3.3.1.4.2 CdSe thin films annealed at 250 ºC

The effect of covering with MP-Sil matrix on the electronic absorption spectra of the CdSe thin films which annealed at 250 ºC under nitrogen atmosphere for 1 hour was studied**,** Figure (3. 41). A relatively obvious absorption was observed for the coated film. This is consistent with the PL spectra result.

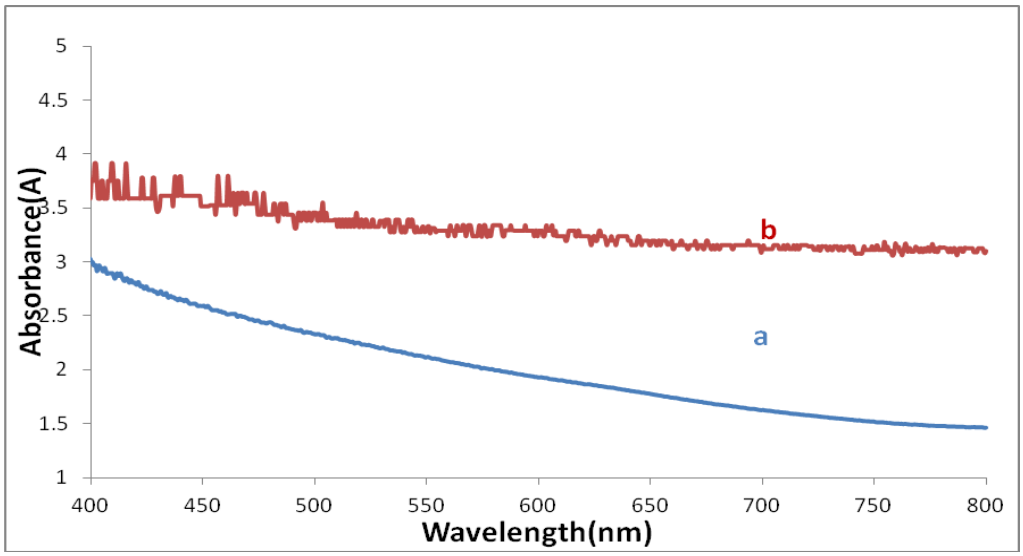

Figure (3.41): Electronic absorption spectra for ECD/CBD CdSe thin films annealed at 250ºC, a) naked, b) coated.

3.3.1.4.1 CdSe thin films annealed at 350 ºC

The effect of covering with MP-Sil matrix on the electronic absorption spectra of the CdSe thin films which annealed at 350 ºC under nitrogen atmosphere for 1 hour was studied. Spectra could not be clearly observed here due to the thickness of the prepared film.

3.4 ECD/CBD thin film PEC studies

PEC characteristics including dark J-V plots, photo J-V plots, value of short-circuit current and efficiency, were studied for ECD/CBD CdSe films in aqueous S^{2-}/S_x^{2-} redox couples at room temperature.

3.4.1 Dark *J-V* plots of CdSe thin film electrodes

Dark *J-V* plots were measured for ECD/CBD -CdSe thin film electrodes with controlling different parameters (deposition time, annealing temperature, cooling rate and covering with MP-Sil matrix). It should be

noted that dark J-V plots were inconclusive in this study. This is due to current leakage in system during the experiment.

3.4.1.1 Effect of deposition time on CdSe thin film electrodes

Dark *J-V* Plots were measured for ECD/CBD -CdSe thin film electrodes deposited in different times (15 min ECD + 120 min CBD), (15 min ECD + 240 min CBD), Figure (3.42). The dark *J-V* plots of films don't give good indication here.

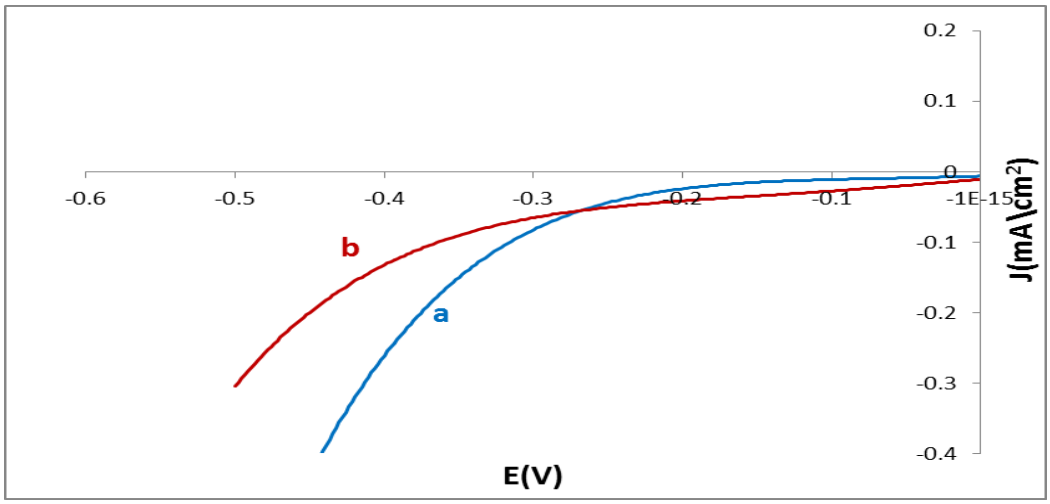

Figure (3.42): Dark *J-V* plots for ECD/CBD -CdSe thin film electrodes, *a)* 15 min ECD and 120 min CBD, *b*) 15 min ECD and 240 min CBD. All measurements were conducted in aqueous S^{2-}/S_x^{2-} redox system at room temperature.

3.4.1.2 Effect of annealing temperature on CdSe thin film electrodes

Dark *J-V* plots were measured for ECD/CBD -CdSe thin film electrodes deposited annealed at different temperatures, Figure (3.43). The positive dark current occurred, due to current leakage in system during the experiment. The dark J-V plots of films don't give good indication here.

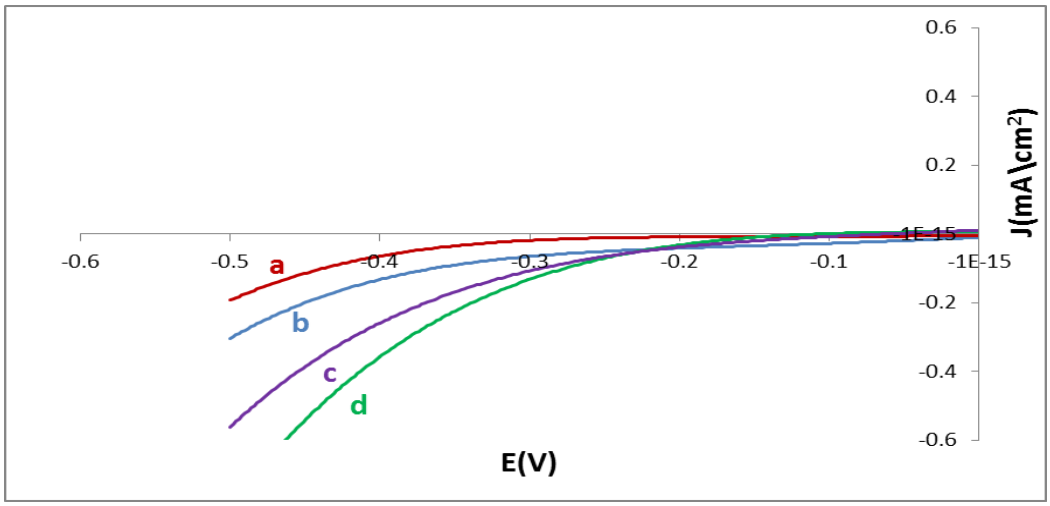

Figure (3.43): Dark *J-V* plots for ECD/CBD -CdSe thin film electrodes, *a)* non-annealed, *b*) 150ºC, c) 250ºC, d) 350 ºC. All measurements were conducted in aqueous S^{2-}/S_x^{2-} redox system at room temperature**.**

3.4.1.3 Effect of cooling rate in CdSe thin film electrodes

Dark *J-V* plots were measured for slowly cooled and quenched ECD/CBD-CdSe thin film electrode**s** which annealed at different temperatures (150ºC, 250ºC, and 350ºC) under nitrogen for 1 hour.

3.4.1.3.1 CdSe thin film annealed at 150ºC

Dark *J-V* plot was measured for slowly and quickly cooled ECD/CBD-CdSe thin film electrode**s**, Figure (3.44). The dark *J-V* plots of films don't give a good indication in our study.

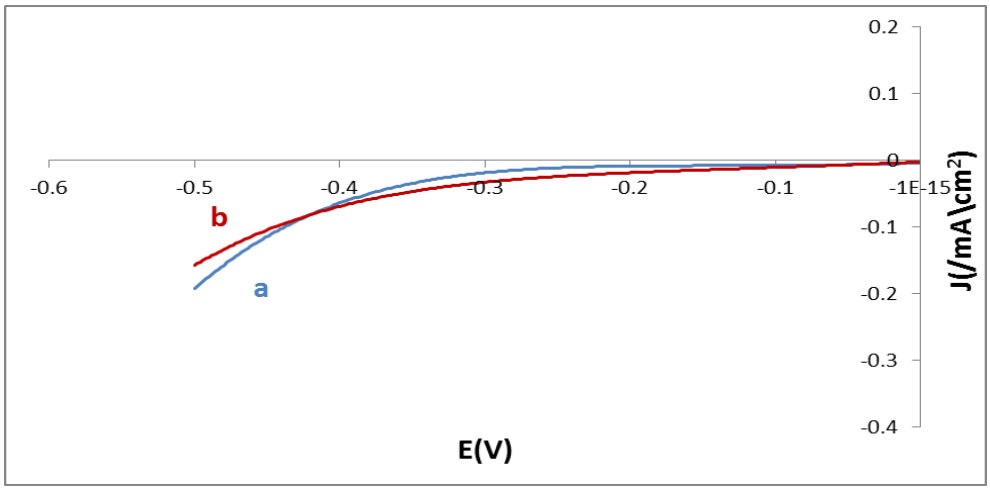

Figure (3.44): Dark *J-V* plots for ECD/CBD -CdSe thin film electrodes annealed at 150ºC, *a)* slowly cooled, *b*) quenched. All measurements were conducted in aqueous S^{2-}/S_x^{2-} redox system at room temperature**.**

3.4.1.3.2 CdSe thin films annealed at 250 ºC

Dark *J-V* plots were measured for slowly and quickly cooled ECD/CBD-CdSe thin film electrode**s**, Figure (3.45). The dark J-V plots of films don't give good indication in our study.

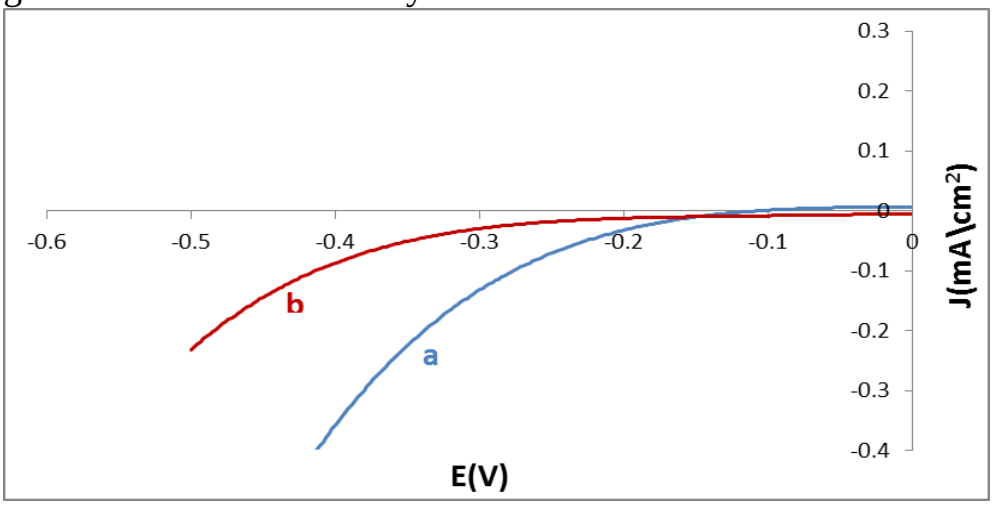

Figure (3.45): Dark *J-V* plots for ECD/CBD-CdSe thin film electrodes annealed at 250ºC, *a)* slowly cooled, *b*) quenched. All measurements were conducted in aqueous S^{2-}/S_x^{2-} redox system at room temperature.

3.4.1.3.3 CdSe thin films annealed at 350 ºC

Dark *J-V* plot was measured for slowly and quickly cooled ECD/CBD-CdSe thin film electrodes, Figure (3.46). The positive dark current occurred, due to current leakage in system during the experiment. The dark J-V plots of films don't give good indication here.

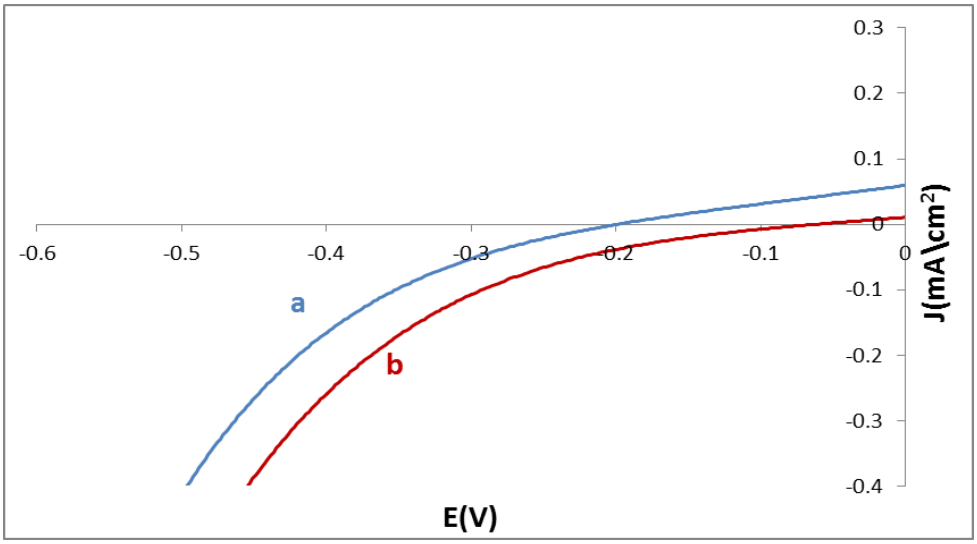

Figure (3.46): Dark *J-V* plots for ECD/CBD-CdSe thin film electrodes annealed at 350ºC, *a)* slowly cooled, *b*) quenched. All measurements were conducted in aqueous S^{2-}/S_x^{2-} redox system at room temperature.

3.4.1.4 Effect of covering with MP-Sil matrix on CdSe thin film electrodes

3.4.1.4.1 CdSe thin films annealed at 150ºC

Dark *J-V* plot was measured for naked and coated ECD/CBD-CdSe thin film electrodes, Figure (3.47). The dark J-V plots of films don't give good indication here.

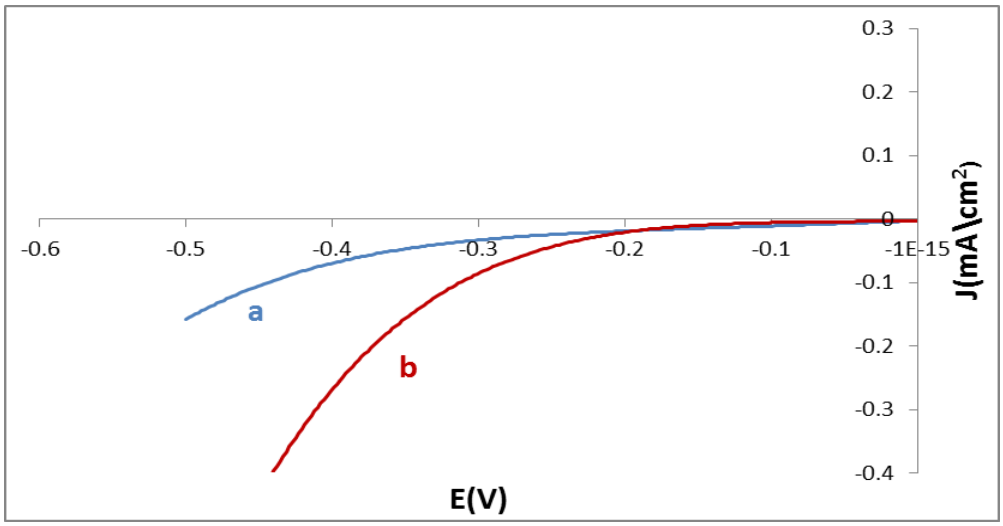

Figure (3.47): Dark *J-V* plots for ECD/CBD-CdSe thin film electrodes annealed at 150ºC, *a)* naked, *b*) coated. All measurements were conducted in aqueous S^{2-}/S_x^{2-} redox system at room temperature.

3.4.1.4.2 CdSe thin films annealed at 250ºC

Dark *J-V* plot was measured for naked and coated ECD/CBD -CdSe thin film electrodes which annealed at 250ºC, Figure (3.48). The dark J-V plots of films don't give good indication here.

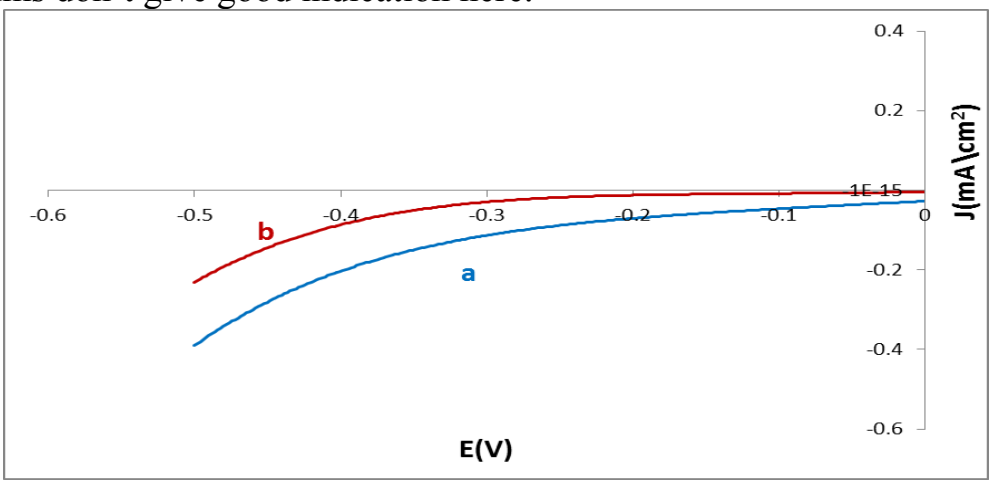

Figure (3.48): Dark *J-V* plots for ECD/CBD-CdSe thin film electrodes annealed at 250ºC, *a)* naked, *b*) coated. All measurements were conducted in aqueous S^{2-}/S_x^{2-} redox system at room temperature.

3.4.1.4.3 CdSe thin films annealed at 350ºC

Dark *J-V* plot was measured for naked and coated ECD/CBD -CdSe thin film electrodes, Figure (3.49). The positive dark current occurred, due to current leakage in system during the experiment. The dark J-V plots of films don't give good indication here.

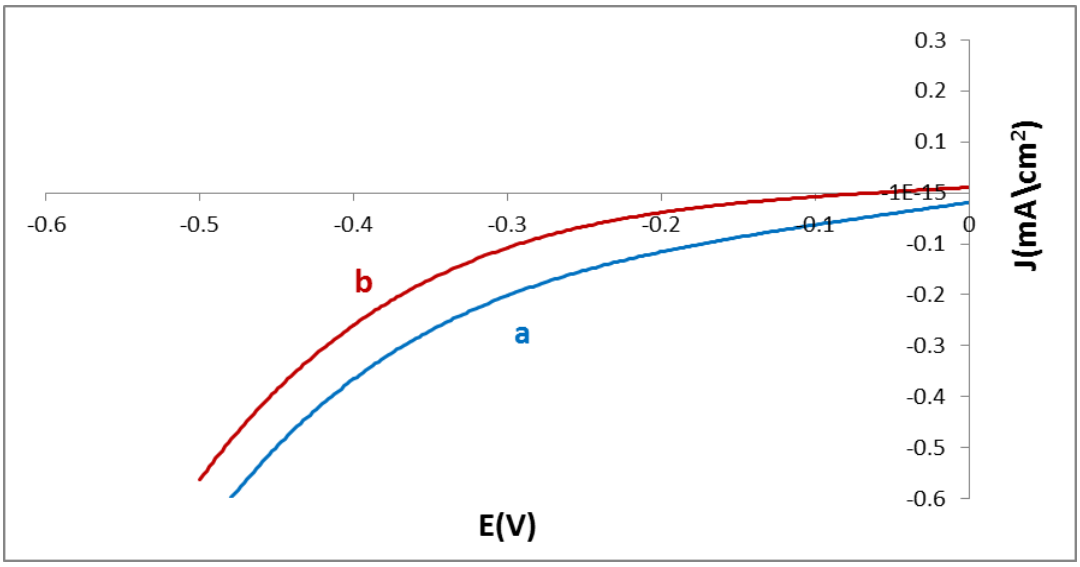

Figure (3.49): Dark *J-V* plots for ECD/CBD-CdSe thin film electrodes annealed at 350ºC, *a)* naked, *b*) coated. All measurements were conducted in aqueous S^{2-}/S_x^{2-} redox system at room temperature.

3.4.2 Photo *J-V* plots of CdSe thin film electrodes

Photo *J-V* plots were measured for ECD/CBD -CdSe thin film electrodes prepared under different conditions (deposition time, annealing temperature, cooling rate, and covering with MP-Sil matrix). The PEC measurements indicate that the CdSe films are n-type in electrical conduction.

3.4.2.1 Effect of deposition time on CdSe thin film electrodes

Photo *J-V* plots were measured for ECD/CBD -CdSe thin film electrodes prepared in different deposition times (15 min ECD + 120 min CBD), (15 min ECD + 240 min CBD), Figure (3.50). The results of the Figure are summarized in Table (3.15).

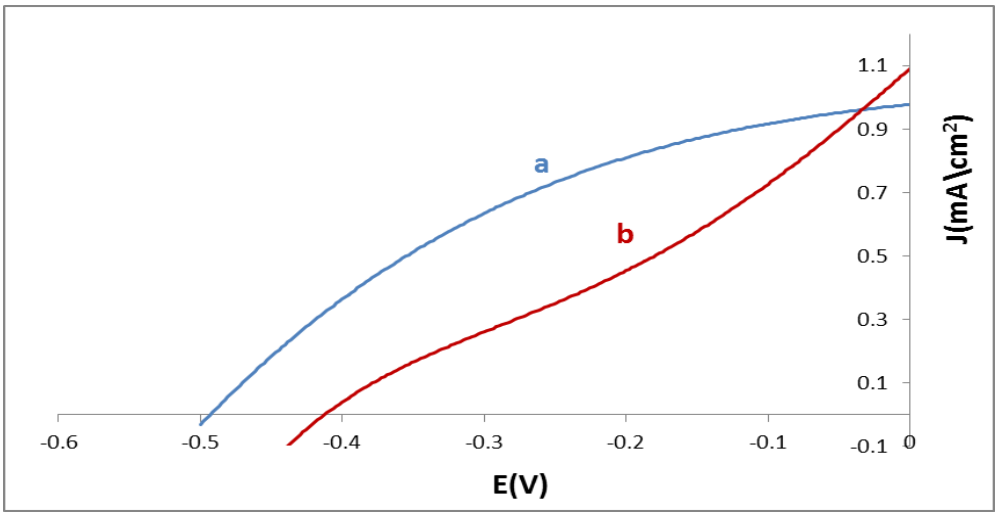

Figure (3. 50): Photo J-V plots for ECD/CBD-CdSe thin film electrodes at different deposition time: a) 15 min ECD and 240 min CBD, b) 15 min ECD and 120 min CBD. All measurements were conducted in aqueous S^{2-}/S_x^{2-} redox system at room temperature

Table (3.15): Effect of deposition time on PEC characteristics of ECD/CBD -CdSe thin film electrode.

sample	description	V_{oc} (V)	J_{sc} (A/cm^2)	[a] η %	[b] FF%
a	15 min & 240 min	-0.49	0.94×10^{-3}	4.40	41.9
b	15 min & 120 min	-0.41	1.08×10^{-3}	1.36	23.5

[a] η (%) = [(maximum observed power density)/(reach-in power density)]×100%.

[b] FF = [(maximum observed power density)/ J_{sc} ×V_{oc}]×100%.

The film deposited in (15 min ECD +240 min CBD) showed higher V_{oc} value, it also gave higher percent conversion efficiency (η % ~ 4.40) and higher fill factor value (FF% ~ 41.9), Table (3.7), in agreement with the PL and the electronic absorption spectra results.

3.4.2.2 Effect of annealing temperature on CdSe thin film electrodes

Photo *J-V* plots were measured for ECD/CBD-CdSe thin film electrodes annealed at different temperatures (150, 250, and 350ºC) and quenched. Figure (3.51). The results of the Figure are summarized in Table (3.16).

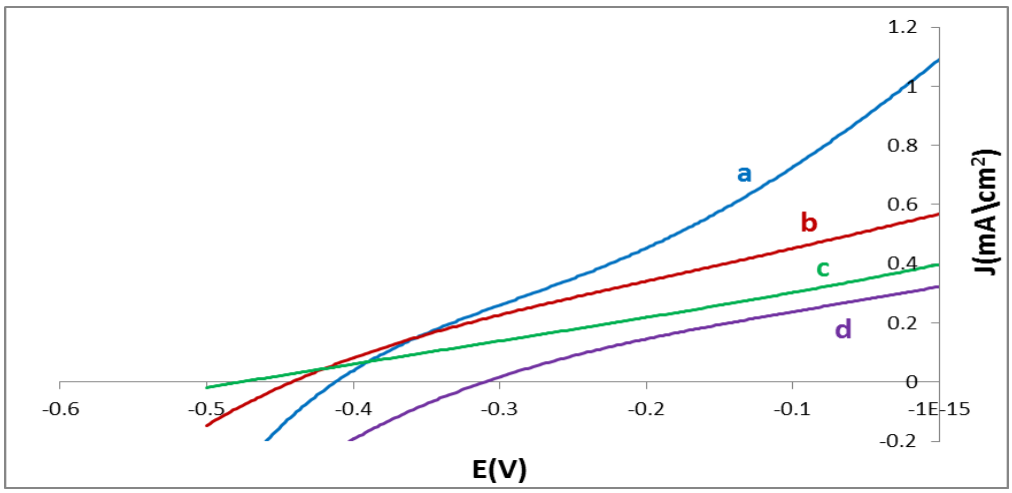

Figure (3.51): Photo J-V plots for naked ECD/CBD -CdSe thin film electrodes, a) non-annealed, b) annealed at 150 ºC and quenched, c) annealed at 250 ºC and quenched, d) annealed at 350 ºC and quenched. All measurements were conducted in aqueous S^{2-}/S_x^{2-} redox system at room temperature.

Table (3.16): Effect of annealing on PEC characteristics of ECD/CBD-CdSe thin film electrode.

Sample	description	V_{oc} (V)	J_{sc} (A/cm^2)	[a] η %	[b] FF%
a	Non-annealed	-0.41	1.08×10^{-3}	1.67	23.5
b	150ºC	-0.44	0.56×10^{-3}	1.36	22.9
c	250ºC	-0.47	0.40×10^{-3}	0.867	27.2
d	350ºC	-0.31	0.34×10^{-3}	0.624	36.1

[a] η (%) = [(maximum observed power density)/(reach-in power density)]×100%.

[b] FF = [(maximum observed power density)/ J_{sc} ×V_{oc}]×100%.

V_{oc} values for the films annealed at different temperatures (150, 250, and 350ºC) were close to each other, the film annealed at 250 ºC film showed the highest V_{oc} value, while the non- annealed one showed the highest J_{sc} value, and gave the highest percent conversion efficiency (η % ~ 1.67), Table (3.16), this is in agreement with the PL spectra and ECD-CdSe thin films results.

3.4.2.3 Effect of cooling rate on CdSe thin film electrodes

Photo *J-V* plots were measured for ECD/CBD-CdSe thin film electrodes annealed at different temperatures (150, 250, and 350ºC) under N_2 atmosphere for 1 hour.

3.4.2.3.1 CdSe thin films annealed at 150ºC

Photo *J-V* plots were investigated for both slowly cooled and quenched ECD /CBD -CdSe thin film electrodes annealed at 150ºC under nitrogen, Figure (3.52). The results of the Figure are summarized in Table (3.17).

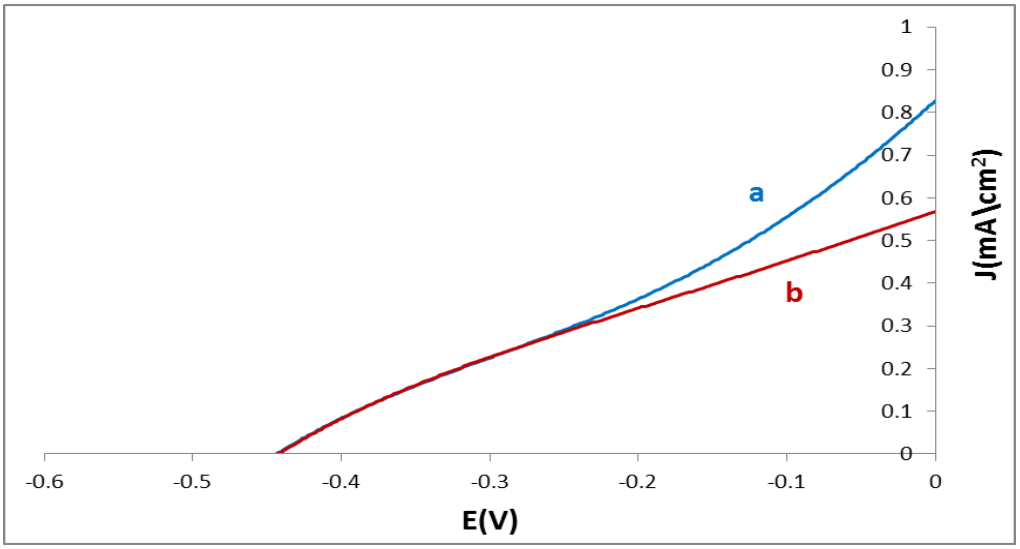

Figure (3.52): Photo J-V plots for ECD/CBD -CdSe thin film electrodes annealed at 150 ºC, a) slowly cooled, b) quenched. All measurements were conducted in aqueous S^{2-}/S_x^{2-} redox system at room temperature.

Table (3.17): Effect of cooling rate on PEC characteristics of ECD/CBD -CdSe thin film electrodes (annealed at 150 ºC).

sample	description	V_{oc} (V)	J_{sc} (A/cm^2)	[a] η %	[b] FF%
a	Slowly cooled	-0.44	0.83×10^{-3}	1.58	22.9
b	Quenched	-0.44	0.56×10^{-3}	1.22	30.4

[a] η (%) = [(maximum observed power density)/(reach-in power density)]×100%.

[b] FF = [(maximum observed power density)/ $J_{sc} \times V_{oc}$]×100%.

The V_{oc} values for the slowly cooled and quenched films were the same, the slowly cooled film showed higher J_{sc} and higher percent conversion efficiency (η % ~ 1.58), Table (3.17), in agreement with the spectra result and XRD results.

3.4.2.3.2 CdSe thin films annealed at 250ºC

Photo *J-V* plots were investigated for both slowly cooled and quenched ECD /CBD CdSe thin film electrodes annealed at 250ºC under nitrogen for 1 hour. Figure (3. 53). The results of the Figure are summarized in Table (3.18).

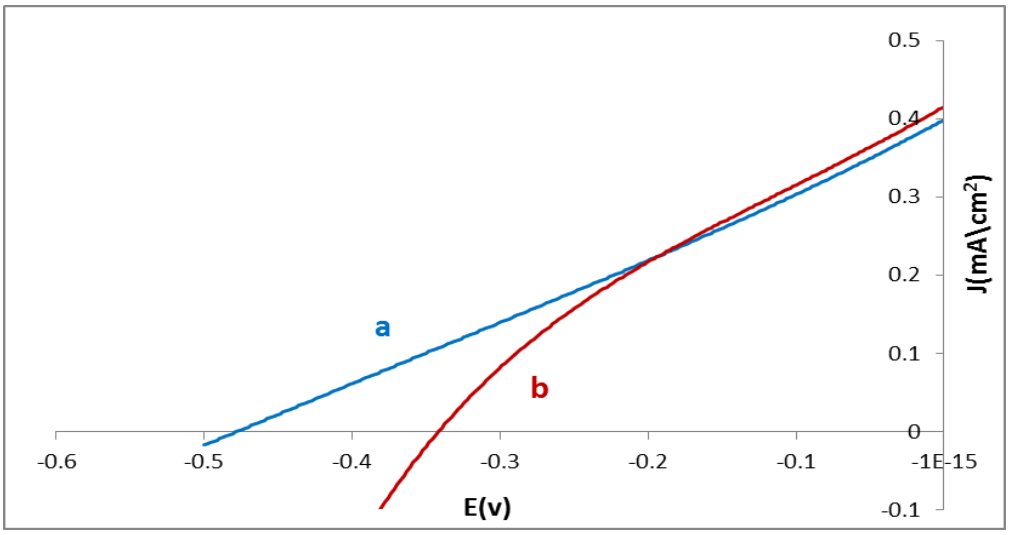

Figure (3. 53): Photo J-V plots for ECD/CBD -CdSe thin film electrodes annealed at 250 ºC, a) quenched, b) slowly cooled. All measurements were conducted in aqueous S^{2-}/S_x^{2-} redox system at room temperature

Table (3.18): Effect of cooling rate on PEC characteristics of ECD/CBD-CdSe thin film electrodes (annealed at 250 ºC).

sample	description	V_{oc} (V)	Jsc (A/cm^2)	[a] η %	[b] FF%
A	Slowly cooled	-0.47	0.40×10^{-3}	1.14	24.46
B	Quenched	-0.34	0.41×10^{-3}	0.93	31.5

[a] η (%) = [(maximum observed power density)/(reach-in power density)]×100%.

[b] FF = [(maximum observed power density)/ $J_{sc} \times V_{oc}$]×100%.

The slowly cooled film showed higher V_{oc} value and gave higher percent conversion efficiency (η % ~ 1.14) than the quenched one, Table (3.18), in agreement with the spectra result and XRD results.

3.4.2.3.3 CdSe thin films annealed at 350 ºC

Photo *J-V* plots were investigated for both slowly cooled and quenched ECD/CBD -CdSe thin film electrodes which annealed at 350ºC under nitrogen for 1 hour, Figure (3.54). The results of the Figure are summarized

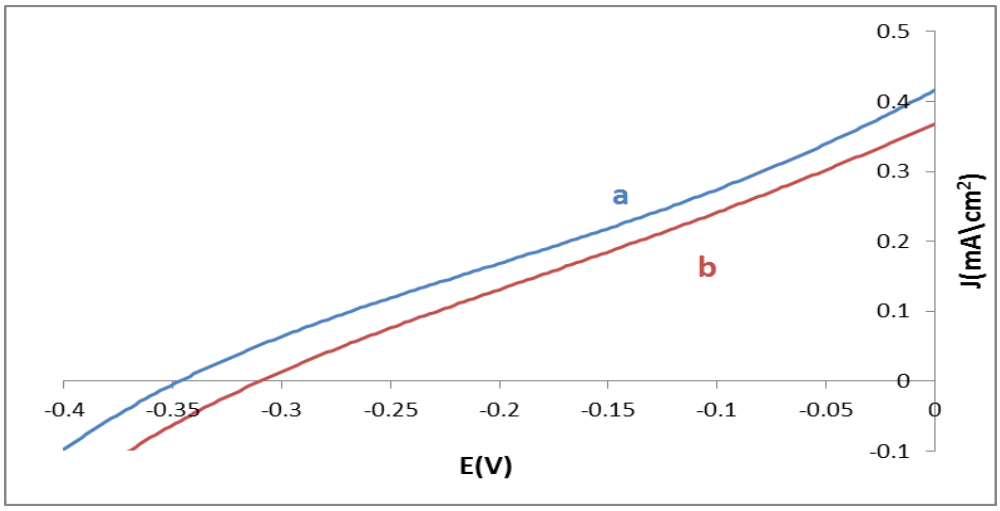

Figure (3.54): Photo J-V plots for ECD/CBD -CdSe thin film electrodes annealed at 350 ºC, a) slowly cooled, b) quenched. All measurements were conducted in aqueous S^{2-}/S_x^{2-} redox system at room temperature**.**

Table (3.19): Effect of cooling rate on PEC characteristics of ECD/CBD-CdSe thin film electrodes (annealed at 350 ºC).

sample	**description**	***Voc* (V)**	***Jsc* (A/cm^2)**	**[a] η %**	**[b] *FF*%**
a	Slowly cooled	-0.35	0.41×10^{-3}	0.924	26.4
b	Quenched	-0.32	0.36×10^{-3}	0.50	26.5

[a]η (%) = [(maximum observed power density)/(reach-in power density)]×100%.

[b]FF = [(maximum observed power density)/ J_{sc} ×V_{oc}]×100%.

The V_{oc} values for the slowly cooled and quenched films were close to each other, in otherwise the slowly cooled film showed higher J_{sc} value and higher percent conversion efficiency (η % ~ 0.924) than the quenched one, Table (3.19), in agreement with the spectra result and XRD results.

3.4.2.4 Effect of covering with MP-Sil matrix on CdSe thin film electrodes

Photo *J-V* plots were investigated for naked and coated ECD /CBD -CdSe thin films, annealed at different temperatures (150, 250, 350ºC) under nitrogen for 1 hour, and slowly cooled to room temperature.

3.4.2.4.1 CdSe thin films annealed at 150ºC

Photo *J-V* plots were investigated for naked and coated ECD /CBD -CdSe thin film electrodes annealed at 150ºC under nitrogen for 1 hour, Figure (3.55). The results of the Figure are summarized in Table (3.20).

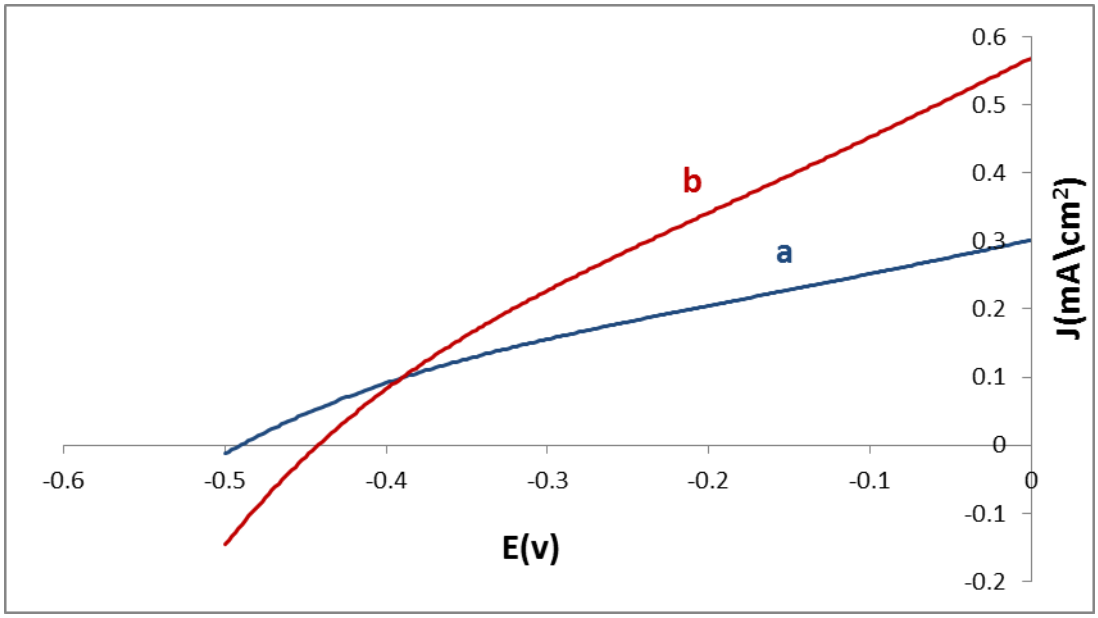

Figure (3.55): Photo J-V plots for ECD/CBD-CdSe thin film electrodes annealed at 150ºC and slowly cooled, a) naked, b) coated. All measurements were conducted in aqueous S^{2-}/S_x^{2-} redox system at room temperature.

Table (3.20): Effect covering with MP-Sil matrix on PEC characteristics of ECD-CdSe thin film electrode (annealed at 150 ºC).

sample	description	V_{oc} (V)	Jsc (A/cm^2)	$^{a}\eta$ %	^{b}FF%
a	Naked	-0.49	0.29×10^{-3}	1.50	30.40
b	Coated	-0.44	0.56×10^{-3}	2.00	33.90

[a]η (%) = [(maximum observed power density)/(reach-in power density)]×100%.

[b]FF = [(maximum observed power density)/ $J_{sc}\times V_{oc}$]×100%.

The coated film showed higher V_{oc} and J_{sc} values, higher percent conversion efficiency (η % ~ 2.00) and higher fill factor value FF% ~ 33.9) than the naked film, Table (3.20). This is consistent with the spectra result.

3.4.2.4.2 CdSe thin films annealed at 250ºC

Photo *J-V* plots were investigated for naked and coated ECD /CBD -CdSe thin film electrodes annealed at 250ºC under nitrogen for 1 hour. Figure (3.56). The results of the Figure are summarized in Table (3.21).

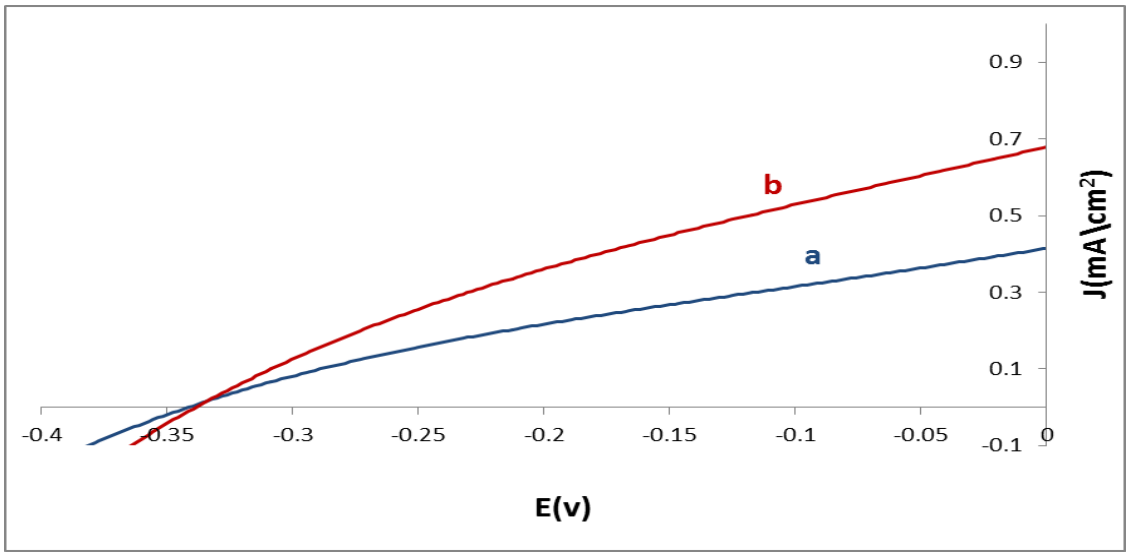

Figure (3.56): Photo J-V plots for ECD/CBD-CdSe thin film electrodes annealed at 250 ºC and slowly cooled, a) naked, *b*) coated. All measurements were conducted in aqueous S^{2-}/S_x^{2-} redox system at room temperature.

Table (3.21): Effect of covering with MP-Sil matrix on PEC characteristics of ECD/CBD-CdSe thin film electrode (annealed at 250 ºC).

sample	description	*Voc* (V)	*Jsc* (A/cm^2)	[a] η %	[b] *FF*%
a	Naked	-0.34	0.41×10^{-3}	0.92	30.8
b	Coated	-0.34	0.67×10^{-3}	1.58	32.5

[a] η (%) = [(maximum observed power density)/(reach-in power density)]×100%.

[b] FF = [(maximum observed power density)/ $J_{sc} \times V_{oc}$]×100%.

The *Voc* values for the coated and naked films were the same, the coated film exhibited higher J_{sc} value and higher percent conversion efficiency (η % ~ 1.58) than the naked one, Table (3.21). This is consistent with the spectra result.

3.4.2.4.3 CdSe thin films annealed at 350ºC

Photo *J-V* plots were investigated for naked and coated ECD /CBD-CdSe thin film electrodes which annealed at 350ºC under nitrogen for 1 hour. **Figure (3.57)**.The results of the Figure are summarized in Table (3.22).

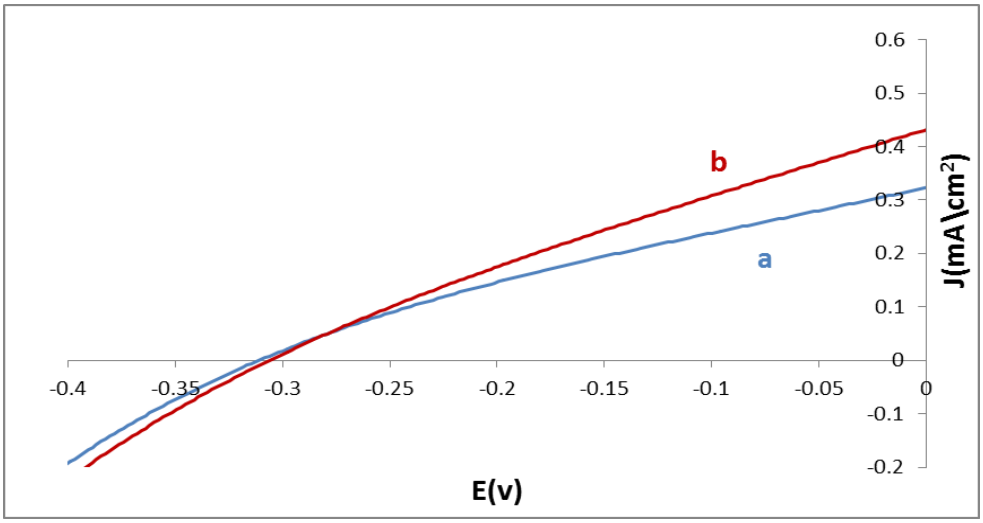

Figure (3.57): Photo J-V plots for ECD/CBD-CdSe thin film electrodes annealed at 350 ºC and slowly cooled, a) naked, b) coated. All measurements were conducted in aqueous S^{2-}/S_x^{2-} redox system at room temperature**.**

Table (3.22): Effect covering with MP-Sil matrix on PEC characteristics of ECD/CBD-CdSe thin film electrode (annealed at 350 ºC).

sample	description	V_{oc} (V)	J_{sc} (A/cm^2)	[a] η %	[b] FF%
a	Naked	-0.315	0.34×10^{-3}	0.62	28.5
b	Coated	-0.307	0.44×10^{-3}	0.92	28.2

[a] η (%) = [(maximum observed power density)/(reach-in power density)]×100%.

[b] FF = [(maximum observed power density)/ $J_{sc} \times V_{oc}$]×100%.

The V_{oc} values for the naked and coated films were close to each other, the coated film showed higher J_{sc} and higher percent conversion efficiency (η

% ~ 0.92) than the naked one, Table (3.22). This is consistent with the spectra result.

Part III

A comparison between different preparation methods (ECD, CBD and ECD/CBD) of CdSe thin film electrodes

The films were comparatively characterized by a number of techniques including PL emission spectra, electronic absorption spectra and XRD. PEC studies including dark J-V plots, photo J-V plots, conversion efficiency, value of short-circuit current, stability and fill-factor (FF) were also studied.

3.5 ECD, CBD and ECD/CBD- CdSe thin film characteristics

The films of ECD, CBD and ECD/CBD-CdSe films were comparatively characterized by using different techniques as shown below.

3.5.1 XRD measurements for CdSe thin film electrodes

XRD measurements were obtained for naked CdSe film electrodes prepared by different techniques (ECD, CBD and combined ECD/CBD), XRD data showed that all the prepared films exhibited crystallinity. The average particle size for ECD-CdSe was~ 3.69 nm, Figure (3.58). CBD-CdSe particle size was~ 3.98 nm and it was~ 4.13 for the combined ECD/CBD-CdSe thin film. All films involved cubic phase (zinc-blende

structure).This was based on comparison with earlier reports (35, 38-40) only. Table (3.23) shows the positions of observed peaks. The peaks of FTO substrate for the ECD/CBD CdSe films don't appear here clearly. This is attributed to the fact that ECD/CBD-CdSe film has higher thickness than either ECD-CdSe film or CBD-CdSe film.

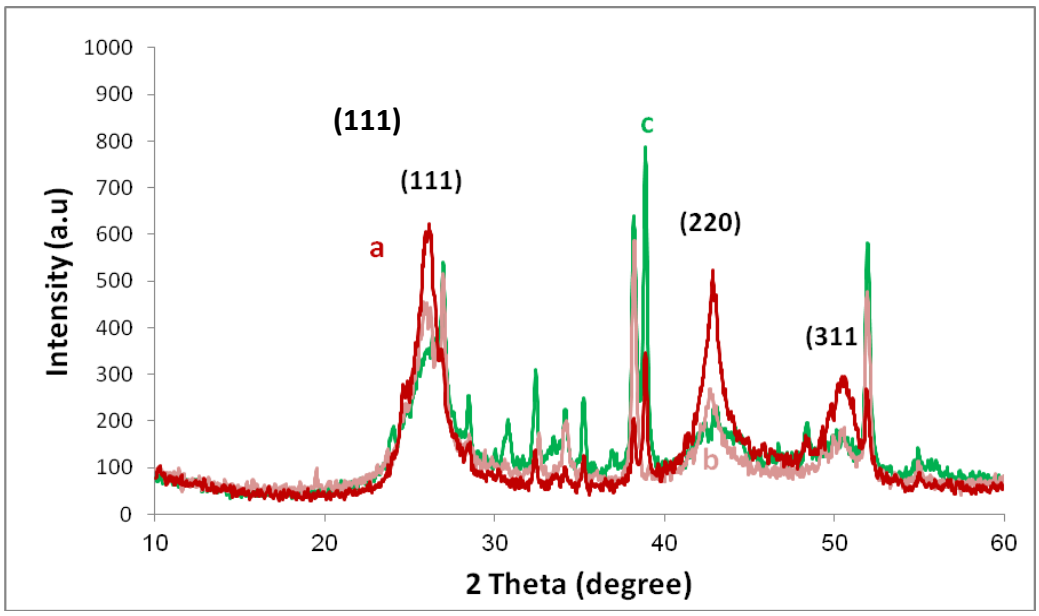

Figure (3.58): XRD patterns measured for naked CdSe thin film a) ECD-CdSe film, b) CBD-CdSe film, c) ECD/CBD CdSe film.

Table (3.23): XRD results for CdSe film electrodes prepared by different techniques (ECD, CBD and combined ECD/CBD).

Position of observed peak (2 theta)		Plane	Reference	Particle size (nm)
ECD-CdSe	**26.34**	**C(111)**	[38]	**3.69**
	29.90	FTO subs	[42]	
	34.09	FTO subs	[42]	
	38.16	FTO subs	[42]	
	38.80	FTO subs	[42]	
	42.90	**C(220)**	[38]	
	50.32	**C(311)**	[38]	
	51.80	FTO subs	[42]	
CBD-CdSe	26.10	**C(111)**	[38]	**3.98**
	26.90	FTO subs	[42]	
	34.12	FTO subs	[42]	
	38.14	FTO subs	[42]	
	42.68	**C(220)**	[38]	
	50.28	**C(311)**	[35]	
	51.88	FTO subs	[30]	
ECD/CBD-CdSe	25.93	**C(111)**	[38]	**4.31**
	34.06	FTO subs	[30]	
	38.13	FTO subs	[30]	
	42.70	**C(220)**	[38]	
	50.35	**C(311)**	[38]	
	51.85	FTO subs	[30]	

3.5.2 Photoluminescence spectra for CdSe thin film electrodes

Photoluminescence spectra were investigated for naked CdSe thin films prepared in different methods (ECD, CBD and combined ECD/CBD), Figure (3.59). The systems were excited at wavelength 385 nm. The Figure

showed different weak peaks, the highest intensity peaks appeared at wavelength range of (600-540) nm with a band gap range (2.06-2.29) eV, for the combined ECD\CBD- CdSe thin film, while the ECD-CdSe thin film showed blue shift at wavelength range (580-520) nm, with a band gap range (2.13-2.38) eV. The lowest intensity peak was for CBD-CdSe thin film at wavelength range (600-540) nm, with a band gap range (2.06-2.29) eV. Band gap values for different prepared films were in agreement with the band gap range of CdSe thin films in literature [22, 35].

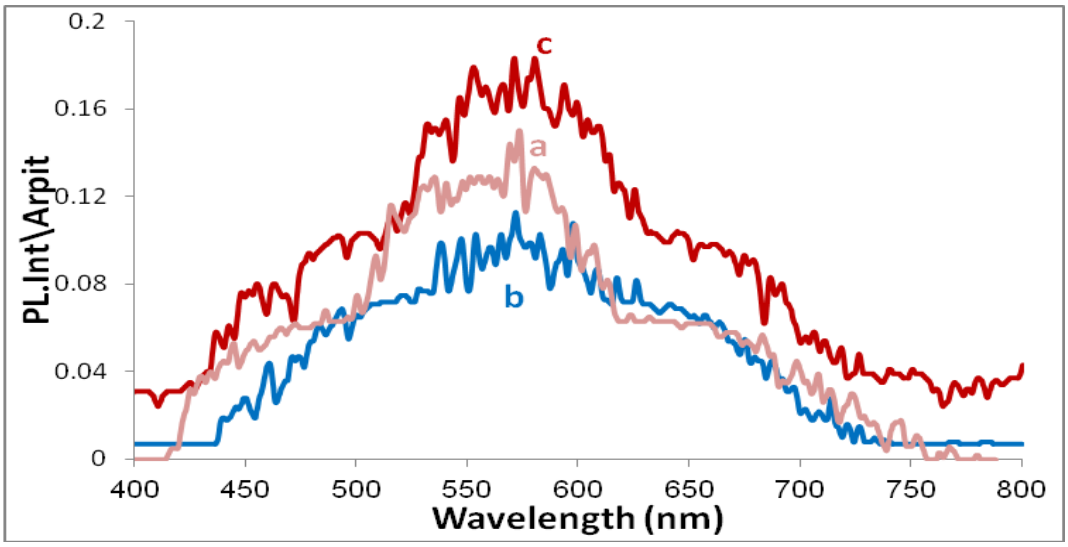

Figure (3.59): Photo-luminescence spectra for CdSe thin films prepared by: a) ECD, b) CBD, c) combined ECD\CBD technique.

3.5. 3 Electronic absorption spectra for CdSe thin film electrodes

Electronic absorption spectra were measured for naked CdSe thin films prepared by different methods (ECD, CBD and combined ECD/CBD), Figure (3.60). The absorption spectra were difficult to conclude and analyze. This is due to the prepared films, being either too thin (ECD) or too thick (ECD/CBD). A relatively obvious absorption was observed for

ECD-CdSe and CBD-CdSe films. While spectra could not be clearly observed here for the combined ECD/CBD CdSe thin film.

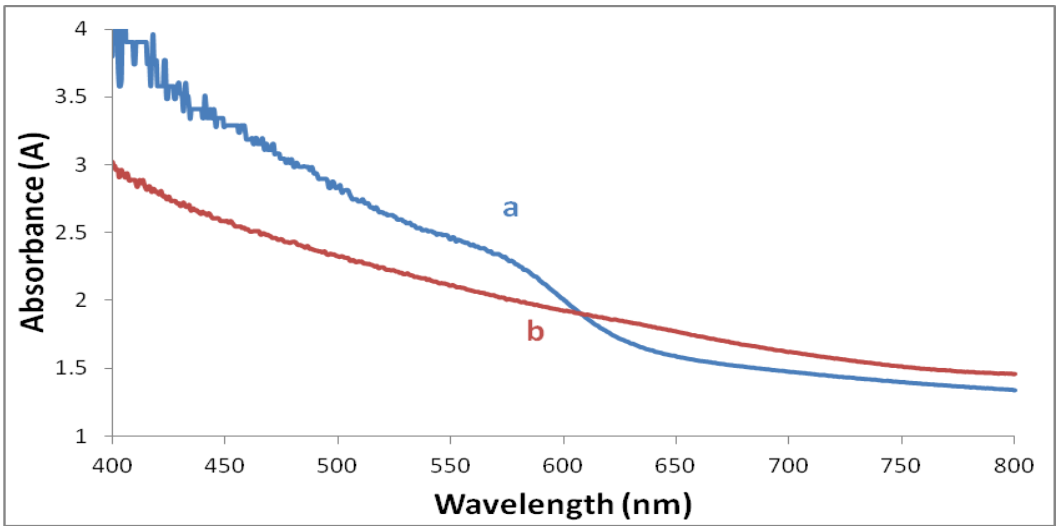

Figure (3.60): Electronic absorption spectra for CdSe thin films prepared by a) ECD technique, b) CBD technique.

3.6 CdSe thin films PEC studies

PEC studied including dark J-V plots, photo J-V plots, conversion efficiency, value of short-circuit current, stability and fill-factor (FF), were investigated for different types of prepared CdSe films in aqueous S^{2-}/S_x^{2-} redox couples at room temperature.

3.6.1 Dark *J-V* Plots of CdSe thin film electrodes

The films were comparatively characterized for ECD, CBD and combined ECD/CBD –CdSe thin films by measuring dark *J-V* plots. The positive dark current occurred, due to current leakage in system during the experiment. The dark J-V plots of films don't give good indication here.

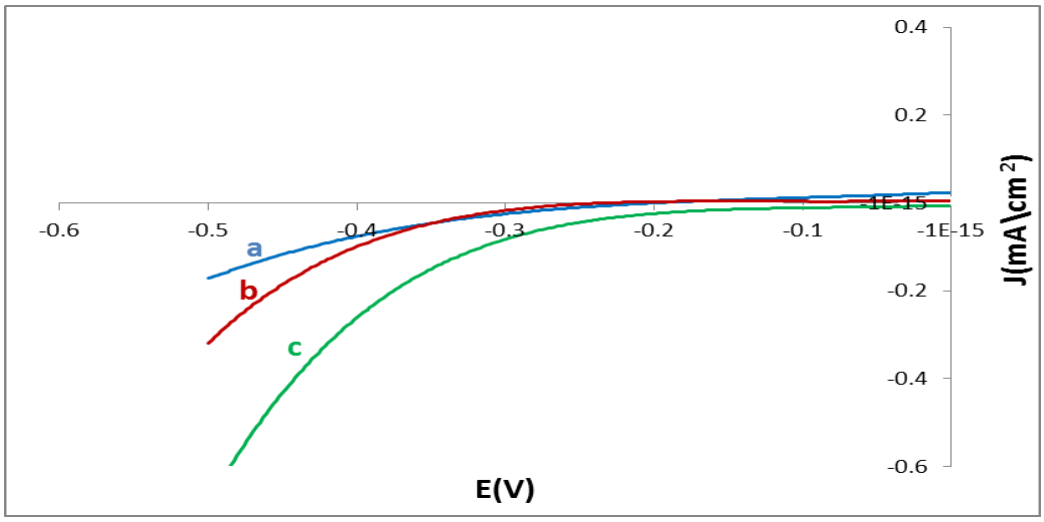

Figure (3.61): Dark J-V plots for CdSe thin film electrodes prepared by: a) ECD, b) CBD, c) combined ECD\CBD technique. All measurements were conducted in aqueous S^{2-}/S_x^{2-} redox system at room temperature.

3.6.2 Photo *J-V* Plots of CdSe thin film electrodes

The films were comparatively characterized for ECD, CBD and combined ECD/CBD –CdSe thin films by measuring photo *J-V* plots.

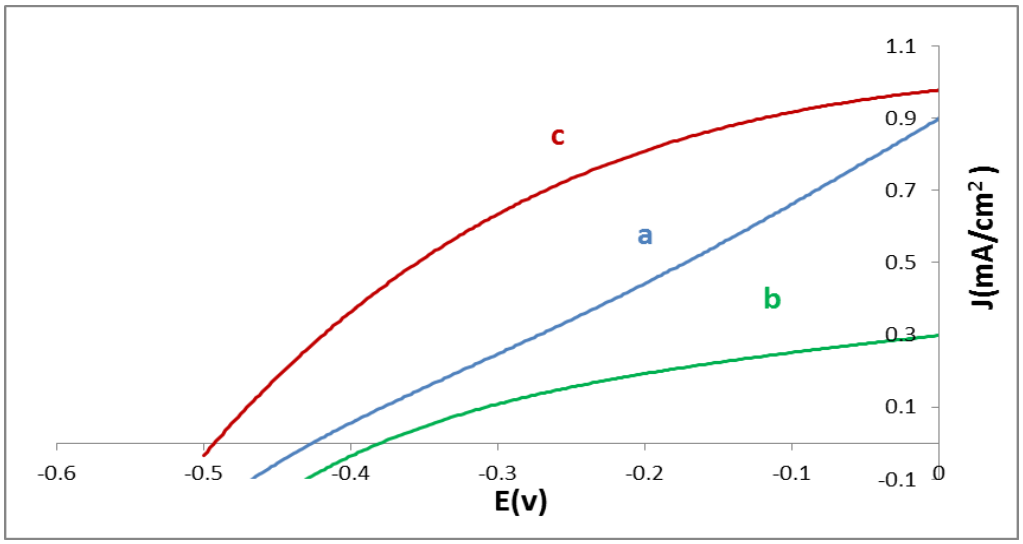

Figure (3.62): Photo *J-V* plots for CdSe thin film electrodes, *a)* prepared by ECD, *b*) prepared by CBD, c) prepared by ECD\CBD. All measurements were conducted in aqueous S^{2-}/S_x^{2-} redox system at room temperature**.**

Table (3.24): Effect of preparation technique on PEC characteristics of CdSe thin film electrode.

Sample	Preparation method	*Voc* (V)	*Jsc* (A/cm^2)	[a] η %	[b] *FF*%
a	**ECD**	-0.45	0.91×10^{-3}	1.72	20.7
b	**CBD**	-0.38	0.27×10^{-3}	1.16	42.8
c	**ECD/CBD**	-0.49	0.98×10^{-3}	4.40	40.2

[a] η (%) = [(maximum observed power density)/(reach-in power density)]×100%.

[b] FF = [(maximum observed power density)/ $J_{sc} \times V_{oc}$]×100%.

The CdSe film prepared by the combined ECD/CBD technique shows the best PEC characteristics with highest *Voc*, *Jsc* values and highest percent conversion efficiency *(*η % ~ 4.40), Table (3.24). This is consistent with the PL and XRD results.

Chapter four

Discussion

Different methods were used here to prepare CdSe thin film electrodes including electrochemical deposition (ECD), chemical bath deposition CBD), and combining the two techniques together (ECD/CBD). The combined technique has been earlier applied to CdS thin film electrode preparation [30], and has now been applied here again in preparing CdSe films for the first time. A comparison between the CdSe film electrodes prepared by different techniques has been made.

Several methods were used here, in order to enhance CdSe thin film characteristics including: Annealing at different temperatures, cooling rate control, deposition time and covering the prepared films with electro-active species Tetra (-4-pyridyl) porphyrinatomanganese (III/II) sulfate embedded inside polysiloxane films (MnPyP/Polysil) matrices.

Characteristics of the enhanced films were studied using different techniques including PL emission spectra, electronic absorption spectra and XRD, PEC studies including dark *J-V* plots, photo *J-V* plots, conversion efficiency, value of short-circuit current and fill-factor (FF).

4.1 Enhancement of ECD-prepared CdSe thin films

Effect of deposition time on the non- annealed ECD-CdSe films has been studied, Figures (3.5, 3.11, 3.17, 3.23). The PL spectra showed similar emission wavelengths for all films, with highest emission intensities at

wave length range (630-540) nm showing a band gap range of (2.06-2.30) eV. The film prepared in shorter time showed higher PL intensity than the other two counterparts. The PL results are consistent with the electronic absorption spectra results. The results are explained based on surface and crystalline order. The surface of the film prepared in shorter time was more uniform and smoother than the other two counterparts. Photo *J-V* plots indicated that the CdSe films were n-type in electrical conduction, and it showed that the film prepared in shorter time gave higher PEC characteristics than the other two films. All PL, electronic absorption spectra and PEC results are consistent. The dark J-V plots showed positive currents indicating leakage. Therefore it didn't give good indication and were ignored here.

Effects of annealing temperature and cooling rate on CdSe thin film characteristics have been studied. In general, annealing process is known to enhance the crystalline particle characteristics, giving more homogenous and higher crystalline quality. Annealing reduces crystal defects, increases inter particle connection, lowers surface roughness and removes surface states [9, 28]. All SCs contain different types of defects such as vacancies. While heating, the defect concentration increases, and gradually spreads throughout the crystal (from surface to the bulk). On cooling the defect concentration is lowered by diffusion of the vacancies to grain boundaries or dislocations, the rate at which vacancies move from point to point in the lattice decreases exponentially with decreasing temperature, thus fast or slow cooling rate affects the crystal [31, 32]. In this study, the non-

annealed film gave higher PL intensity, more obvious electronic absorption spectra and better PEC characteristics than the annealed counterparts at different temperatures (150, 250, 350℃), Figures (3.6, 3.12, 3.24). This is acceptable as the ECD-CdSe thin films are expected to be relatively uniform and crystalline even with no annealing. Heating increases the kinetic energy of the particles, it may thus increase their disorder and arrange them in a random manner [33].

On the other hand, lower annealing temperature (150℃) with fast cooling showed higher PL intensity, clearer electronic absorption spectra and better PEC characteristics than the other annealed counterparts (250 and 350℃) , Figures (3.6, 3.7, 3.12, 3.13, 3.24 and 3.25). This is because the concentration of the selenium in the films decreases slightly with increased annealing temperature. The selenium totally evaporates at 500ºC as reported earlier [34]. This increases the possibility of film distortion. Fast cooling prevents the crystal from prolonged exposure to high temperature and possibly lowers of film distortion. Film electrode annealed at high temperature with slow cooling involved more crystal imperfection for the same reason, similar arguments were reported for different systems [28]. The optical absorption measurements, Figure (3.12), showed that energy band gap has been decreased from 2.17 to 2.06 eV with annealing, this comes in agreement with an earlier study [34].

Dark J-V plots were measured for slowly cooled and quenched CdSe film electrodes annealed at (150, 250, 350ºC). Figures (3.19-3.21) showed that

dark J-V plots didn't give good indication here. The positive dark current occurred due to current leakage in the system during the experiment. Dark current results were inconclusive in this study.

The XRD pattern, measured for the annealed film confirmed its CdSe nature with a cubic phase (zinc-blende structure). This was based on comparison with earlier reports [35, 38-41]. There are three dominant diffraction peaks: (111), (220) and (311). Annealing the film at 350 ºC enhanced the XRD peaks, in terms of peak height and width, Figure (3.1). According to Scherer equation using (111) plane, the calculated particle size values were 3.69 and 4.38 nm for the non-annealed and the annealed films, respectively, this indicates that annealing slightly affected the particle sizes of the CdSe film. The particle sizes for CdSe films annealed at different temperatures (150 and 350 ºC) were 4.47 and 3.15 nm, respectively, Table (3.2). The particle sizes were 4.38 and 3.51 nm for the quenched CdSe films and the slowly cooled, respectively, Table (3.3). The XRD pattern indicates that annealing at lower temperature (150ºC) followed by fast cooling, gives higher crystallinty than annealing at higher temperature and slow cooling. The XRD results are thus in good agreement with above discussions.

Effect of covering with MP-Sil matrix on non-annealed CdSe thin film electrodes was studied. Figures (3.10, 3.16, 3.28) showed that coated film gave higher PL intensity, more obvious electronic absorption spectra and better PEC characteristics than naked counterpart. This is consistent with

earlier reported results observed for CBD-CdSe film electrodes [35] and for other types of SC thin films [28, 30]. Coating the film with MP-Sil eliminates surface states and defects, which are responsible for lowering PL intensity, electronic absorption and PEC characteristics. MP-Sil matrix works as charge transfer catalyst and there is evidence that the positively charged metalloporphyrin lies closer to the SC surface. The presence of such positive charges would affect positions of flat band edges of the SC and cause positive shifting (lowering) in the value of the flat-band potential, as documented earlier for n-GaAs [37] and for CBD-CdSe [35]. Figure (4.1) shows how lowering the flat band edge will kinetically enhance hole transfer across solid/redox couple interference, and thus protects CdSe surface from corrosion. Coating the film with MP-Sil Matrix may physically protect the film from oxygen and water. This system enhanced the thin film electrode efficiency and stability at the same time [35, 37].

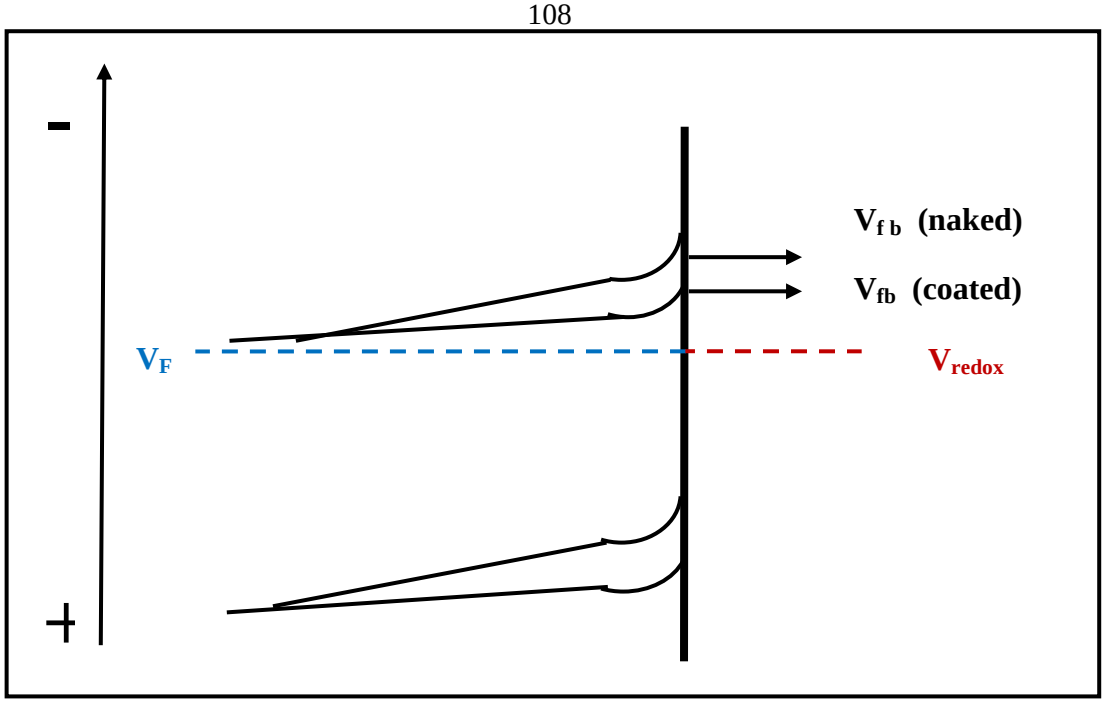

Figure (4.1): Effect of MP-Sil mdatrix coverage on the flat band edges of the SC. *Reproduced from [37]*.

XRD patterns were measured for naked and coated ECD-CdSe thin films, Figure (3.4). According to Scherrer equation, the calculated particle size values were 3.69 and 3.31 nm for the naked and the coated films, respectively. This indicates that coating films with MP-Sil matrix did not affect crystallinty and particle sizes of the CdSe films, since coating involved the outer surface of the film and caused no real sintering.

4.2 Enhancement of ECD/CBD-prepared CdSe thin films

Effect of deposition time on the non- annealed ECD/CBD-CdSe films deposited in (15 min ECD + 120 min CBD, 15 min ECD + 240 min CBD) has been studied. The PL spectra showed similar emission wavelengths for all films, with highest emission intensities at wave length range (600-550) nm showing a band gap range (2.06-2.25) eV. The film deposited in longer

time showed higher PL intensity and better PEC characteristics than its counterpart, Figures (3.33, 3.42, 3. 50). The CBD-CdSe layer needs extra time to be well adhered to the ECD-CdSe layer and getting more uniform surface. Dark *J-V* plots didn't give good indication and were ignored here.

Effects of annealing temperature and cooling rate on ECD/CBD-CdSe thin film characteristics have been studied. The non-annealed film gave higher PL intensity and better PEC characteristics than the films annealed at different temperatures (150ºC, 250ºC and 350ºC). Figures (3.34, 3.51), which is consistent with results observed for ECD-CdSe films. As mentioned previously, annealing was reported to enhance the particle characteristics, giving more uniform and compact surface, depending on the annealing temperature and way of cooling. In this study annealing is undesirable, because heating may increase the kinetic energy of the particles and may thus increase their disorder and arrange them in a random manner. It may also increase ECD-CdSe layer distortion, since ECD-CdSe layer is expected to be relatively uniform and crystalline even before annealing [33].

On the other hand, lower annealing temperature (150ºC) with slow cooling showed higher PL intensity and better PEC characteristics than the other temperatures (250 and 350ºC), Figures (3.34-3.37, 3.51-3.54). Lower annealing temperature is favored for ECD/CBD-CdSe films, which is consistent with results observed for ECD-CdSe films. Higher annealing temperatures increase the possibility of the film electrode distortion, since

excessive Se evaporation from the film may also occur at elevated temperatures [28, 34]. Slow cooling gives enough time to help annealed crystals to regain their original order and retain their stable positions, giving more crystal uniformity [36]. However, slow cooling may also expose the heated crystal to high temperature for longer time.

Fast cooling is preferred for ECD-CdSe films, while slow cooling is preferred for ECD/CBD films. This is attributed to the fact that ECD/CBD-CdSe film has higher thickness and disorder than CBD-CdSe. It needs extra time for the metastable atoms/ions to retain to their original order.

Electronic absorption spectra couldn’t be obtained here clearly, due to the high thickness of the combined ECD/CBD films. Dark current results were inconclusive in this study. The positive dark current occurred, due to current leakage in system during the experiment. XRD pattern, measured for the annealed ECD/CBD film confirmed its CdSe nature with a cubic phase (zinc-blende structure). This was based on comparison with earlier reports [35, 38-40]. There are three dominant diffraction peaks: (111), (220) and (311). Annealing the film at 350 ºC enhanced the XRD peaks, in terms of peak height and width, Figure (3.29). According to Scherer equation using (111) plane, the calculated particle size values were 4.13 and 4.32 nm for the non-annealed and the annealed films, respectively. This indicates that annealing slightly affected the particle sizes of the CdSe film. The particle sizes for CdSe films annealed at different temperatures (150 and 350 ºC) were 3.32 and 3.19 nm, respectively, Table (3.12), the

particle sizes were 3.56 and 3.19 nm for the quenched and the slowly cooled CdSe, respectively, Table (3.13). The XRD pattern indicates that annealing at lower temperature (150ºC) followed by slow cooling, gives higher crystallinty than annealing at higher temperature and slow cooling. The XRD results are thus in good agreement with above discussions.

Effect of covering with MP-Sil matrix on pre-annealed ECD/CBD-CdSe thin film electrodes was studied. Figures (3.38-3.40, 3.55-3.57) showed that coated films gave higher PL intensity and better PEC results than naked counterparts. This is consistent with results which observed for coated ECD-CdSe films discussed earlier.

As discussed above, coating the film with MP-Sil matrix protects the film from oxidation and behaves as charge transfer catalyst across solid/redox couple interference. This speeds up hole transfer and enhances photocurrent. MP-Sil matrix also eliminates surface states and defects, which are responsible for lowering PL intensity. Clear electronic absorption spectra couldn't be obtained here, due to the high thickness of the ECD/CBD-CdSe films. The dark *J-V* plots didn’t give good indication here, Figures (3.47-3.49). XRD patterns were measured for naked and coated ECD/CBD-CdSe thin films, Figure (3.32). According to Scherrer equation, the calculated particle size values were 3.41and 3.31 nm for the naked and the coated films, respectively. This indicates that coating films with MP-Sil matrix did not affect crystallinty and particle sizes of the CdSe

films, since coating involved the outer surface of the film and caused no real sintering.

4.3 A comparison between different preparation methods

CdSe films have been deposited by three different techniques, electrochemical deposition (ECD), chemical bath deposition (CBD) and combined method (based on electrochemical deposition (ECD) followed by chemical bath deposition (CBD). The combined technique has been earlier applied on CdS- film electrodes [30]. And it has now been applied again here in preparing CdSe film electrode for the first time. The films were comparatively characterized by different techniques (photoluminescence spectra, electronic absorption spectra and XRD). PEC characteristic of the electrodes, including dark J-V plots, photo J-V plots, conversion efficiency, value of short-circuit current, stability and fill-factor (FF) were also studied.

The PL spectra measured for ECD, CBD and combined ECD/CBD-CdSe films (non- annealed), Figure (3.59). PL spectra shows that CBD and ECD/CBD films have emission band with almost similar wavelength range (600-540 nm), while ECD shows some blue shift (580-520 nm) with an increase of band gap values range from (2.06 - 2.29) eV to (2.13-2.38) eV. As the particle size decreases the band gap value increases, so it is expected that ECD film have smaller particle size than the other two prepared counterparts, which is in good agreement with XRD results.

The PL intensities showed different values for the three prepared films. The highest emission intensity for ECD/CBD film is attributed to the fact that ECD/CBD-CdSe film has higher thickness than either CBD-CdSe or ECD-CdSe films.

Only rough conclusion could be made based on electronic absorption spectra. This is because CdSe films being either too thin (ECD) or too thick (ECD/CBD), obvious absorptions were observed for ECD-CdSe and CBD-CdSe films, Figure (3.60). While it could not be observed for the combined ECD/CBD CdSe thin film.

Photo J-V plots were measured for the different prepared films, Figure (3.62) showed that the CdSe films are n-type in electrical conduction, and

it showed that the combined ECD/CBD film electrode gave the best PEC characteristics. It exhibited the highest values of V_{oc}, J_{sc}, conversion

efficiency (η) and fill factor in comparison with the other two counterparts. This supports the basic hypothesis of this work where the ECD/CBD film

is assumed to combine the advantages of both ECD (good adherent to FTO surface) and CBD (suitable thickness) together.

Table (3.24) showed the efficiency of different electrodes varied as CBD < ECD < ECD/CBD. The fact that ECD is more efficient than CBD electrode indicates that ECD electrode has higher crystallinity and uniformity than the CBD electrode.

XRD patterns, Figure (3.58), measured for naked ECD, CBD and combined ECD/CBD films show that the films were mostly cubic type crystals [35, 38-41]. Scherrer equation showed that ECD-film involved nano-crystal of 3.69 nm average diameter. The CBD film involved 3.98 nm particles, while the combined ECD/CBD film involved slightly larger nano-particles (4.13 nm) with higher crystallinity, Table (3.23). This is in agreement with results discussed above. The FTO peaks didn't appear clearly in the combined ECD/CBD XRD patterns due to the fact that ECD/CBD has higher thickness than either ECD or CBD films.

Conclusion

- CdSe thin films have been deposited onto FTO/glass substrates by three different techniques, ECD, CBD and combined ECD/CBD for solar cell applications.

- ECD/CBD-CdSe thin film electrodes were more effective in PEC processes than either ECD or CBD systems, while ECD-CdSe film showed better PEC characteristic than CBD-CdSe counterpart.

- Effect of deposition times on PEC characteristic were studied for both ECD and ECD/CBD films. The film deposited in shorter time showed better characteristics for ECD-CdSe system, while the ECD/CBD film deposited in longer time showed better characteristic.

- Effect of annealing temperatures on the prepared ECD and ECD/CBD films (non-annealed, annealed at 150, 250, 350ºC) were studied. The non-annealed films showed better characteristics than the annealed films. The 150 ºC annealing temperature gave better results than the higher temperatures.

- Cooling rate (slow or fast cooling) affects ECD and ECD/CBD-CdSe films characteristics like (XRD, PL and electronic spectra, photo J-V plots).

- Covering ECD and ECD/CBD CdSe films with MP-Sil matrix enhanced their PEC characteristics.

Suggestions for future work

The following recommendations are suggested for future works:

1) Prepare ECD, CBD and ECD/CBD-CdSe thin films with Multi-deposition layers.

2) Modify the CdSe thin films with coating materials using different types of electro-active species and polymers.

3) Apply different PEC cells using different experimental conditions and different redox couples to enhance electrode efficiency and stability.

4) Modify the CdSe films by doping with different metals.

References

[1] J.Wallace, P.Hobbs, "**Atmospheric Science: An introductory Survey**", ed. Academic Press, New York, (1977), 54.

[2] V.Ryan, "**What is solar energy**?", 2005. http ://www.technologystudent. com/energy1/solar7. htm, (date accessed 22/03/2014).

[3] J. Bratley," **Disadvantages of solar energy**",2007. http://www.clean-energy-ideas.com/articles/disadvantages_of_solar_ energy.html, (date accessed 10/04/2014)

[4] H.O Finklea, **Semiconductor Electrodes Concepts and Terminology, in '' Semiconductor Electrodes "**, ed. H.O Finklea, Elsevier, Amsterdam, (1988).

[5] Singleton, James. **Band theory of Solid**,1st ed. oxford university, USA,2001,http://chemwiki.ucdavis.edu/Physical_Chemistry/Quantum_Mechanics/Eletronic_Structure/Band_Theory_of_Semiconductors, (date accessed 05/04/2014).

[6] K. W. Frese, Jr., in "**Semiconductor Electrodes**", ed. H.O Finklea, Elsevier, Amsterdam, (1988), 5.

[7] J. Portier, H. S. Hilal, I. Saa'deddin, S. J. Hwang, M . A. ubramanian, G. Campet, **Thermodynamic correlations and band gap calculations in metal oxides,** *Progress in Solid State Chemistry*, **32** (2004) 207-217.

[8] B. Finnstr M, in "**Solar Energy Photochemical Processes Available for Energy Conversion",** 14, eds. S. Claesson and B. Holmstr, National Swedish, Board for Energy Source Development (1982).

[9] M. Marie, " **Thin Film CdS/FTO/Glass Electrodes Prepared by Combined Electrodeposition/Chemical Bath Deposotion: Enhancement of PEC Characteristics by Coating with Metalloporphyrinate/Polysiloxane Matrices,** " *Master's Thesis*, An-Najah National University, Nablus, Palestine, (2013).

[10] P. Asogwa, **Optical and structural properties of chemical bath deposited CdSe nanoparticles thin films for photovoltaic applications,** *Journal of Non-Oxide Glasses* 2, **4** (2010), 183 – 189.

[11] D. Yt, S. Ks (Sep 2005). "**Chemical aerosol flow synthesis of semiconductor nanoparticles** " *Journal of the American Chemical Society* **127** (35), 12196–1307.

[12] V. L. Colvin, M. C. Schlamp, A. P. Alivisatos,. "**Light-emitting diodes made from cadmium selenide nanocrystals and a semiconducting polymer"**. *Nature* **370** (1994), 648- 654.

[13] http://en.wikipedia.org/wiki/Cadmium_selenide. (date accessed 13/04/2014).

[14] http://en.wikipedia.org/wiki/File:Wurtzite_polyhedra.png. (date accessed 15/04/2014).

[15] N. Gopakumar, P. S. Anjana, P. K. Vidyadharan Pillai , **Chemical bath deposition and characterization of CdSe thin films for optoelectronic applications”**, *Journal of Materials Science*”, **45** (2010), 6653-6656.

[16] Y. Guo, Alan L. Porter, Lu Huang, **Nanotechnology-Enhanced Thin-Film Solar Cells: Analysis of Global Research Activities with Future Prospects**, [article on line]. A vailable from: http://www.thevantagepoint/resources/articles/NANO-ENHANCED%20%20%CELLS.pdf (date accessed 15/04/2014)

[17] A. Zyoud, I. Saa’deddin, S. Khudruj, Z. M. Hawash, D. Park, G. Campet, H. S. Hilal, **CdS/FTO thin film electrodes deposited by chemical bath deposition and by electrochemical deposition: A comparative assessment of photo-electrochemical characteristics,** *Solid State Sciences* ,**18** (2013), 83-90.

[18] H. Sabri, "**Modification of the properties of cadmium selenide thin films in photovoltaic solar cells",** *Master's Thesis*, An-Najah National University, Nablus, Palestine, (2009).

[19] S. Chandra, in "**Photoelectrochemical Solar Cells** ", ed. Gordon and Breach Science Publishers, New York, (1986), 88-103.

[20] R. Memming, in "**Comprehensive Treating of Electrochemistry**", **7** eds. B. E. Conway, et al., **Plenum Publishing Corporation**, New York, (1983), 540-544.

[21] K.War, p.Singh, J.Dubow, "**Energy conversion in hotoelectrochemical systems-a review"**, *Electrochim. Acta*, **23** (1978), 1117-1144.

[22] R. Chowdhury, M. Islam, F. Sabeth, G. Mustafa, S. Farhad, D. Saha, F. Chowdhury, S. Hussain, A. Islam1, **Characterization of electrodeposited cadmium selenide thin films,** *Dhaka university Journal of Science*, **60** (2012), 137-140.

[23] J. Kois, S. Bereznev, O.Volobujeva, J. Gurevits, E. Mellikov, **Electrocrystallization of CdSefromaqueouselectrolytes: Structural arrangementfromthinfilmstoself-assemblednanowires,** *Journal of Crystal Growth*, **320** (2011) 9–12.

[24] M. Deshpande, N. Garg, S. Bhatt, Pa. Sakariya, S. Chaki, **Characterization of CdSe thin films deposited by chemical bath solutions containing triethanolamine**, *Materials Science in Semiconductor Processing*, **16** (2013), 915–922.

[25] W. Mansour," **Hydrosolation reaction catalyzed by novel Metalloporphyrin catalysts instercatalted inside Nano- and micro particles",** Master's thesis, An-Najah National University, Nablus, Palestine, (2013).

[26] H. S. Hilal, W. M. Ateereh, T. Al-Tel, R. Shubeita, I. Saadeddin, G .Campet**, Enhancement of n-GaAs characteristics by combined heating,**

cooling rate and metalloporphyrine modification techniques, *Solid State Sciences*, **6** (2004), 139-146.

[27] H. S. Hilal, M. Masoud, S. Shakhshir, N. **Jisrawi"n-GaAs band-edge reposition by modification with metaloporphorin-polysiloxane matrices"**, *Active and Passive Electronic Components*, **26**(1) (2001), 11-21.

[28] R. AL-Kerm, " **Modification of CuSe thin film electrodes prepared by electrodeposition: Enhancement of photoelectrochemical characteristics by controlling cooling rate and covering with polymer/metalloporphyrin''**, *Master's thesis*, An-Najah National University, Nablus, Palestine, (2013).

[29] Md. S. Mina, H. Kabir, M. M. Rahman ,Md.A. Kabir, M. Rahaman, M. S. Bashar, Md. S. Islam, A. **Sharmin, F.Ahmed, Optical and Morphological Characterization of BaSe Thin Films Synthesized via Chemical Bath Deposition,** *IOSR Journal of Applied Physics*, **4** (2013), 30-35

[30] A. Zyoud, I. Saadeddin, S. Khudruj, M.I. Marie, Z. M. Hawash, M. Faroun, G. Campet, D.Park, H.S.Hilal, **Combined lectrochemical/chemical bath depositions to prepare CdS film electrodes with enhanced PEC characteristics,** *Journal of Electroanalytical Chemistry*, **707**(2013), 117-121.

[31] L. Smart, **"Elaine Moore, Solid State Chemistry an introduction"** Champman & Hall, 1955, PP 159-214.

[32] A.R.West, **"Basic Solid State Chemistry"** JHONE WILEY & SONS, 1984.1988. PP 206-255.

[33] S. Khudruj, "**CdS Thin Film Photo-Electrochemical Electrodes: Combined Electrochemical and Chemical Bath Depositions",** Master's thesis, An-Najah National University, Nablus, Palestine, (2011).

[34] S. Erat, H. Metin, M. Ari, **Influence of the annealing in nitrogen atmosphere on th XRD, EDX, SEM and electrical properties of chemical bath deposited CdSe thin films,** *Material Chemistry and Physics*, **111**(2008) ,114-120.

[35] H. Sabri, S. Saleh, A. Zyoud, N. N. Abdel-Rahman, I. Saadeddin, G. Campet, D. Park, M. Faroun, H. S. Hilal, **Enhancement of CdSe film electrode PEC characteristics by metalloporphyrin/pilysiloxane matrices**, *Electrochimica Acta*, **136** (2014),138-145.

[36] H. S. Hilal, S. K. Salih, I. A. Saadeddin, G. Campet, **Effect of annealing and of cooling rates on n-GaAs electrode photoelectrochemical characteristics,** *Active and Passive Electonic comp*nents, **27** (2004), 69-81.

[37] H. S. Hilal, M. Masoud, S. Shakhir, N. Jisrawi, n-**GaAs band-edge repositioning by modification with metalloporphyrin/polysiloxane matrices,** *Active and Passive Elecronis Comp*onents, **26** (2003), 11–21.

[38] Y. Zhao, Z. Yan, J. Liu, A. Wei, **Synthesis and characterization of CdSe nanocrystalline thin films deposited by chemical bath deposition,** *Material Science in Semiconductor Processing.***10**(2013), 1592-1598.

[39] P. Gupta, M. Ramrakhiani, **Influence of the particle size on the optical propertiesof CdSe nanoparticles,** *Open Nanosci. J.* **3**(2009), 15–19.

[40] M. R. S. Mahajan, R. B. Dubey, Jagrati Mahajan, **Characteristics and properties of CdSe quantum dots,** *Intenational Journal. Latest Research Science Technology*. **2**(2013), 457–459.

[41] M. Dhanam, R. R. Prabhu, P. K. Manoj, **Investigation on chemical bath deposited Cadmiun selenide thin films,** *Materials Chemistry and Physics*, **107** (2008), 289–296.

[42] Y. S. Jin, K. H. Kim, H. W. **Choi, Properties of TiO_2 Films Prepared for Use in Dye-sensitized Solar Cells by Using the Sol-gel Method at Different Catalyst Concentrations,** *Journal of the Korean Physical Society*, **57**(2010), 1049-1053.

جامعة النجاح الوطنية
كلية الدراسات العليا

أقطاب من الافلام الدقيقة ل CdSe

في التحويل الفوتوكهروكيميائي: جمع طريقتي الترسيب الكهربي والكيميائي

اعداد

نور نايف عبد الرحمن

اشراف

أ.د. حكمت هلال

د. عاهد الزيود

قدمت هذه الرسالة استكمالا لمتطلبات الحصول على درجة الماجستير في الكيمياء بكلية الدراسات العليا في جامعة النجاح الوطنية في نابلس، فلسطين
2014

أقطاب من الافلام الدقيقة ل CdSe
في التحليل الفوتوكهروكيميائي: جمع طريقتي الترسيب الكهربي والكيميائي

اعداد

نور نايف عبد الرحمن

اشراف

أ.د. حكمت هلال

د. عاهد الزيود

الملخص

تم تحضير أفلام CdSe الرقيقة النانوية على شرائح زجاجية مغطاة بطبقة رقيقة موصلة شفافة من أكسيد القصدير المزود بالفلور FTO بطريقة الترسيب الكهربي ECD والترسيب الكيميائي CBDوتم ايضا الجمع بين الطريقتين ECD\CBD. كما تمت المقارنة بين الأفلام المحضرة بالطرق المختلفة و دراسة خصائصها باستخدام طرق مختلفة منها : أطياف انحراف أشعة اكس (XRD)، أطياف الوميض (photoluminescence spectra) وأطياف الامتصاص

(electronic absorption spectra)، ثم تم دراسة كفاءة الأفلام المحضرة في تحويل الضوء الى كهرباء بالطريقة الفوتوكهروكيميائية، حيث بنيت هذه الدراسة على اساس عدة عوامل مثل: منحنيات كثافة تيار الظلمة (dark J–V plots) مقابل الجهد، منحنيات كثافة تيار الاضاءة (Photo J–V plots)، مقابل الجهد، كثافة تيار الدارة القصيرة (J_{sc})، جهد الدارة المفتوح (V_{oc}) وكفاءه الخلية في تحويل الضوء الى كهرباء (percent conversion efficiency).

أظهرت الدراسة الفوتوكهروكيميائية للأفلام المحضرة بالطرق المختلفة سلوكا ومسارات مختلفة. حيث وجد أن الخلية الفوتوكهروكيميائية للأفلام المحضرة بطريقة الجمع أعلى كفاءة من خلية الافلام المحضرة بطريقتي الترسيب الكهربي والترسيب الكيميائي.

علاوة على ما سبق، تم دراسة تاثير عوامل متعددة على كفاءة الأفلام المحضرة بطريقتي الترسيب الكهربي وطريقه الجمع بين االترسيب الكهربي والكيميائي، وذلك استكمالا لدراسة اجريت سابقا على أفلام CdSe حضرت بطريقة الترسيب الكيميائي [18] وتشمل هذه العوامل: تأثير زمن الترسيب،

تأثير تسخين الأفلام المحضرة، تأثير طريقة تبريد الأفلام (تبريد بطيء او سريع) وتأثير طلاء سطوح أفلام CdSe بمادة (MP-Sil).

وجد أن الأفلام غير المشوية أكثر كفاءة في تحويل الضوء الى كهرباء مقارنة بتظائرها المشوية، في حين أن الافلام المشوية على درجة حرارة منحفضه (150درجة مئوية) أعلى كفاءة في تحويل الضوء الى كهرباء من الأفلام المشوية على درجة حرارة عالية(350 درجة مئوية)، كما قد أثرت طريقة تبريد الأفلام (تبريد بطيء او سريع) في الخصائص الفوتوكهروكيميائية والفيزيائية للأفلام.

وقد خرجت هذه الدراسة بنتيجة مفادها أن طلاء سطوح أفلام CdSe بمادة (MP-Sil) تحسن من كفاءة الالكترود المحضر في عمليات التحويل الضوئي الي تيار كهربائي.